Synthesis of End-Functionalized π-Conjugated Polymers by Suzuki–Miyaura Catalyst-Transfer Polycondensation of Triolborate Satl-Type Monomers

A Dissertation for the Degree of Doctor of Philosophy

Saburo Kobayashi

Graduate School of Chemical Sciences and Engineering

Hokkaido University

March 2022

Acknowledgments

The study presented in this dissertation has been performed under the direction of Professor Toshifumi Satoh, Division of Applied Chemistry, Faculty of Engineering, Hokkaido University, from 2017 to 2022. The author wishes to express his sincere appreciation to Professor Toshifumi Satoh, for his kind instruction, helpful advice, and unstinting encouragement during the course of this work. The author is deeply grateful to Associate Professor Takuya Isono, Division of Applied Chemistry, Faculty of Engineering, Hokkaido University, for his helpful and valuable suggestions with continuous encouragement throughout this study. The author also would like to express his sincere thanks to Associate Professor Kenji Tajima and Associate Professor Takuya Yamamoto, Division of Applied Chemistry, Faculty of Engineering, Hokkaido University, Associate Professor Yasunori Yamamoto, Institute for Chemical Reaction Design and Discovery, Hokkaido University, Professor Hisaho Hashimoto and Professor Hiroyuki Kono, Division of Applied Chemistry and Biochemistry, National Institute of Technology, Tomakomai College, Professor Wen-Chang, Department of Chemical Engineering, National Taiwan University, and Assistant Professor Yu-Cheng Chiu, Department of Chemical Engineering National Taiwan University of Science and Technology, whose kind understanding and generous supports have been indispensable throughout this work.

The author enjoyed working with colleagues because the friendship and good humor of the members in the laboratory created a pleasant and stimulating environment in which to work. The author thanks all of members of Professor Satoh's and Associate Professor Yamamoto's groups.

The author would like to give his special thanks to Messrs. Mayoh Ashiya, Kaiyu Fujiwara, Dai-Hua Jiang, Li-Che Hsu, Yun-Chi Chiang, and Hui-Ching Hsieh for their fine contributions to this dissertation work.

Finally, the author would like to express his deep gratitude for his family for their kind understanding, support, and encouragement throughout his study.

March 2022

Saburo Kobayashi

Contents

Chapter 1

General Introduction

1.1 π-Conjugated Polymers

Historically, polymers were used as insulators and dielectrics because of the lack of mobile electrons. For this reason, they possessed inefficient conductivity. Still, π-conjugated polyenes with alternating double and single bonds were theoretically conductive. In 1958, Natta synthesized polyenes (polyacetylenes) by polymerizing acetylene using a Ziegler-Natta catalyst,[1] but they were unstable, insoluble, and infusible; therefore, they were not studied for a long time. In 1977, Shirakawa et al. reported that a synthesized polyacetylene film exhibited high conductivity owing to chemical doping. [2–4]

Although polyacetylene exhibits high electrical conductivity, it is highly susceptible to degradation by oxygen and moisture, and thus its use is not practical. In recent research on electrically conductive polymers, *π*-conjugated polymers including poly(p-phenylene), poly(p-phenylene vinylene), and polyfluorene polycarbazole, polypyrrole, and polythiophene have been widely employed because of their aromatic main chains that are highly resistant to oxidation in air. [5–10]

Polypyrrole is stable in air and can be polymerized in aqueous solutions; hence, it has been used in polymer solid electrolytic capacitors and biosensors.[11,12] Additionally, polythiophene has been used in organic photovoltaics (OPVs),[13–15] organic field-effect transistors (OEFTs), [16–18] and sensor materials [19] owing to its thermal and environmental stabilities. Polyphenylene, polyfluorene, and polycarbazole have been used in organic light-emitting diodes (OLEDs) [20, 21–24, 31,32] and organic memory devices [25-30, 33, 34] because of their high fluorescence quantum yields, thermal stabilities, and hole mobilities in addition to possessing good solubilities in common organic solvents (Figure 1-1).

In addition to their oxidation stability, *π*-conjugated polymers with aromatic main chains are lightweight. They have been used in processes such as coatings while contributing to the miniaturization, weight reduction, and performance enhancement of electronic devices.[35]

When combined with printing technology, they will bring about a significant revolution in printable electronics, a bottom-up technology different from conventional electronic device fabrication technology. [36–38]

π-conjugated polymers usually possess alkyl groups on their side chains, which increase their solubility in common organic solvents. However, despite a long alkyl chain, π-conjugated polymers aggregate due to the strong π-π stacking interaction. This leads to the deterioration of the electrical and fluorescent properties.[39,40] There is a need for technology for molecularly oriented π-conjugated polymers. Nanoconfinement strategies have been proposed to achieve the molecular orientation of conjugated polymers. For example, π-conjugated polymer-containing block copolymers (conjugated BCP) have been employed to create microphase-separated structures, in which the π-conjugated polymer chains are confined and arranged in the microdomain. Furthermore, polymer blending and electrospinning approaches have been used to achieve molecular orientation. [41–44]

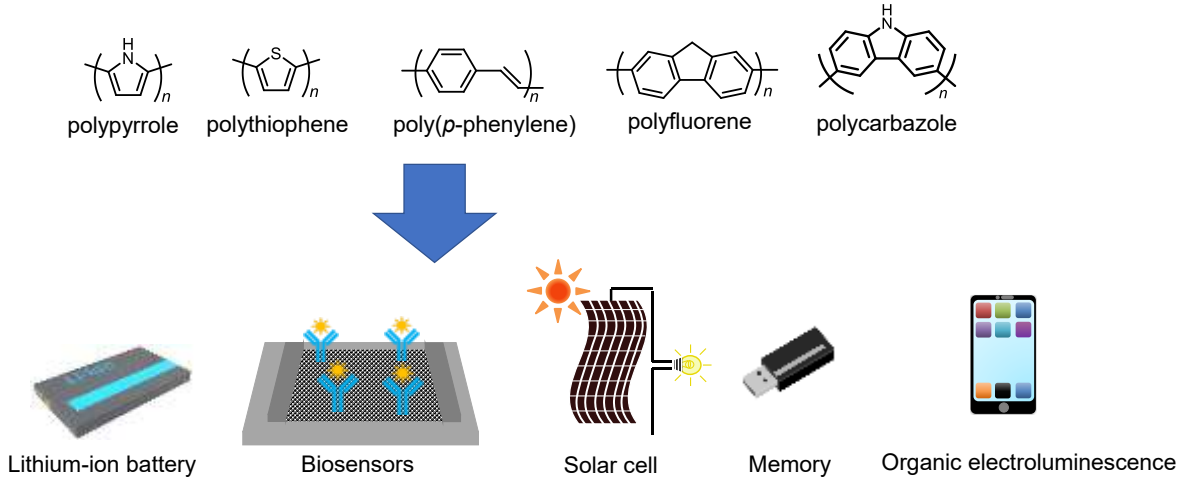

Figure 1-1. π-Structures of conjugated polymers and their applications.

1.2 π-Conjugated Polymer-Containing Block Copolymers

1.2.1 Electronic Devices Based on π-Conjugated Polymers

Among the methods used to molecularly orient π-conjugated polymers, the use of BCP is highly attractive. BCPs consist of two or more covalently linked polymers, which generally exhibit self-assembly properties. The solubility differences of the polymer segment cause them to spontaneously repel each other, resulting in micellar aggregates in a selective solvent and microphase-separated structures in the solid state.[45–48] The microphase separation of BCP has been widely studied for application in next-generation nanotechnology because it can construct dense periodic structures at the nanometer scale. [49–52] The conjugated BCPs are composed of π-(rigid "rod segment") and non-π-conjugated polymers (flexible "coil segment"). Among the BCPs, conjugated BCPs provide self-assembled structures different from conventional coil-coil BCPs because of the π–π stacking interaction and chain rigidity. [53–58] The device applications of conjugated BCPs have been reported in recent years.[59]

Chen et al. have created OFET consisting of a BCP of poly(3-hexylthiophene) (P3HT) and syndiotactic polypropylene (sPP). They measured the field-effect mobility of this device and found that it was 30-fold higher than that of homo P3HT. This was due to the self-assembly of BCPs, which improved the packing of the P3HT segments (Figure 1-2A).[60]

Segalman et al. reported that BCPs composed of poly(diethylhexyloxy-phenylenevinylene) (PPV) and poly(vinyl oxadiazole) (OX) self-assembled into lamellar structures with microphase-separated structures both parallel and perpendicular to the electrode (Figure 1-2B). Furthermore, OLED devices fabricated from this BCP showed 2.7 times higher efficiency and brightness than OLEDs made from pure PPV or a blend of two similar homopolymers. The improved performance with microphase separation mainly resulted from the maximum effective interfacial area between the electron-and hole-transporting domains, which facilitated exciton formation.[61]

Fréchet et al. used a BCP consisting of P3HT and perylene diimide (PDI) as a compatibilizer for the P3HT and PDI blend as the active layer of OPVs (Figure 1-2C). They measured the external quantum efficiency (EQE) of the OPVs with and without the compatibilizer and found a 3% increase compatibilizer was used. Adding the compatibilizer to the mixture of P3HT and PDI reduced the interfacial tension and decreased the domain size.[62] Conjugated/elastic BCPs that combine π-conjugated polymers with elastic materials, are expected to be used in stretchable modern electronic devices for stretchable transistors, [63–66] memories, [67–71] sensors,[72,73] and their integrated devices. [74–79] For example, Higashihara et al. reported triblock copolymers of P3HT/polyisobutylene (PIB),[80] and Chen et al. reported diblock and triblock copolymers of P3HT/poly(δ-decanolactone) (PDL) and diblock copolymers of PF/PDL as stretchable OFETs (Figure 1-3A, 3 B, and 3C).[18,29] In addition, Kuo et al. reported that diblock copolymers of PF/polybutyl acrylate (PBA) and diblock copolymers of PF/PDL are efficient touch-responsive OLEDs with mechanical durability (Figure 1-3C and 3D).[24,81]

As described above, conjugated BCPs dramatically improve the device performance over π-conjugated homopolymers by controlling the polymer orientation through self-assembly. Moreover, conjugated/elastic BCPs that combine π-conjugated polymers with elastic materials possesing mechanical strength made it possible to create stretchable electronic devices that maintain their respective properties.

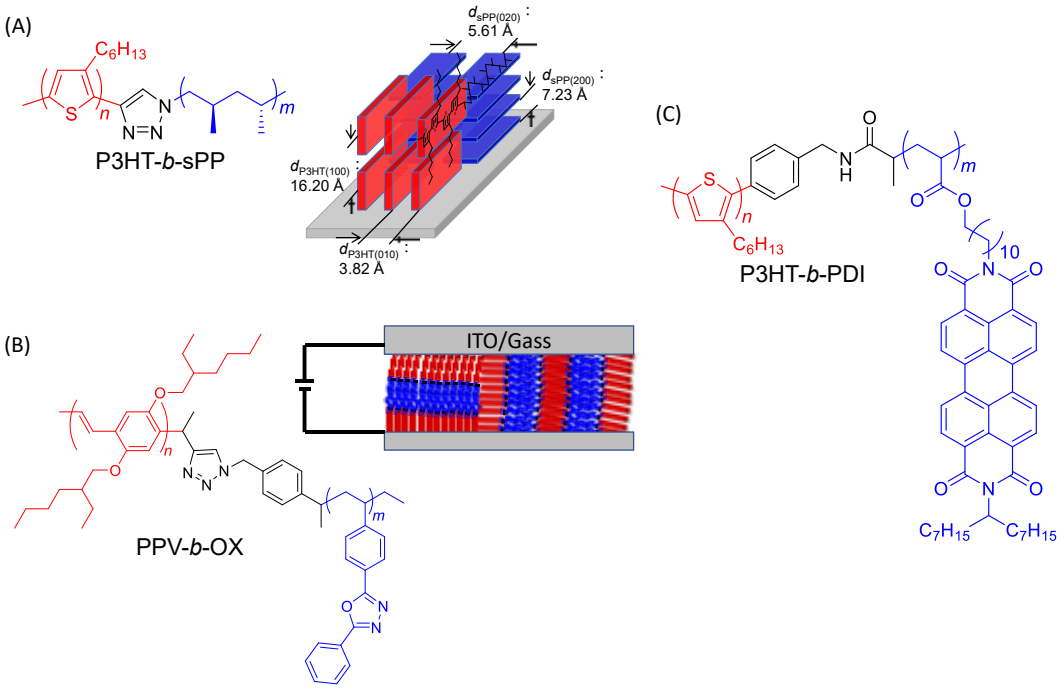

Figure 1-2. Electronic devices using P3HT and PPV-containing block copolymers.

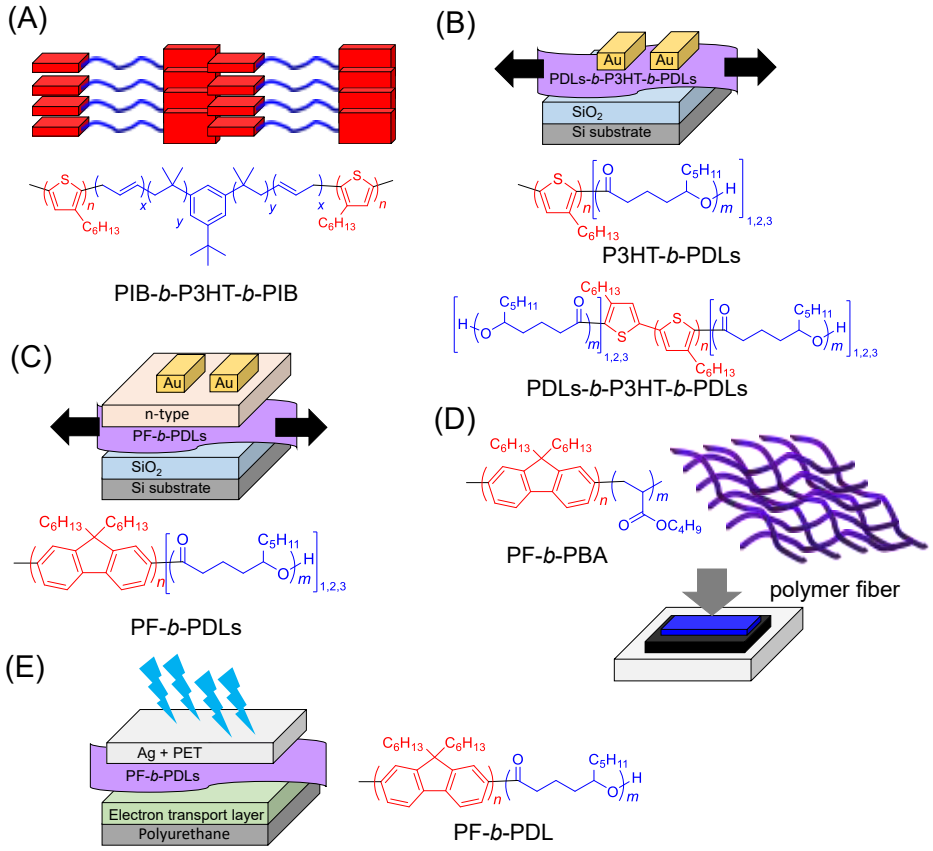

Figure 1-3. Stretchable electronic devices using conjugated BCPs.

1.2.2 Synthesis of π-Conjugated Polymer-Containing Block Copolymers

There are two ways to synthesize π-conjugated polymer-containing BCPs, the coupling and the macroinitiator method. In the coupling method, a pair of end-functionalized polymers are synthesized first and then linked by an end-to-end coupling reaction. The examples include condensation reactions such as esterification, and addition reactions, for instance, copper-catalyzed azido-alkyne cycloaddition and thiol-ene reaction (Figure 1-4A).[82–94] This approach requires one reactant in excess to complete the reaction, making it difficult to isolate the product.

The macroinitiator method involves the advance synthesis of end-functionalized polymers and their use as initiators to elongate another polymer. This is extremely useful from a practical point of view because it avoids tedious purification to remove unreacted components. The macroinitiator approach using π-conjugated polymers as the macroinitiator (rod-type macroinitiator method) is limited to the combination of atom transfer radical polymerization (ATRP),[95–98], anionic ring-opening polymerization (ROP),[99,100] and reversible addition-fragmentation chain transfer (RAFT) polymerization [101] (Figure 1-4B). More complex polymer architectures, including rod-coil-rod triblock copolymers, are also inaccessible through the rod-type macroinitiator method. Furthermore, the rod-type macroinitiator method often has low solubility in organic solvents, making it challenging to grow coil segments. [102–105]

In contrast, the coil-type macroinitiator method has a high solubility in organic solvents, making it easier to grow the rod segment. Therefore, the coil-type macroinitiator method effectively overcame the limitations of the rod-type macroinitiator method. The coil-type macroinitiator method provides a convenient synthesis route for complex polymer structures, such as conjugated triblock, star, and graft copolymers, which previously required multiple synthetic steps to construct (Figure 1-4C).

As mentioned, the performance of polymeric electronic devices based on conjugated polymers can be dramatically improved by molecularly orienting *the* π-conjugated polymer

chains by the BCP self-assembly. It has been reported that the self-assembling structure varies depending on the architecture of the BCPs, which is remarkable from an academic point of view,[18,29,106] and it is expected that future research will focus on the relationship between polymer architectures and self-assembly properties. The conjugated BCPs had been synthesized by either the polymer-polymer coupling method or the macroinitiator method. A well-controlled polymerization system to produce well-defined π-conjugated polymers is essential, independent of the methods used.

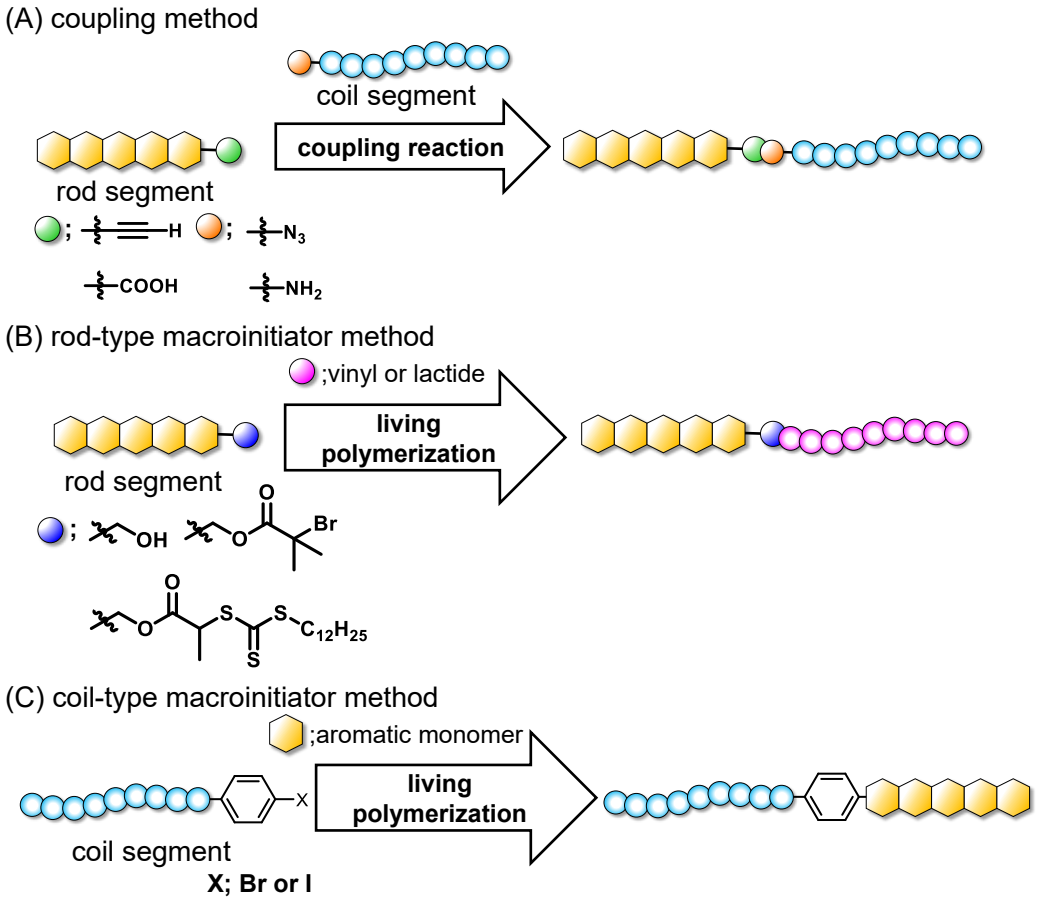

Figure 1-4. Synthesis of conjugated BCPs using approaches (A) coupling method, (B) rod-type macroinitiator method, and (C) coil-type macroinitiator method.

1.3 Controlled Polymerization of π-Conjugated Polymers

Synthesis methods of π-conjugated polymers can be broadly classified into two types, electrolytic and chemical polymerization. In the electrolytic polymerization method, monomers are oxidized or reduced on the electrode surface for polymerization, and chemical doping is performed. [107–110] As a result, polymer properties, including film thickness and doping amount, can be controlled by monomer concentration, electrolyte composition, the magnitude of applied voltage, and temperature. The main drawback of this method is the narrow application range of copolymerization.[111,112]

Chemical polymerization methods can be classified into chain- and step‐growth polymerization according to the polymerization mechanism.

In step-growth polymerization, π-conjugated polymers are synthesized by elementary reactions, including aromatic nucleophilic substitution,[113–116] aromatic electrophilic substitution,[117,118] transition metal-catalyzed coupling,[119–127] and oxidative coupling reactions. [128,129] Transition-metal-catalyzed coupling reactions (Suzuki-Miyaura coupling, Kumada-Tamao-Corriu coupling, and Negishi coupling) have shown exceptionally high reactivity and selectivity under mild conditions, and many π-conjugated polymers have been synthesized using this approach.

A variety of bifunctional monomers including aryl halide and arylboronic acid for Suzuki–Miyaura coupling, aryl halides, and aryl magnesium halides for Kumada–Tamao–Corriu coupling, and aryl halide and aryl zinc halide for Negishi coupling are commercially available and relatively easy to design and prepare. These bifunctional monomers are used to synthesize π-conjugated polymers through metal-catalyzed coupling reactions. The reaction must proceed quantitatively to obtain a high-molecular-weight material, and high-purity monomers must be used to ensure the 1:1 stoichiometry of the two monomers. The number of

reactive groups in the polymerization system decreases as the step-growth polymerization progresses, and intramolecular reactions of the linear polymer occur to produce cyclic polymers.[130–132] Therefore, it is challenging to synthesize polymers with distinct terminal structures in step-growth polymerization. Overall, it has been challenging to obtain π-conjugated polymers with well-defined structures and synthesize conjugated BCPs through a step-growth polymerization approach.

Chain-growth polymerization is advantageous for producing high molecular weights in a short time because the activated monomer reacts to the growing chain end promptly, one after another.[133,134] The precise synthesis of π-conjugated polymers is possible by using chain-growth polycondensation.

Conversely, McCullough and Yokozawa (2004) independently reported the precise synthesis of P3HT with high stereoregularity by Ni-catalyzed polymerization of a Grignard-type thiophene monomer.[135–137] The polymerization mechanism involves the transmetalation of two molecules of a Grignard-type thiophene monomer and a Ni catalyst to form a C–Ni–C bond. The Ni catalyst immediately reduces the dissociation and oxidation between the intramolecular C–Br bonds because of the weak C–Ni–C bond while being attracted to the electrons of the thiophene ring. The thiophene dimer generated in this reaction serves as the initiating species, and the condensation reaction proceeds via repeated transmetalation, reductive desorption, and oxidative addition. Notably, the Ni catalyst was inserted between the C and Br bonds of the same molecule without diffusion (Scheme 1-1). Therefore, the polymerization proceeds in a chain-growth rather than a step-growth manner, and this polymerization is known as catalyst-transfer chain polycondensation (CTP). In this polymerization method, all thiophene repeating units are bonded in a head-to-tail fashion, except the α-end, resulting in P3HT with high regioregularity.

CTPs based on Kumada–Tamao–Corriu coupling (KCTP) and Suzuki–Miyaura reaction (SCTP) [138–147] were previously reported; however, a variety of CTPs based on various coupling reactions have recently been described, for example, Negishi coupling,[148–151] Murahashi coupling,[152] Migita–Kosugi–Stille coupling,[153,154] and Sonogashira–Hagihara coupling.

Scheme 1-1. Polymerization mechanism of KCTP

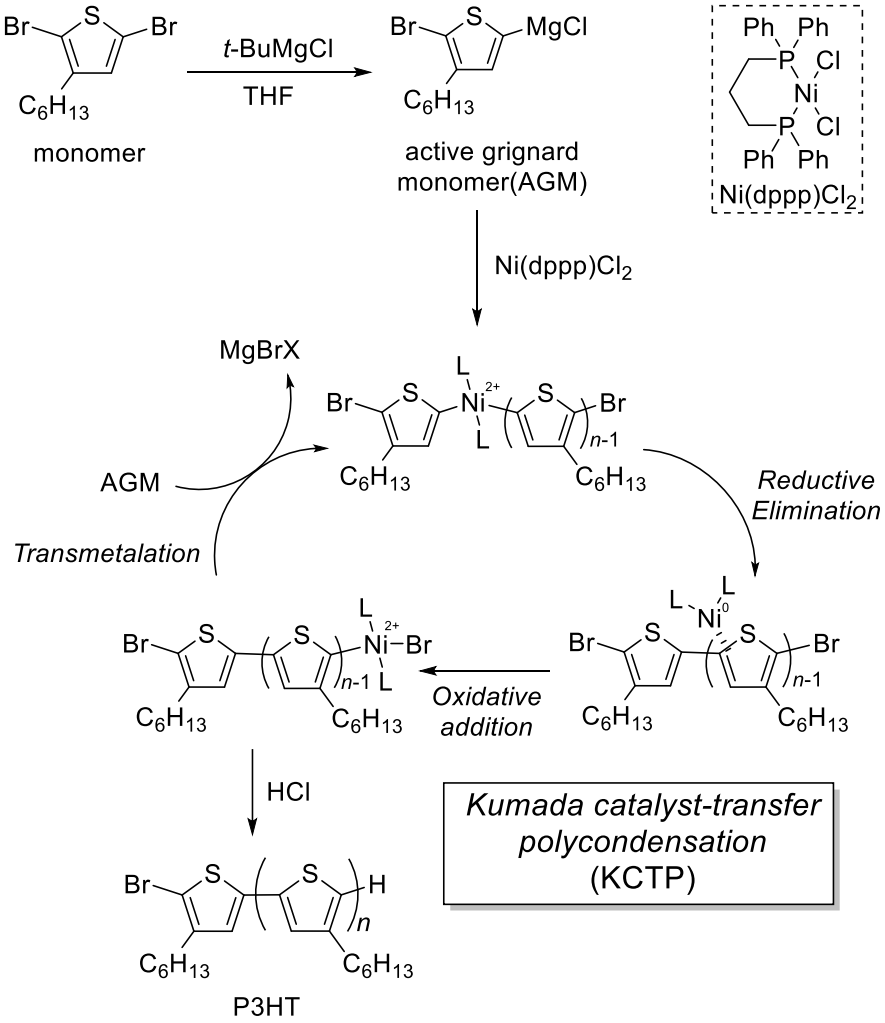

There are still many challenges and limitations associated with chain-growth polycondensation. Owing to the high reactivity and low functional group tolerance of Grignard reagents, it is challenging to introduce reactive groups, such as hydroxyl and amino groups, to the polymer chain ends. Therefore, monomers containing milder transmetalating agents than the Grignard reagents are required during polymerization. The organotin reagent (X–Ar–SnR_3) is probably the mildest coupling method used to date, although tin byproducts are toxic. Organoboron reagents have received increasing attention due to their excellent functional group tolerance and environmentally friendly by-products.

In 2006, Yokozawa et al. reported the first example of the chain-growth polymerization of fluorene monomer using the Suzuki–Miyaura coupling reaction.[141,142] Hu et al. synthesized end-functionalized PF by SCTP of a pinacolboronate-type fluorene monomer using iodobenzene *para*-substituted derivative (R–Ar–I)/$Pd_2(dba)_3$/*t*-Bu_3P as the initiator.[156–161] In the SCTP polymerization mechanism, the Pd-aryl complex of the initiator and the pinacolboronate-type fluorene monomer are transmetalated. The reductively desorbed Pd catalyst is attracted onto the electrons of the fluorene ring. At the same time, oxidative addition occurs between the intramolecular C–Br bonds, resulting in PF with an initiating terminal residue (Scheme 1-2).

Scheme 1-2. Polymerization mechanism of SCTP

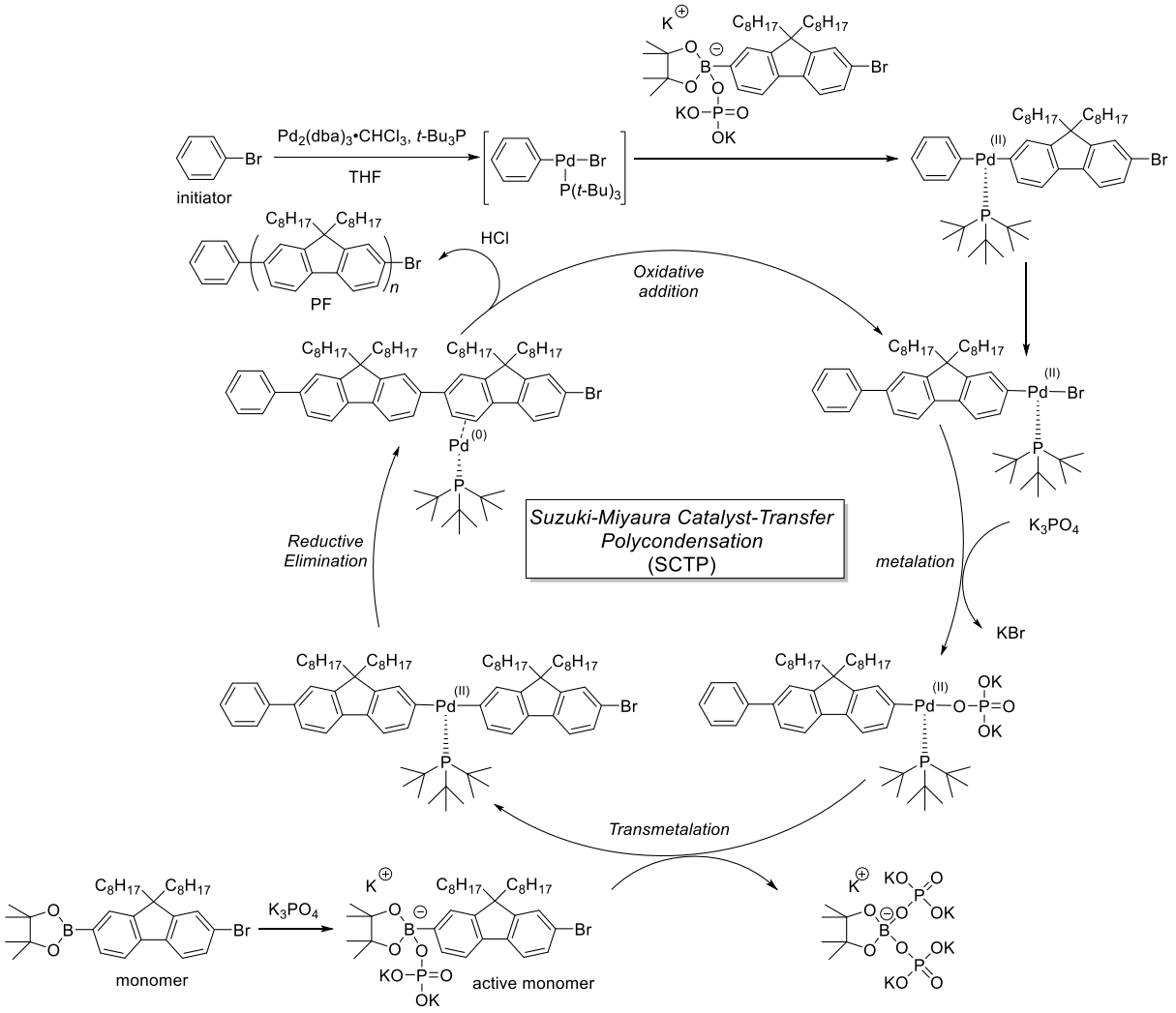

It is challenging to obtain hetero-π-conjugated polymers under the reported conditions using the SCTP method because of the progressive protodeboronation of heteroaromatic boronic acid monomers (Scheme 1-3).[162,163] For example, SCTP of pinacolboronate-type thiophene monomers produces polymers with wide dispersity. This is due to the competition between polymerization and protodeboronation.[164] This protodeboronation reaction is promoted by water and a base in the reaction mixture, although they are essential components for the coupling reaction.

Boronic acid C–B bonds are completely covalent and inert. [165–171] Nevertheless, by

adding a base to form a tetracoordination art complex, the nucleophilicity of the organic group increases, and transmetalation to the transition metal–X bond occurs. For this reason, the Suzuki–Miyaura coupling reaction must be carried out in the presence of a base. The use of trifluoroborate (RBF_3K), trihydroxyborate sodium salt ($RB(OH)_3Na$), triisopropylboronate ($RB(O\textit{i}\text{-}Pr)_3Li$), and tetraaryl borate (Ar_4B) has made it possible to carry out the Suzuki-Miyaura coupling reaction without a base. Many limitations still need to be addressed for synthesizing boronic acid derivatives (Figure 1-4).[172–175] Therefore, organoboron reagents do not require the addition of a base during the Suzuki-Miyaura coupling reaction and are easy to prepare.

Scheme 1-3 Base catalyzed protodeboronation of thiophen boronic acids

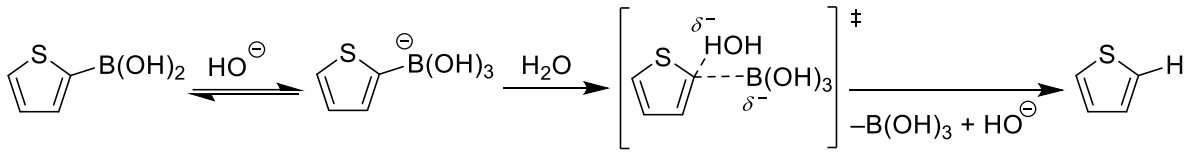

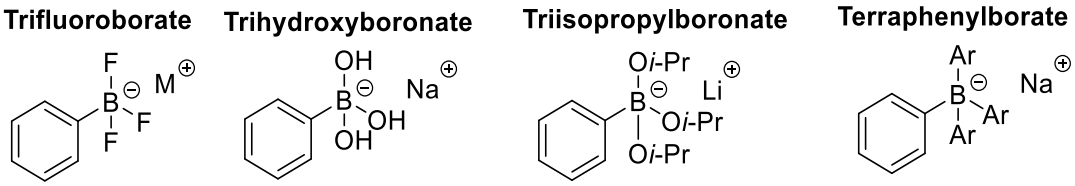

Figure 1-4. Most common boronates used in Suzuki–Miyaura coupling reaction.

1.4 Triolborate Salt

Miyaura and Yamamoto developed a triolborate salt soluble in organic solvents and stable in air and water. Triolborate salts can be easily synthesized from boronic acid or boronic acid ester (Scheme 1-4).[176,177] The Suzuki–Miyaura coupling reaction using triolborate salts proceeds even without the addition of water and base. It has also been reported that triolborate salts show high reactivity to heteroaromatic compounds, which are usually inactive for the Suzuki–Miyaura coupling reaction (Scheme 1-5).[178] As described above, triolborate salts provide higher nucleophilicity to the organic group than other boronic acid derivatives.[179] Additionally, adding water and base for the Suzuki–Miyaura coupling reaction is unnecessary. Thus, it is highly expected that the side reactions in the SCTP, protodeboronation, which limits access to high-molecular-weight and well-defined π-conjugated polymers, can be suppressed by employing the triolborate salt-type aryl monomer.[180]

Scheme 1-4. Synthesis of triolborate salts via boronic acid or a boronic acid ester

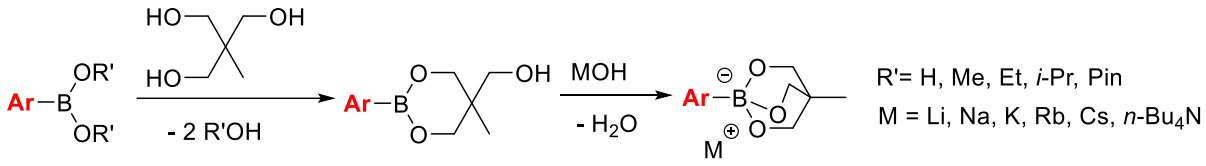

Scheme 1-5. The Suzuki–Miyaura coupling reaction using heteroaromatic triolborate salts

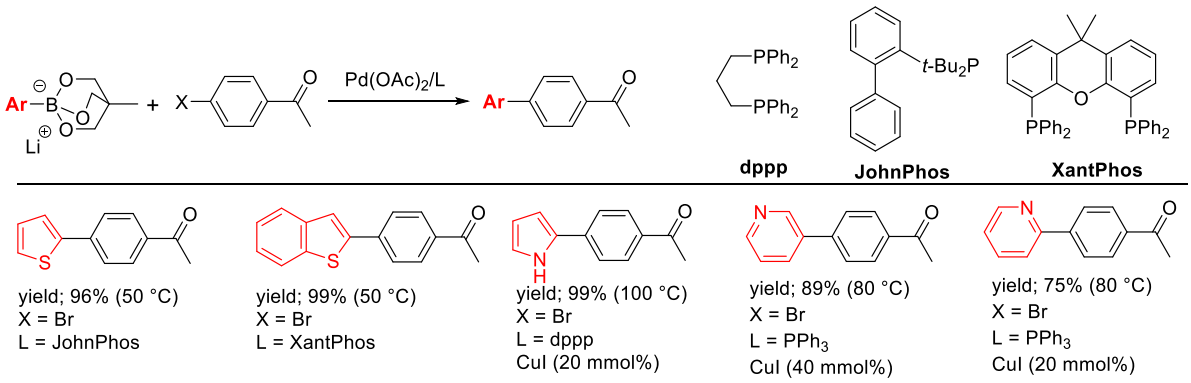

Yokozawa et al. investigated the synthesis of P3HT through SCTP of a triolborate lithium salt monomer (Scheme 1-6).[181] However, molecular weight control and end-functionalization were not achieved, and no successful SCTP of triolborate salt-type monomers was reported.

Scheme 1-6. Polymerization of triolborate lithium salt monomer

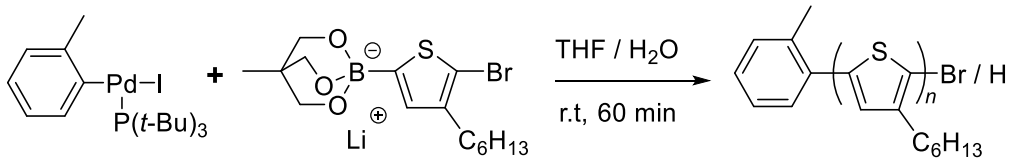

1.5 Objective and Outline of the Thesis

There is a need to synthesize π-conjugated polymers that are efficient and versatile from the perspective of organic electronics. The self-assembly of conjugated BCPs has further attracted attention to enhance electronic device performance. As described in Section 1.2, it is necessary to synthesize conjugated BCPs simple and high-yield manner. Most π-conjugated polymers are synthesized by step-growth polycondensation; however, it is difficult to control the molecular weight, dispersity, and end group using this method. Therefore, for the precise synthesis of end-functionalized π-conjugated polymers, CTPs using cross-coupling reactions as elementary reactions have been developed over the past 20 years.

SCTP is currently one of the most used methods for the precise synthesis of π-conjugated polymers. It has good functional group tolerance compared to other CTPs, allowing the introduction of various aryl monomers end-functional groups. There are very few reported examples of the SCTPs of heteroaromatic boronic acids. For example, the SCTP of pinacolboronate-type thiophene monomers gives rise to polymers with wide dispersity because of the competition between polymerization and protodeboronation. For the coupling method and rod-type macroinitiator method to prepare conjugated BCPs, it is necessary to precisely synthesize π-conjugated polymer segments with a reactive group at the chain end. In the case of conjugated BCP synthesis using the coil-type macroinitiator method, it is necessary to have high functional group tolerance and high initiation efficiency when the π-conjugated polymer is extended from the coil-type macroinitiator. At present, SCTP is the best choice for the synthesis of π-conjugated polymers in terms of the functional group. There is still room for improvement to achieve a precise synthesis of conjugated BCP.

It was envisioned that well-defined π-conjugated polymers could be synthesized by polymerizing triolborate salt-type monomers with higher nucleophilicity than other boronic acid derivatives. If the well-controlled SCTP can be achieved using the triolborate salt-type

monomers, it will be possible to easily synthesize not only conjugated linear diblock copolymers but also star block copolymers and graft copolymers, which have been difficult to synthesize in the past.

This thesis aims to establish an SCTP using triolborate salt-type monomers, which can be polymerized with a minimal amount of base and water and has higher nucleophilicity than boronic acid derivatives for the precise synthesis of conjugated BCPs. The polymerizability of triolborate salt-type monomers was investigated to synthesize PF as a π-conjugated polymer. Following this, PF-containing block and graft copolymers were synthesized via SCTP using various coil macroinitiators. SCTP of triolborate salt-type carbazole monomers was also carried out to investigate whether triolborate salt-type monomers are helpful for heteroaromatics. These developments will significantly advance the fabrication of high-quality π-conjugated polymers with unique structures and functions, ultimately contributing to the field of organic electronics.

An outline of the thesis is as follows.

Chapter 2 describes the SCTP of the triolborate-salt-type fluorene monomer potassium 2-(7-bromo-9,9-dihexyl-9*H*-fluorene-2-yl)triolborate (**M1**), which is an efficient and versatile approach for the precise synthesis of poly[2,7-(9,9-dihexylfluorene)]s (PFs). The SCTP of the triolborate salt-type monomer proceeded rapidly in a THF/H_2O mixed solvent at –10 °C with an iodobenzene derivative/$Pd_2(dba)_3$•$CHCl_3$/*t*-Bu_3P initiating system. Kinetic and post-polymerization experiments revealed that the reaction proceeded following the chain-growth and controlled/living polymerization mechanism. The most important feature of the present polymerization system is that only small amounts of base and water can sufficiently promote the reaction. This suppressed the side reaction and improved the initiation efficiency, enabling the synthesis of high-molecular-weight PFs (M_n = 5–80 kg mol^{-1}) with narrow dispersity ($Đ_M$ = 1.14–1.38) and α- and ω-end-functionalized PFs. Most importantly, PF-containing block and graft copolymers were successfully synthesized, beginning with various iodobenzene-functionalized macroinitiators; this was difficult to achieve using the conventional SCTP of pinacolboronate-type fluorene monomers (Figure 1-6).

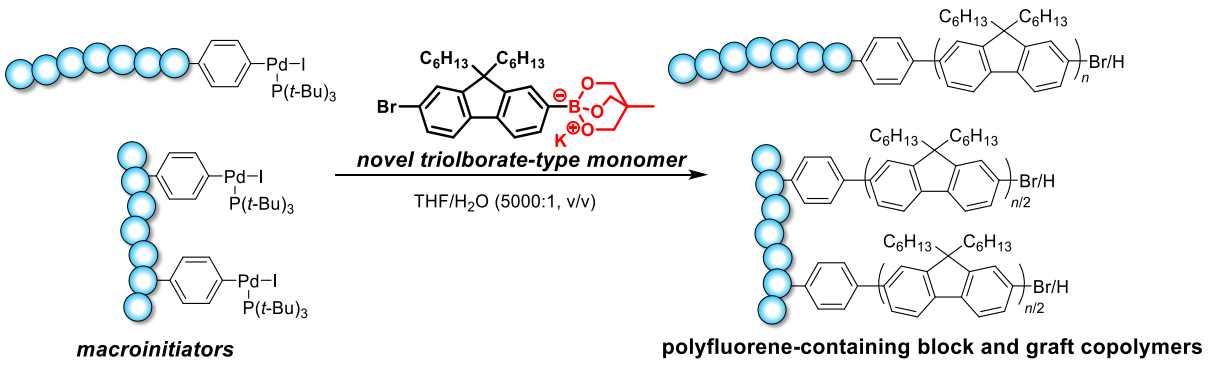

Figure 1-6. Synthesis of PF-containing BCPs using macroinitiators.

Chapter 3 describes the SCTP of triolborate salt-type carbazole monomers, that is, potassium 3-(6-bromo-9-(2-octyldodecyl)-9*H*-carbazole-2- yl)triolborate (**M3**) and potassium 2-(7-bromo-9-(2-octyldodecyl)-9*H*-carbazole-2-yl) triolborate (**M4**), as an efficient and versatile approach for the precise synthesis of poly[9-(2-octyldodecyl)-3,6-carbazole] (3,6-PCz) and poly[9-(2-octyldodecyl)-2,7-carbazole] (2,7-PCz). SCTP of the triolborate salt-type carbazole monomers was performed in a mixture of THF/H_2O using an initiating system consisting of 4-iodobenzyl alcohol, $Pd_2(dba)_3$•$CHCl_3$, and *t*-Bu_3P. Cyclic byproduct formation was confirmed in the SCTP of **M3**, as reported for the corresponding pinacolboronate-type monomer. By optimizing the reaction temperature and time, linear end-functionalized 3,6-PCz was successfully synthesized for the first time. The SCTP of **M4** proceeded with almost no side reactions, yielding 2,7-PCz with a functional initiator residue at the α-chain end. Kinetic and block copolymerization experiments demonstrated that the SCTP of **M4** proceeds in a chain-growth and controlled/living polymerization manner. This is a novel synthesis route of 2,7-PCz via SCTP. High-molecular-weight 2,7-PCzs (M_n = 5–38 kg mol^{-1}) with a relatively narrow $Đ_M$ (1.35–1.48) was achieved by taking advantage of the well-controlled nature of this polymerization system. Fluorene/carbazole copolymers and 2,7-PCz-containing diblock copolymers were successfully synthesized, demonstrating the versatility of the present polymerization system as a novel synthetic strategy for well-defined polycarbazole-based materials (Figure 1-7).

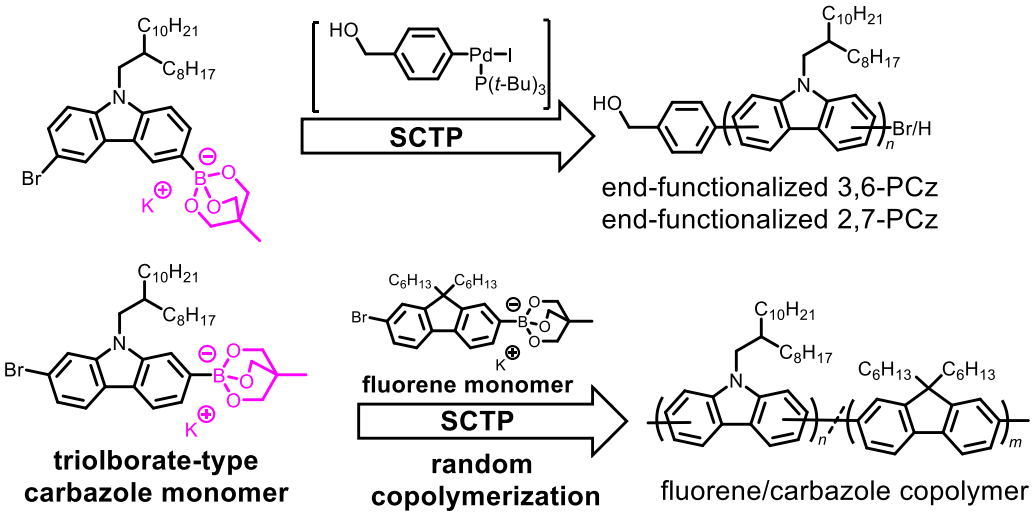

Figure 1-7. Synthesis of linear PCz and carbazole/fluorene copolymers using the triolborate salt-type monomer

Chapter 4 summarized the overall conclusions of this dissertation.

1.6 References

1. G. Natta, G. Mazzanti, P. Corradini, *Atti Acad. Naz. Lincei Cl. Sci. Fis. Mater. Nat. Rend*. **1958**, *8*, 25.
2. T. Ito, H. Shirakawa and S. Ikeda, *J. Polym.Sci., Polym.Chem. Ed*. **1974**, *12*, 11−20.
3. H. Shirakawa, E.J. Louis, A.G. MacDiarmid, C.K. Chiang and A. J. Heeger, *J Chem. Soc. Chem. Comm*. **1977**, *16*, 579−580.
4. C. K. Chiang, C. R. Fincher, Jr., Y. W. Park, A. J. Heeger, H. Shirakawa, E. J. Louis, S. C. Gau, and A. G. MacDiaemid, *Phys. Rev. Lett*. **1977**, *39*, 1098−1101.
5. A. D. Schluter, *In Handbook of Conducting Polymers*, 2 ed.; Marcel Dekker, INC. USA, **1998**, pp.209−224.
6. S. C. Maratti, In Handbook of Conducting Polymers; 2 ed.; Marcel Dekker, INC. USA, **1998**, pp. 343−362
7. U. W. F. Bunz, *In Handbook of Conducting Polymers*; 3 ed.; CRC Press: Boca Raton, FL, **2007**.
8. E. M. Genies, A. Boyle, M. Lapkowski, C. Tsintavis, *Synthetic Metals* **1990**, *36*, 139−182.
9. D. Curran, J. Grimshaw, S. Perera, *Chemical Society Reviews* **1991**, *20*, 391−404.
10. J. Roncali, *Chemical Reviews* **1992**, *92*, 711−738.
11. S. Asavapiriyanont, G. K. Chandler, G. A. Gunawardena, D. Pletcher, *J. Electroanal. Chem*. **1984**, *177*, 229−244.
12. N. C. Foulds, C. R. Lowe, *J. Chem. Soc. Faraday Trans. 1* **1986**, *82*, 1259−1264.
13. M. T. Dang, L. Hirsch, G. Wantz, J. D. Wuest, *Chem. Rev*. **2013**, *113*, 3734−3765.
14. S. Gunes, H. Neugebauer, N. D. Sariciftci, *Chem. Rev*. **2007**, *107*, 1324−1338.
15. M. T. Dang, L. Hirsch, G. Wantz, *Adv. Mater*. **2011**, *23*, 3597−3602.
16. J.-Yu. Lee, C.-J. Lin, C.-T. Lo, J.-C. Tsi, W.-C. Chen, *Macromolecules* **2013**, *46*, 3005−3014.
17. J.-T. Wang, S. Takashima, H.-C. Wu, Y.-C. Chiu, Y. Chen, T. Isono, T. Kakuchi, T. Satoh, W.-C. Chen, *Adv. Funct. Mater*. **2016**, *26*, 2695−2705.
18. L.-C. Hsu, S. Kobayashi, T. Isono, Y.-C. Chiang, B. J. Ree, T. Satoh and W.-C. Chen, *Macromolecules* **2020**, *53*, 7496−7510.
19. B. Li, G. Sauvé, M. C. Iovu, M. J.-EL, R. Zhang, J. Cooper, S. Santhanam, L. Schultz, J. C. Revelli, A. G. Kusne, T. Kowalewski, J. L. Snyder, L. E. Weiss, G. K. Fedder, R. D. McCullough, and D. N. Lambeth, *Nano Lett*. **2006**, *6*, 1598–1602.
20. A. C. Grimsdale, K. L. Chen, R. E. Martin, P. G. Jokisz, A. B. Holmes, *Chem. Rev*. **2009**, *109*, 897–1091.
21. J. H. Burroughes, D. D. C. Bardley, A. R. Brown, R. N. Marks, K. Mackay, R. H. Friend, P. L. Burns, and A. B. Holmes, *Nature* **1990**, *347*, 539−541.
22. M.-C. Choi, Y. Kim, and C.-S. Ha, *Prog. Polym. Sci*. **2008**, *33*, 581−630.
23. A. C. Grimsdale, K. L. Chan, R. E. Martin, P. G. Jokisz, and A. B. Holmes, *Chem. Rev*., **2009**, *109*, 897−1091.

24. D.-H. Jiang, S. Kobayashi, C.-C. Jao, Y. Mato, T. Isono, Y.-H. Fang, C.-C. Lin, T. Satoh, S.-H. Tung, and C.-C. Kuo, *Polymers* **2020**, *12*, 84−95.
25. Q.-D. Ling, D.-J. Liaw, C. Zhu, D. S.-H. Chan, E.-T. Kang, and K.-G. Neoh, *Prog. Polym. Sci*. **2008**, *33*, 917−978.
26. B. Cho, S. Song, Y. Ji, T.-W. Kim, and T. Lee, *Adv. Funct. Mater*. **2011**, *21*, 2806−2829.
27. Y.-C Chiu, C.-C. Shih, and W.-C. Chen, *J. Mater. Chem. C*. **2015**, *3*, 551−558.
28. J.-C. Hsu, A. Hirao, and W.-C. Chen, *J. Mater. Chem*. **2012**, *22*, 5820−5827.
29. L.-C. Hsu, T. Isono, Y.-C. Lin, S. Kobayashi, Y.-C. Chiang, D.-H. Jiang, C.-C. Hung, E. Ercan, W.-C. Yang, H.-C. Hsieh, K. Tajima, T. Satoh, W.-C. Chen, *ACS Appl. Mater. Interfaces* **2021**, *13*, 2932−2943.
30. Y.-C. Chen, Y.-C. Lin, H.-C. Hsieh, L.-C. Hsu, W.-C. Yang, T. Isono, T. Satoh and W.-C. Chem, *J. Mater. Chem. C*. **2021**, *9*, 1259-1268.
31. F. M. A. Hide, D. Garciäa, B.J. Schwartz, A.J. Heeger, *Acc. Chem. Res*. **1997**, *30*, 430–436.
32. A. C. Grimsdale, K. L. Chan, R. E. Martin, P. G. Jokisz, A. B. Holmes, *Chem. Rev*. **2009**, *109*, 897–1091.
33. P. Heremans, G. H. Gelinck, R. Müller, K.-J. Baeg, D.-Y. Kim, Y.-Y. Noh, *Chem. Mater*. **2010**, *23*, 341–358.
34. S. T. Han, Y. Zhou, V. A. L. Roy, *Adv. Mater*. **2013**, *25*, 5425–5449.
35. T. Yamamoto, *Macromol. Rapid Commun*. **2002**, *23*, 583–606.
36. W. Wu, *Nanoscale*, **2017**, *9*, 7342-7372.
37. C. C.-Raya, Z. Z. Denchev, S. F. Cruz, J. C. *Viana, Applied Materials Today* **2019**, *15*, 416–430.
38. Y.-R. Jang, S.-J. Joo, J.-H. Chu, H.-J. Uhm, J.-W. Park, C.-H. Ryu, M.-H. Yu, and H.-S. Kim, *International Journal of Precision Engineering and Manufacturing-Green Technology* **2021**, *8*, 327–363.
39. Y. H. Geng, D. Katsis, S. W. Culligan, J. J. Ou, S. H. Chen, L. J. Rothberg, *Chem Mater*. **2002**, *14*, 463−470.
40. J. Pei, X.-L. Liu, Z.-K. Chen, *Macromolecules* **2003**, *36*, 323-327.
41. Y.-C. Chiu, C.-C. Shih, W.-C. Chen, *J. Mater. Chem. C*. **2015**, *3*, 551−558.
42. A. P. Kulharni, S. A. Jenekhe, *Macromolecules* **2003**, *36*, 5285−5296.
43. Y.-C. Chiu, Y. Chen, T. Kakuchi, W.-C. Chen, *ACS Appl. Mater. Interfaces* **2012**, *4*, 3387−3395.
44. Y. Tian, W.-C. Chen, A. K.-Y. Jen, *Macromolecules* **2010**, *43*, 282−291.
45. G. Daniel, *Rev Environ Sci Biotechnol*. **2010**, *9*, 301−306.
46. J. Beilstein, *Nanotechnol*. **2018**, *9*, 2332−2344.
47. E. W. Cochran, C. J. G.-Cervera, G. H. Fredrickson, *Macromolecules* **2016**, *39*, 2449−2451.
48. H.-C. Kim, S.-M. Park, W. D. Hinsberg, *Chem. Rev*. **2010**, *110*, 146−177.
49. H.-F. Fei, W. Li, A. Bhardwaj, S. Nuguri, A. Ribbe and J. J. Watkins, *Chem. Soc*. **2019**, *141*, 17006−17014.
50. A. Rahman, P. W. Majewski, G. Doerk, C. T. Black and K. G. Yager, *Nature communications* **2016**,

13988−13995.

51. J. K. Kim, S. Y. Yang, Y. Lee and Y. Kim. *Progress in Polymer Science* **2010**, *35*, 1325−1349.
52. Y. Pang, X. Jin, G. Huang, L. Wan, and S. Ji, *Macromolecules* **2019**, *52*, 2987−2994.
53. H.-C. Kim, S.-M. Park, W. D. Hinsberg, *Chem. Rev*. **2010**, *110*, 146−177.
54. A. D. Cuendias, R.C. Hiorns, E. Cloutet, L. Vignauc, H. Cramaila, *Polym. Int*. **2010**, *59*, 1452−1476.
55. Y.-C. Chiu, C.-C. Shih, W.-C. Chen, *J. Mater. Chem. C.* **2015**, *3*, 551−558.
56. N. Surin, D. Marsitzky, R. Lazzaroni, P. Leclere, *Adv. Funct. Mater*. **2004**, *14*, 708−715.
57. P. Leclere, M. Surin, R. Lazzaroni, *Eur. Polym. J.* **2004**, *40*, 885−892.
58. C. L. Chochos, P. K. Tsolakis, J. K. Kallitsis, *Macromolecules* **2004**, *37*, 2502−2510.

59. C.-L. Liua, C.-H. Lina, C.-C. Kuo, S.-T. Linb, W.-C. Chen, *Progress in Polymer Science* **2011**, *36*, 603–637.
60. J.-Y. Lee, C.-J. Lin, C.-T. Lo, J.-C. Tsi, W.-C. Chen, *Macromolecules* **2013**, *46*, 3005−3014.
61. Y. F. Tao, B. Ma, R. A. Segalman, *Macromolecules* **2008**, *41*, 7152–9.
62. R. A. Segalman, B. McCulloch, S. Kirmayer, J. J. Urba, *Macromolecules* **2009**, *42*, 9205.
63. J. Y. Oh, S. R.-Gagné, Y.-C. Chiu, A. Chortos, F. Lissel, G.-J. N. Wang, B. C. Schroeder, T. Kurosawa, J. Lopez, T. Katsumata, J. Xu, C. Zhu, X. Gu, W.-G. Bae, Y. Kim, L. Jin, J. W. Chung, J. B.-H. Tok, Z. Bao, *Nature* **2016**, *539*, 411−415.
64. J.-T. Wang, S. Takshima, H.-C. Wu, C.-C. Shih, T. Isono, T. Kakuchi, T. Satoh, and W.-C. Chen, *Macromolecules* **2017**, *50*, 1442−1452.
65. C. Lu, W.-Y. Lee, C.-C. Shih, M.-Y. Wen, and W.-C. Chen, *ACS Appl. Mater. Interfaces* **2017**, *9*, 25522−25532.
66. J. Mun, G.-J. N. Wang, J. Y. Oh, T. Katsumata, F. L. Lee, J. Kang, H.-C. Wu, F. Lissel, S. R.-Gagné, J. B.-H. Tok, and Z. Bao, *Adv. Funct. Mater*. **2018**, *28*, 1804222−1804232.

67. J.-T. Wang, K. Saito, H.-C. Wu, H.-S. Sun, C.-C. Hung, Y. Chen, T. Isono, T. Kakuchi, T. Satoh, and W.-C. Chen, *NPG Asia Mater*. **2016**, *8*, 298−306.
68. L-C. Hsu, C.-C. Shih, H.-C. Hsieh, Y.-C. Chiang, P.-H. Wu, C.-C. Chueh and W.-C. Chen, *Polym. Chem*., **2018**, *9*, 5145–5154.
69. Y.-C. Chiang, S. Kobayashi, T. Isono, C.-C. Shih, T. Shingu, C.-C. Hung, H.-C. Hsieh, S.-H. Tung, T. Satoh and W.-C. Chen, *Polym. Chem*., **2019**, *10*, 5452–5464.
70. C.-C. Hung, S. Nakahira, Y.-C. Chiu, T. Isono, H.-C. Wu, K. Watanabe, Y.-C. Chiang, S. Takashima, R. Borsali, S.-H. Tung, T. Satoh, and W.-C. Chen, *Macromolecules* **2018**, *51*, 4966−4975.
71. C.-C. Hung, Y.-C. Chiu, H.-C. Wu, C. Lu, C. Bouilhac, I. Otsuka, S. Halila, R. Borsali, S.H. Tung, and W.-C. Chen, *Adv. Funct. Mater*. **2017**, *27*, 1606161−1606174.
72. J. T. Muth, D. M. Vogt, R. L. Truby, Y. Mengüç, D. B. Kolesky, R. J. Wood, J. A. Lewis, *Adv. Mater*. **2014**, *26*, 6307–6312.

73. S. Yao and Y. Zhu, *Nanoscale* **2014**, *6*, 2345–2352.
74. D. Son, J. Lee1, S. Qiao, R. Ghaffari, J. Kim, J. E. Lee, C. Song, S. J. Kim, D. J. Lee, S. W. Jun, S. Yang, M. Park, J. Shin, K. Do, M. Lee, K. Kang, C. S. Hwang, N. Lu, T. Hyeon and D.-H. Kim, *Nature nanotechnology* **2014**, *9*, 397–404.
75. J. Kim, D. Son, M. Lee, C. Song, J.-K. Song, J. H. Koo, D. J. Lee, H. J. Shim, J. H. Kim, M. Lee, T. Hyeon, and D.-H. Kim, *Sci. Adv*. **2016**, *2*, 1501101–1501110.
76. D. Son, J. H. Koo, J.-K. Song, J. Kim, M. Lee, H. J. Shim, M. Park, M. Lee, J. H. Kim, and D.-H. Kim, *ACS Nano* **2015**, *9*, 5585–5593.
77. T. Sekitani, H. Nakajima, H. Maeda, T. Fukushima, T. Aida, K. Hata, and T. Somey, *Nat. Mater*. **2009**, *8*, 494–499.
78. Y. Qian, X. Zhang, L. Xie, D. Qi, B. K. Chandran, X. Chen, and W. Huang, *Adv. Mater*. **2016**, *28*, 9243–9265.
79. T. Q. Trung and N.-E. Lee, *Adv. Mater*. **2017**, *29*, 1603167–1603196.
80. T. Higashihara, S. Fukuta, Y. Ochiai, T. Sekine, K. Chino, T. Koganezawa, and I. Osaka, *ACS Appl. Polym. Mater*. **2019**, *1*, 315−320.
81. D.-H. Jiang, B. J. Ree, T. Isono, X.-C. Xia, L.-C. Hsu, S. Kobayashi, K. H. Ngoi, W.-C. Chen, C.-C. Jao, L. Veeramuthu, T. Satoh, S. H. Tung, and C.-C. Kuo, *Chemical Engineering Journal* **2021**, *418*, 129421−129430.
82. T. Higashihara, K. Ohshimizu, A. Hirao, M. Ueda, *Macromolecules* **2008**, *41*, 9505−9507.
83. M. H. M. Cativo, D. K. Kim, R. A. Riggleman, K. G. Yager, S. S. Nonnrnmann, H. Chao, D. A. Bonnell, C. T. Black, C. R. Kagan, S.-J. Park, *ACS Nano* **2014**, *12*, 12755−12762.
84. K. Yoshida, J.-F. Chang, C.-C. Chueh, and T. Higashihara, *ACS Appl. Polym. Mater*. **2021**, *3*, 4450−4459.
85. C. S. Fisher, M. C. Baier, S. Mecking, *J. Am. Chem. Soc*. **2013**, *135*, 1148−1154.
86. Y. K. Kwon, and M. S. Kim, *Macromolecules* **2009**, *42*, 887−891.
87. H. H. Ahn and Y. K. Kwon, *Polymer* **2013**, *54*, 4864−4872.
88. P. Chen, G. Yang, T. Liu, T. Li, M. Wang, and W. Huang, *Polym. Int*., **2006**, *55*, 473−490.
89. Y.-C. Chiu, C.-C. Kuo, C.-J. Lin, and W.-C. Chen, *Soft Matter* **2011**, *7*, 9350−9358.
90. P. Leclere, M. Surin, and R. Lazzaroni, *Eur. Polym. J.* **2004**, *40*, 885−892.
91. Y.-C. Chiu, Y. Chen, C.-C. Kuo, S.-H. Tung, T. Kakuchi, and W.-C. Chen, *ACS Appl. Mater. Interfaces* **2012**, *4*, 3387–3395.
92. H.-C. Hsieh, C.-C. Hung, K. Watanabe, J.-Y. Chen, Y.-C. Chiu, T. Isono, Y.-C. Chiang, R. R. Reghu, T. Satoh, and W.-C. Chen, *Polym. Chem*. **2018**, *9*, 3820−3831.
93. C. S. Fisher, M. C. Baier, and S. Mecking, *J. Am. Chem. Soc*. **2013**, *135,* 1148−1154.
94. J.-T. Wang, K. Saito, H.-C. Wu, H.-S. Sun, C.-C Hung, Y. Chen, T. Isono, T. Kakuchi, T. Satoh and W.-C. Chen, *NPG Asia Materials* **2016**, *8*, 1−11.
95. J.-J. Li, J.-J. Wang, Y.-N. Zhou, and Z.-H. Luo, *RSC Adv*. **2014**, *4*, 19869−19877.

96. A. Bolonesi, F. Galeotti, U. Giovanella, F. Bertini, and S. Yunus, *Langmuir*, **2009**, *25*, 533−5338.
97. S. Huber, and S. Mecking, *Macromolecules* **2019**, *52*, 5917−5924.
98. B. Y.-K. Fang, C.-L. Liu, C. Li, C.-J. Lin, R. Mezzenga, and W.-C. Chen, *Adv. Funct. Mater*. **2010**, *20*, 3012−3024.
99. I. Botiz and S0 B. Darling, *Macromolecules* **2009**, *42*, 8211−8217.
100. K. Saito, T. Isono, H.-S. Sun, T. Kakuchi, W.-C. Chen and T. Satoh, *Polym. Chem*. **2015**, *6*, 6959–6972.
101. A.-N. A.-Duong, C.-C Wu, Y.-T. Li, Y.-S. Huang, H.-Y. Cai, I J. Hai, Y.-H. Cheng, C.-C. Hu, J.-Y. Lai, C.-C. Kuo, and Y.-C. Chiu, *Macromolecules* **2020**, *53*, 4030−4037.
102. S. Kang, R. J. Ono, C. W. Bielawski, *J. Polym. Sci., Part A: Polym. Che*m. **2013**, *51*, 3810−3817.
103. L.-M. Gao, Y.-Y. Hu, Z.-P. Yu, N. Liu, J. Yin, Y.-Y Zhu, Y. Ding, Z.-Q. Wu, *Macromolecules* **2014**, *47*, 5010−5018.
104. X. Yu, K. Xiao, J. Chen, N. V. Lavrik, K. Hong, B. G. Sumpter, D. B. Geohegan, *ACS Nano* **2011**, *5*, 3559−3567.
105. H.-N. Choi, H.-S. Yang, J.-H. Chae, T.-L. Choi, and I.-H. Lee, *Macromolecules* **2020**, *53*, 5497−5503.
106. M. H. M. Cativo, D. K. Kim, R. A. Riggleman, K. G. Yager, S. S. Nonnrnmann, H. Chao, D. A. Bonnell, C. T. Black, C. R. Kagan, S.-J. Park, *ACS Nano* **2014**, *12*, 12755−12762.
107. Y. Cao, A. Andreatta, A. J. Heeger, P. Smith, *Polymer* **1989**, *30*, 2305−2311.
108. J. Huang, R. B. Kaner, *Angew. Chem.* **2004**, *116*, 5941−5945.
109. A. F. Diaz, K. K. Kanazawa, *J. Chem. Soc., Chem. Commun*. **1979**, *14*, 635−636.
110. T. Ohsaka, Y. Ohnuki, N. Oyama, *J. Electroanal. Chem.* **1984**, *161*, 399−405.
111. T. Yijie, C. Haifeng, Z. Zhaoyang, X. Xiaoqian, Z. Yongjiang, *J. Electroanal. Chem*. **2013**, *689*, 142−148.
112. L. Baoyang, K. Lin, S. Zhen, S. Ming, H. Liu, H. Gu, S. Chen, J. Xu, *Synth. Met*. **2016**, *220*, 202−207.
113. Y. Imai, M. Ueda, and M. li, *J. Polym. lett. Ed*. **1979**, *17*, 85−89.
114. Y. Wamg, K. P. Chen, and A. S. Hay, *J. Polym. Sci., Part A: Polym. Chem*. **1996**, *34*, 375.
115. Y. Imai, M. Ueda, and K. Otaira, *J. Polym. lett. Ed*. **1977**, *15*, 457−461.
116. D. S. Thomopson, L. J. Markoski, and J. S. Moore, *Macromolecules* **1999**, *32*, 4764−4768.
117. A. Fritz and R. W. Rees, *J. Polym. Sci., Part A-1* **1972**, *10*, 2365−2378.
118. M. Zolotukhin, S. Fomine, R. Salcedo and l. Khalilov, *Chem. Commum*. **2004**, 1030−1031.
119. A. D. Schluter, *J. Polym. Sci.: Part A: Polym. Chem*. **2001**, *39*, 1533−1564.
120. T. Yamamoto, *Macromol. Rapid Commun*. **2002**, *23*, 583−606.
121. F. Babudri, G. M. Farinola, F. J. Naso, *Mater. Chem*. **2004**, *14*, 11−34.
122. G. Barbarella, M. Melucci, G. Sotgiu, *Adv. Mater*. **2005**, *17*, 1581−1593.
123. H. Katayama, M. Nagao, R. Moriguchi, F. Ozawa, *J. Organomet. Chem*. **2003**, *676*, 49−54.
124. H. Katayama, M. Nagao, T. Nishimura, Y. Matsui, K. Umeda, K. Akamatsu, T. Tsuruoka, H. Nawafune, F. Ozawa, *J. Am. Chem. Soc*. **2005**, *127*, 4350−4353.
125. H. Katayama, K. Taniguchi, M. Kobayashi, T. Sagawa, T. Minami, F. Ozawa, *J. Organomet. Chem*. **2002**, *645*, 192−200.

126. M. Agao, K. Asano, K. Umeda, H. Katayama, F. Ozawa, *J. Org. Chem*. **2005**, *70*, 10511−10514.
127. A. Hayashi, T. Yoshitomi, K. Umeda, M. Okazaki, F. Ozawa, *Organometallics* **2008**, *27*, 1022−1025.
128. V. Percec and H. Nava, *J. Polym. Sci., Part A: Polym. Chem*. **1988**, *26*, 783−785.
129. S. Amou, K. Takeuchi, M. Asai, K. Niizeki, T. Okada, M. Seino, O. Haba, and M. Ueda, *J. Polym. Sci., Part A: Polym. Chem*. **1999**, *37*, 3702−3709.
130. W. H. Carothers, *J. Am. Chem. Soc*. **1929**, *51*, 2548−2559.
131. P. J. Flory, *Chem. Rev*. **1946**, *39*, 137−197.
132. H. R. Kricheldorf, M. Rabenstein, M. Maskos, and M. Schmidt, **Macromolecules 2001**, *34*, 713−786.
133. H. Weissbach, S. Pestka, *Molecular Mechanism of Protein Biosynthesis, Academic Press* **1977**.
134. E. Bermek, *Mechanism of Protein Synthesis. Structure-Function Relations, Control Mechanisms, and Evolutionary Aspects*, Springer-Verlag **1985**.
135. Loewe, R. S.; Ewbank, P. C.; Liu, J.; Zhai, L.; McCullough, R. D. *Macromolecules* **2001**, *34*, 4324−4333.
136. Yokozawa, T.; Yokoyama, *A. Chem. Rev.* **2009,** *109*, 5595−5619.
137. Miyakoshi, R.; Yokoyama, A.; Yokozawa, T. *J. Am. Chem. Soc.* **2005**, *127*, 17542−17547.
138. H. G. Kuivila, J. F. Reuwer, J. A. Mangravite, *J. Am. Chem. Soc*. **1964**, *86*, 2666−2670.
139. M. Jayakannan, J. L. J. Van Dongen, R. A. J. Janssen, *Macromolecules* **2001**, *34*, 5386−5393.
140. M. Jayakannan, X. Lou, J. L. J. Van Dongen, R.A.J. Janssen, *J. Polym. Sci. Part A: Polym. Chem.* **2005**, *43*, 1454−1462.
141. A. Yokoyama, H. Suzuki, Y. Kubota, K. Ohuchi, H. Higashimura, and T. Yokozawa, *J. Am. Chem. Soc*. **2007**, *129*, 7236−7237.
142. T. Yokozawa, and A. Yokoyama, *Chem. Rev*. **2009**, *109*, 5595−5619.
143. T. Yokozawa, R. Suzuki, M. Nojima, Y. Ohta, A. Yokoyama, *Macromol. Rapid Commun*. **2011**, *32*, 801−806.
144. R. Grisorio, P. Mastrorilli, G. P. Suranna, *Polym. Chem*. **2014**, *5*, 4304−4310.
145. A. Sui, X. Shi, H. Tian, Y. Geng, F. Wang, *Polym. Chem*. **2014**, *5*, 7072−7080.
146. J. A. Carrillo, M. J. Ingleson, M. L. Turner, *Macromolecules* **2015**, *48*, 979−986.
147. K. Kosaka, T. Uchida, K. Mikami, Y. Ohta, and T. Yokozawa, *Macromolecules*, **2018**, *51*, 364−369.
148. G. Koeckelberghs, D. Cornells, A. Persoons, T. Verbiest, *Macromol. Rapid Commun*. **2006**, *27*, 1132−1136.
149. T. Higashihara, E. Goto, *Polym. J.* **2014**, *46*, 381−390.
150. T. Higashihara, E. Goto, M. Ueda, *ACS Macro Lett*. **2012**, *1*, 167−170.
151. R. Tkachov, V. Senkovskyy, T. Beryozkina, K. Boyko, V. Bakulev, A. Lederer, K. Sahre, B. Voit, A. Kiriy, *Angew. Chem. - Int. Ed*. **2014**, *53*, 2402−2407.
152. K. Fuji, S. Tamba, K. Shono, A. Sugie, A. Mori, *J. Am. Chem. Soc*. **2013**, *135*, 12208−12211.
153. Y. Qiu, J. Mohin, C.-H. Tsai, S. Tristram-Nagle, R.R. Gil, T. Kowalewski, K.J.T. Noonan, *Macromol. Rapid Commun*. **2015**, *36*, 840−844.
154. K. Kosaka, Y. Ohta, T. Yokozawa, *Macromol. Rapid Commun*. **2015**, *36*, 373−377.

155. S. Kang, R.J. Ono, C.W. Bielawski, *J. Am. Chem. Soc*. **2013**, *135*, 4984−4987.
156. H.-H. Zhang, C.-H. Xing, and Q.-S. Hu, *J. Am. Chem. Soc*. **2012**, *134*, 13156−13159.
157. H.-H. Zhang, C.-H. Xing, G. B. Tsemo, and Q.-S. Hu. *ACS Macro Lett*. **2013**, *2*, 10−13.
158. H.-H. Zhang, Q.-S. Hu, and K. Hong. *Chem. Commun*. **2015**, *51*, 14869−14872.
159. H.-H. Zhang, C.-H. Xing, Q.-S. Hu, and K. Hong, *Macromolecules* **2015**, *48*, 967−978.
160. H.-H. Zhang, W. Peng, J. Dong, and Q.-S. Hu. *ACS Macro Lett.* **2016**, *5*, 656−660.
161. J. Dong, H. Guo, and Q.-S. Hu. *ACS Macro Lett*. **2017**, *6*, 1301−1304.
162. J. J. L Alastair, C. L. J. Guy, *J. Chem*. **2010**, *50*, 664−674.
163. H. G. Kuivila, K. V. Nahabedian, *J. Am. Chem. Soc*. **1961**, *83*, 2159−2163.
164. T. Yokozawa, R. Suzuki, M. Nojima, Y. Ohta, A.o Yokoyama, *Macromol. Rapid Commun*. **2011**, *32*, 801–806.
165. Organic Synthesis via Boranes, Vol. 2 (Eds.: Brown, H. C.; Zaidlewicz, M.), Aldrich, Milwaukee **2001**.
166. Science of Synthesis, Houben-Weyl Methods of Molecular Transformations, Vol. 6 (Eds.: Kaufmann, D. E.; Matteson, D. S.), Thieme, Stuttgart **2005**.
167. Boronic Acids (Ed.: Hall, D. G.), Wiley-VCH, Weinheim **2005**.
168. N. Miyaura, A. Suzuki, *Chem. Rev*. **1995**, *95*, 2457−2483.
169. N. Miyaura, T*op. Curr. Chem*. **2002**. *219*, 11−59.
170. Organic Synthesis via Boranes, Vol. 3 (Eds.: Suzuki, A.; Brown, H. C.), Aldrich, Milwaukee **2003**.
171. Metal-Catalyzed Cross-Coupling Reactions, 2nd ed. (Eds.: Meijere, A.; Diederich, F.), Wiley-VCH, Weinheim **2004**, pp. 41−123.
172. S. Darses, J.-P. GenÞt, *Eur. J. Org. Chem*. **2003**, 4313−4327.
173. G. A. Molander, N. Ellis, *Acc. Chem. Res*. **2007**, *40*, 275−286.
174. A. N. Cammidge, V. H. M. Goddard, H. Gopee, N. L. Harrison, D. L. Hughes, C. J. Schubert, B. M. Sutton, G. L. Watts, A. J. Whitehead, *Org. Lett*. **2006**, *8*, 4071−7074.
175. J. A. Soderquist, K. Matos, A. Rane, Ramos, J. *Tetrahedron Lett*. **1995**, *36*, 2401−2402.
176. A. Fnrstner, G. Seidel, *Tetrahedron* **1995**, *51*, 11165−11176 51.
177. Y. Yamamoto, M. Takizawa, X.-Q. Yu, N. Miyaura, *Angew. Chem. Int. Ed*. **2008**, *47*, 928−931.
178. G.-Q. Li, Y. Yamamoto, N. Miyaura, *Tetrahedron* **2011**, *67*, 6804−6811.
179. S. Sakashita, M. Takizawa, J. Sugai, H. Ito, Y. Yamamoto, *Org. Lett.* **2013**, *15*, 4308−4311.
180. B. Guillaume, M. Biplab, K. Paul, M. Herbert, *Chem. Sci*. **2012**, *3*, 878–882.
181. K. Kosaka, Y. Ohta, T. Yokozawa, *Macromol. Rapid Commun*. **2015**, *36*, 373−377.

Chapter 2

Suzuki–Miyaura Catalyst-Transfer Polycondensation of Triolborate Salt-Type Fluorene Monomer

2.1 Introduction

Poly[2,7-(9,9-dialkylfluorene)]s (PFs) have attracted considerable attention for their applications in various organic electronic devices, such as sensors, organic photovoltaics (OPVs), organic field-effect transistors (OEFTs), organic light-emitting diodes (OLEDs) and organic memory devices,[10–13] because of their high fluorescence quantum yield, high thermal stability, high hole mobility, and good solubility in common organic solvents.[14,15] Many PFs have been synthesized through step-growth polycondensation based on various cross-coupling reactions (e.g., Suzuki–Miyaura coupling and Kumada–Tamao–Corriu coupling).[16–18] However, gaining control over the molecular weight and dispersity ($Đ_M$) of the synthesized polymers had been difficult owing to the step-growth nature of the polymerization. In 2007, Yokozawa's group reported the Suzuki–Miyaura catalyst-transfer polycondensation (SCTP) of an AB-type monomer with PhPd(*t*-Bu_3P)Br as the initiator, in which narrowly dispersed PFs were obtained (dispersity ≥ 1.33) with a controlled molecular weight. Thus, the SCTP is advantageous over the conventional step-growth polycondensation from the viewpoint of both polymerization and structural control. [19, 20] However, the reported SCTP methods require complicated reaction systems, consisting of a monomer, an initiator (e.g., iodobenzene or bromobenzene derivative), a catalyst (e.g., $Pd_2(dba)_3$), a ligand like *t*-Bu_3P, a solvent like THF, water, a base like K_3PO_4, and a phase-transfer catalyst like crown ether. [21–27] Therefore further expansion of the synthetic utility of SCTP is difficult.

For example, synthesis of PF-containing block copolymer (BCP) has been rarely achieved using the coil-type macroinitiator method, which might be partly attributed to the insufficient initiation efficiency and limited solubility of the macroinitiator in aqueous media. Previously, the PF-containing BCPs had been synthesized either by the coupling reaction of end-functionalized PF with other functionalized polymers (coupling method) or by chain extension from end-functionalized PF as the macroinitiator (rod-type macroinitiator method). In the former approach, it is necessary to add one of the components in excess to complete the reaction, which makes product isolation difficult (Figures 2-1A).[28–36] In contrast, the latter approach can avoid such complicated product isolation, making it more synthetically useful (Figures 2-1B). Nevertheless, the method using PF as the macroinitiator is limited to the combination with atom transfer radical polymerization (ATRP),[37–39] anionic ring-opening polymerization (ROP),[40] and reversible addition fragmentation chain transfer (RAFT) polymerization.[41] Since PF-containing block and graft copolymers are promising for a wide variety of device applications,[4,6,10,12,13,28–42] it is of great interest to realize the synthesis of block and graft copolymers via PF chain extension using various macroinitiators.

Therefore, establishing a simpler SCTP system for fluorene monomers is essential for the successful synthesis of PF-containing block and graft copolymers. In 2008, Miyaura and Yamamoto developed a triolborate salt soluble in organic solvents and stable in air and water, which could be used in Suzuki–Miyaura coupling, even without using water and base. Triolborate salts can be easily synthesized using boronic acid or a boronic acid ester.[43 44] In addition, the triolborate salts reportedly show higher reactivity to heteroaromatic compounds, which are usually inactive to Suzuki–Miyaura coupling.[45–47] Therefore, author envisioned that the SCTP of triolborate salt-type monomers could be performed using a simpler reaction system and eventually offer a drastic improvement in PF synthesis (Figure 2-1C).

In this chapter, the author investigated the SCTP of a triolborate salt-type fluorene monomer, i.e., potassium 2-(7-bromo-9,9-dialkyl-9*H*-fluorene-2-yl)triolborate (**M1**), aiming to

establish a novel precise synthesis strategy for high-molecular-weight and end-functionalized poly[2,7-(9,9-dihexylfluorene)]s. In the presence of a minimal amount of water, controlled/living polymerization of **M1** proceeded employing the chain-growth manner. Using optimized polymerization conditions, PFs with controlled molecular weights (4,800–69,400 g mol^{-1}) and a relatively narrow dispersity ($Đ_M$; 1.14–1.38) were successfully obtained. A variety of α- and ω-end-functionalized PFs were then synthesized by the SCTP using various functional initiators or terminators. The author efficiently synthesized PF-containing BCP as well as graft copolymers by SCTP using various macroinitiators, a task that has not been accomplished using conventional SCTP.

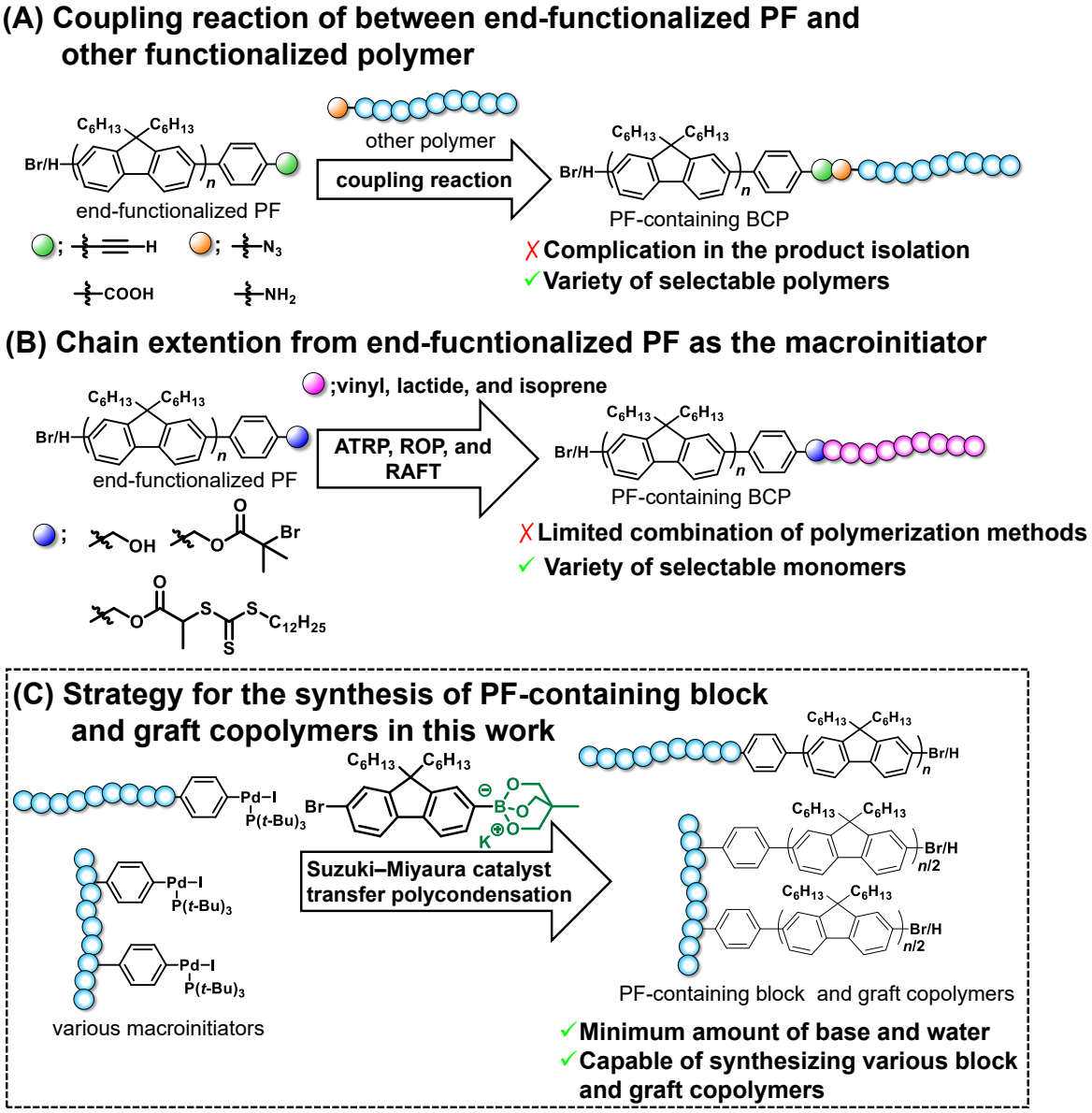

Figure 2-1. Schematic for the synthesis of the PF-containing block and graft copolymers. (A) Coupling reaction between end-functionalized PF and the other functionalized polymer. (B) Chain extension from end-functionalized PF as the macroinitiator. (C) Macroinitiator approach: Author strategy for the synthesis of PF-containing block and graft copolymers by SCTP of triolborate salt-type fluorene monomer.

2.2 Result and Discussion

2.2.1 Suzuki–Miyaura catalyst-transfer condensation polymerization of triolborate salt-type monomer

The author first attempted the polymerization of potassium 2-(7-bromo-9,9-dihexyl-9*H*-fluorene-2-yl)triolborate (**M1**) using the 4-iodobenzyl alcohol (**FI−CH$_2$OH**)/$Pd_2(dba)_3$•$CHCl_3$/*t*-Bu_3P initiating system employing a [**M1**]$_0$/[**FI−CH$_2$OH**]$_0$/[$Pd_2(dba)_3$•$CHCl_3$]/[*t*-Bu_3P] ratio of 15/1/0.3/2.2 at 20 °C in a THF/water (v/v) = 10/1 ([**M1**]$_0$ = 10 mmol L^{-1}) solvent (Scheme 2-1; run 1 in Table 2-1). Although the SCTP of **M1** proceeded, the obtained polymeric product ($M_{n,SEC}$ = 8,500 g mol^{-1}) has a relatively broad $Đ_M$ of 1.36. Nevertheless, encouraged by the promising result, author then attempted to thoroughly optimize the reaction conditions. To investigate the effect of the polymerization temperature, SCTP was carried out at −30, −10, and 0 °C without changing the other factors. At −30 °C (run 4), the product precipitated out during the polymerization. On the other hand, the products obtained at 0 and −10 °C (runs 2 and 3) exhibited narrower $Đ_M$ values of 1.33 and 1.18, respectively. This suggests that possible side reactions, such as chain transfer, were suppressed on lowering the polymerization temperature. Author also undertook SCTP at −10 °C with a small amount of added base (K_3PO_4), which resulted in a further improvement in the $Đ_M$ (run 5, $M_{n,SEC}$ = 4800 g mol^{-1} (THF), $Đ_M$ = 1.14), which can be attributed to the anion ligand exchange of the Pd complex occurring on the addition of the base that further facilitated the catalysis. These results confirmed the promising potential for the triolborate salt-type monomer to produce PFs with a narrow $Đ_M$ (~1.2).

The chemical structure of the obtained PF was characterized in detail by ^{1}H NMR and matrix-assisted laser desorption/ionization time-of-flight mass spectroscopy (MALDI-TOF MS). In the ^{1}H NMR spectrum of the product obtained from run 5 (Figure 2-2A), the major signals observed were due to the polyfluorene backbone (7.93–7.57 ppm: proton A) and hexyl side chain (2.12: proton B, 1.36–0.66 ppm: proton C and D), consistent with reported ^{1}H NMR

data. In addition, a minor signal due to the benzyl proton located at the α-chain end (proton E) was observed at 4.79 ppm, suggesting successful incorporation of the initiator residue. Therefore, the obtained product could be suggested to be the expected poly[2,7-(9,9-dihexylfluorene)] with a benzyl alcohol residue at the α-chain end (**HOCH$_2$−PF**). The number-average molecular weight ($M_{n,NMR}$) values of the **HOCH$_2$−PF (**run 5), calculated by end group analysis based on the ^{1}H NMR spectrum, was 4900 g mol^{-1}. To further confirm the end group fidelity, MALDI-TOF MS analysis was carried out on the obtained **HOCH$_2$−PF** (run 5). The MALDI-TOF MS spectrum showed one series of peaks with a regular interval of 333.46 Da corresponding to the 9,9-dihexylfluorene repeating units (Figure 2-2B). The observed peaks were assigned to the expected chemical structure of **HOCH$_2$−PF** having a benzyl alcohol moiety at the α-chain end and a hydrogen atom at the ω-end because a peak at m/z of 2101.57 matched well with the calculated mass for the 6-mer of **HOCH$_2$−PF** ($[M + H]^+$ = 2101.56 Da). Overall, the SCTP of **M1** was found to proceed in a controlled manner to produce narrowly dispersed PFs with sufficient end group fidelity.

Scheme 2-1. Synthesis of functionalized PFs by SCTP of the triolborate salt-type fluorene monomer

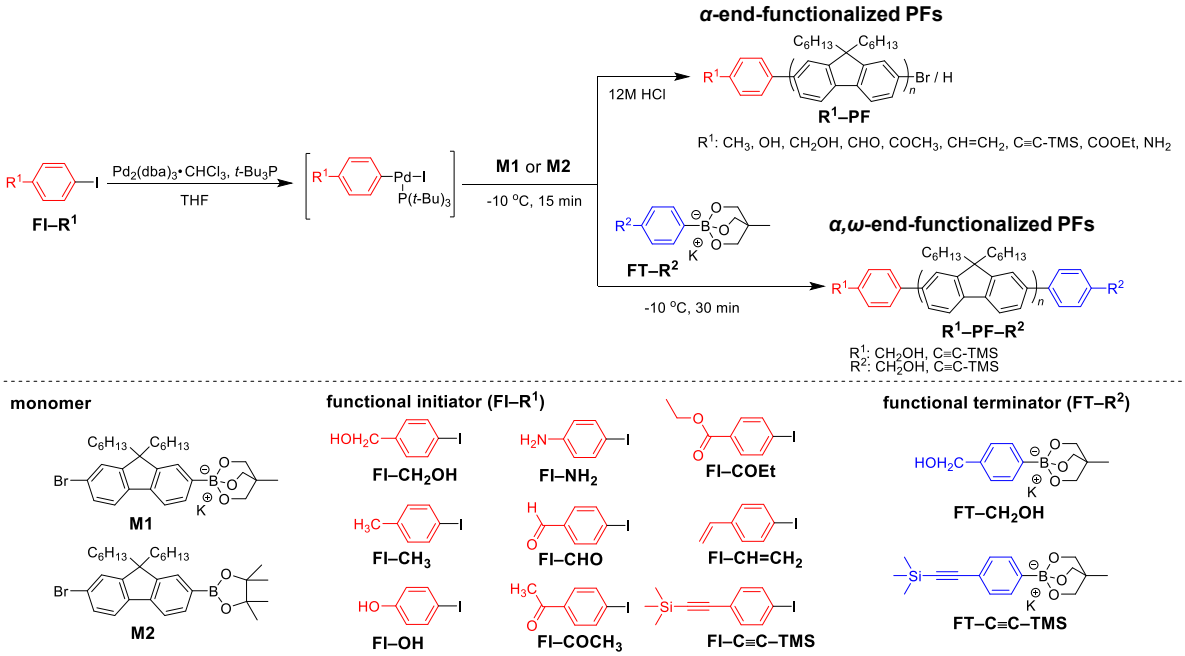

Table 2-1. SCTP of **M1** under various conditions [a]

run	[monomer]$_0$/[**FI−CH$_2$OH**]$_0$	temp (°C)	$M_{n,SEC}$ [b] (g mol^{-1})	$M_{n,NMR}$ [c] (g mol^{-1})	$Đ_M$ [b]	yield [d] (%)
1	15/1	20	8500	9500	1.36	80.3
2	15/1	0	8300	9200	1.33	85.2
3	15/1	−10	5700	5800	1.18	84.3
4	15/1	−30	—	—	—	—
5[e]	15/1	−10	4800	4900	1.14	84.2
6[e]	30/1	−10	10,000	12,600	1.24	83.2
7[e]	45/1	−10	14,200	17,800	1.25	84.3
8[e]	90/1	−10	25,700	29,400	1.28	85.4
9[e]	180/1	−10	44,700	68,300	1.37	82.6
10[e]	270/1	−10	69,400	83,300	1.38	88.9
11[f]	180/1	−10	24,000	26,700	1.48	86.9

[a]Polymerization conditions: Ar atmosphere; solvent, THF/water (v/v) = 10/1; [**M1**]$_0$ = 10 mmol L^{-1}; [**FI−CH$_2$OH**]$_0$/[Pd$_2$(dba)$_3$•CHCl$_3$]/[*t*-Bu$_3$P] = 1/0.3/2.2. [b]Determined by SEC (PSt standards, THF, 40 °C). [c]Determined by ^{1}H NMR spectrum in CDCl$_3$. [d]Isolated yields. [e]K$_3$PO$_4$ (1.5 equiv.) was added during the polymerization. [f]2-(7bromo-9,9-dihexyl-9*H*-fluorene-2-yl)4,4,5,5-tetramethyl-1,2,3dioxaborolane (180 equiv.), K$_3$PO$_4$ (2 mol L^{-1} aqueous, 150 equiv.), 18-crown-6 (50 equiv.).

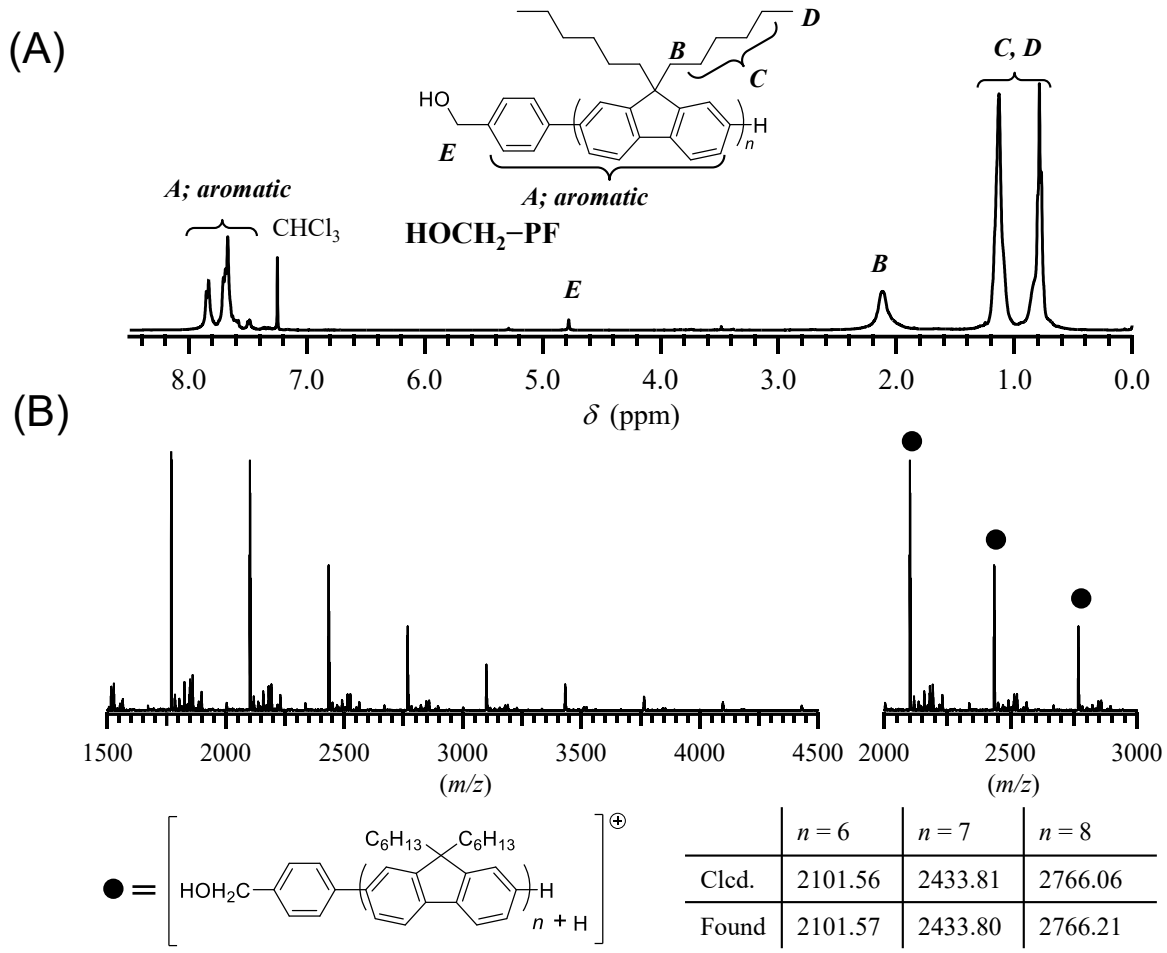

	n = 6	*n* = 7	*n* = 8
Clcd.	2101.56	2433.81	2766.06
Found	2101.57	2433.80	2766.21

Figure 2-2. (A) ^{1}H NMR spectrum of **HOCH$_2$−PF** obtained from run 5 in Table 2-1 (solvent, $CDCl_3$). (B) MALDI-TOF MS spectrum of **HOCH$_2$−PF** obtained from run 5 in Table 2-1.

2.2.2 Living nature of SCTP of triolborate salt-type monomer

The living nature of the SCTP of **M1** was assessed by a kinetic study and post-polymerization experiments. The time-conversion plot for the SCTP of **M1** under optimized conditions showed that monomer conversion (conv.) reached >99% in 10 min (Figure 2-3A). In addition, the $M_{n,NMR}$ of the obtained **HOCH$_2$−PF** increased linearly with increasing monomer conversion while the $Đ_M$s were maintained at less than 1.3 over the course of polymerization (Figure 2-3B). These results strongly suggested a chain-growth nature of polymerization. The kinetic plot revealed distinct first-order kinetic behavior, based on which the rate constant was estimated to be 0.42 s^{-1} mol L^{-1} (Figure 2-3C). The rate constant was 2.8 times greater than that of the conventional SCTP of the corresponding pinacolborate-type monomer, even though the author polymerization was carried out at a temperature 10 °C lower.[30,31] This demonstrates the excellent advantage of the present polymerization system over the conventional one.

The chain extension experiment was carried out to prove the livingness of the propagating chain end. Under the optimized conditions, the SCTP was initially conducted using a [**M1**]$_0$/[**FI−CH$_2$OH**]$_0$ ratio of 15/1 for 12 min to achieve full monomer conversion, affording an intermediate product with a $M_{n,NMR}$ of 11,500 g mol^{-1} and $Đ_M$ of 1.28. Then, an additional 15 eq. of **M1** was added to the reacting mixture for the second polymerization. Importantly, the added monomer was fully consumed, as confirmed by ^{1}H NMR analysis. The SEC traces of the products obtained after the first and second polymerizations are shown in Figure 2-3D, which demonstrates the shift in the elution peak maximum toward the higher-molecular-weight region after the second polymerization. This is strong evidence in favor of the second polymerization having been initiated from the living chain end. These results collectively suggest that polymerization of the triolborate salt-type monomer **M1** proceeded was a controlled/living polymerization that proceeded with the chain-growth mechanism.

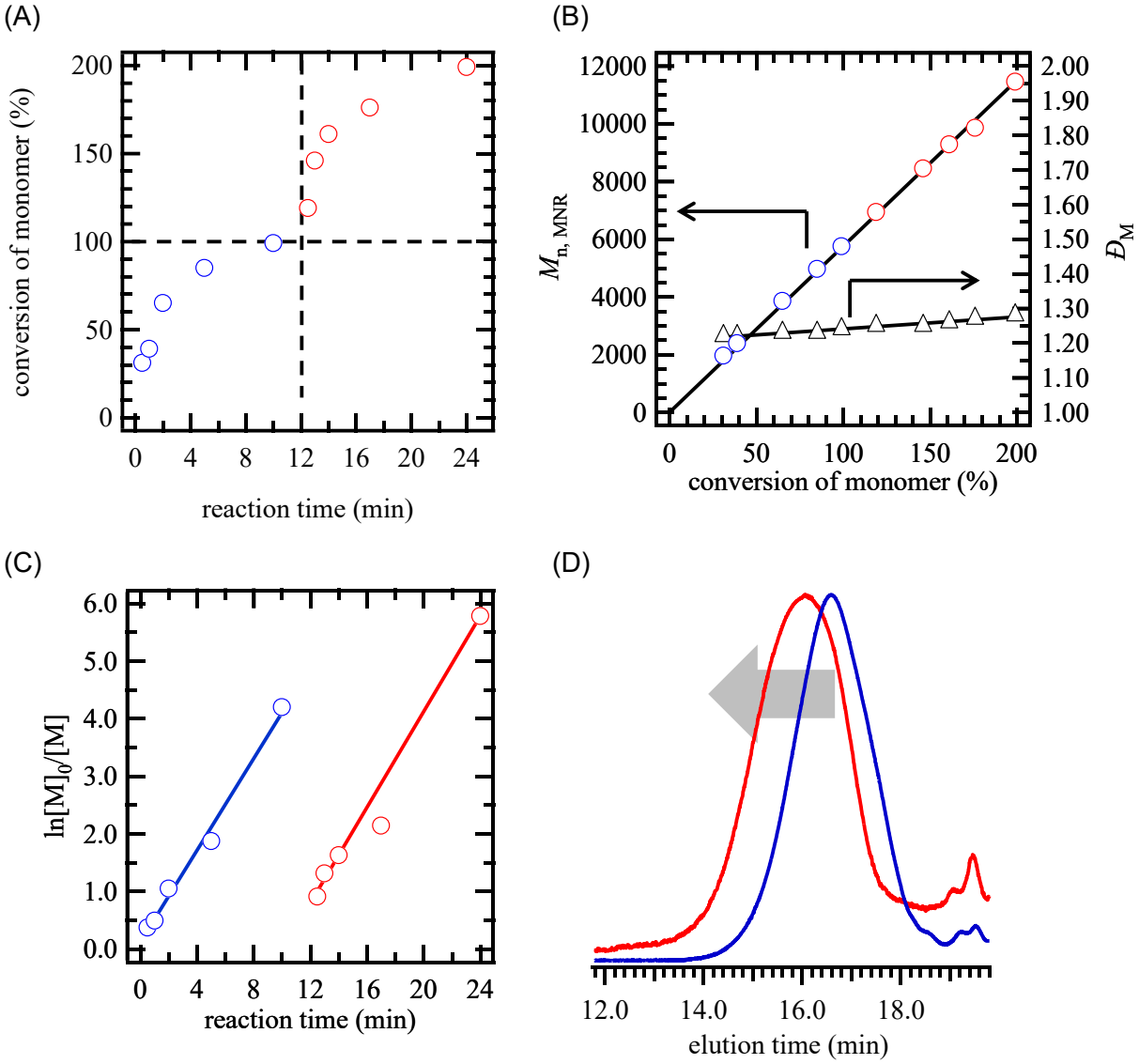

Figure 2-3. (A) Time against conversion plot (blue, first polymerization; red, post-polymerization) for SCTP of **M1** with [**M1**]$_0$/[**FI−CH$_2$OH**]$_0$/[$Pd_2(dba)_3$•$CHCl_3$]/[*t*-Bu_3P] ratio of 15/1/0.3/2.2 in THF/water (v/v) = 10/1 at −10 °C. (B) Dependence of $M_{n,NMR}$ (blue, first polymerization; red, post- polymerization) and $Đ_M$ (triangle, dispersity) on monomer conversion. (C) First-order kinetics plots for SCTP (blue, first polymerization; red, post-polymerization). (D) SEC traces of PFs obtained before (blue line) and after (red line) second polymerization (eluent, THF; flow rate, 1.0 mL min^{-1}).

2.2.3 Molecular weight control

With the optimized polymerization condition in hand, the SCTPs of **M1** were conducted by varying the [**M1**]$_0$/[**FI−CH$_2$OH**]$_0$ ratio (30/1 for run 6, 45/1 for run 7, 90/1 for run 8, 180/1 for run 9, and 270/1 for run 10) with the aim to synthesize PFs with higher molecular weights. As a result, PFs with $M_{n,SEC}$ and $Đ_M$ values of 10,000–69,400 g mol^{-1} and 1.24–1.38, respectively (runs 6–10, Table 2-1, $M_{n,NMR}$; 12,600–83,300 g mol^{-1}) were successfully obtained. It was confirmed that the highest molecular weight achieved by the present polymerization system was higher than that achieved by the SCTP of the pinacolboronate-type fluorene monomer so far (Figure 2-4). For comparison, we examined the polymerization of 2-(7bromo-9,9-dihexyl-9*H*-fluorene-2-yl)4,4,5,5-tetramethyl-1,2,3dioxaborolane (**M2**) as pinacolborate-type monomer, using the **FI−CH$_2$OH**/Pd$_2$(dba)$_3$•CHCl$_3$/*t*-Bu$_3$P/K$_3$PO$_4$/18-crown-6 initiating system for a [**M2**]$_0$/[**FI−CH$_2$OH**]$_0$ ratio of 180/1 at −10 °C in THF. However, the obtained **HOCH$_2$−PF** had a much lower $M_{n,SEC}$ (24,000 g mol^{-1}) as well as a broader $Đ_M$ (1.48) compared to those obtained in run 11, which could be attributable to chain transfer to the monomer. These results demonstrate that the triolborate salt-type monomer is better suited for the synthesis of higher-molecular-weight PFs. To the best of author knowledge, the PF obtained in run 10 ($M_{n,SEC}$ of 69,400 g mol^{-1}) has the highest molecular weight among PFs prepared by the chain-growth polycondensation approach.

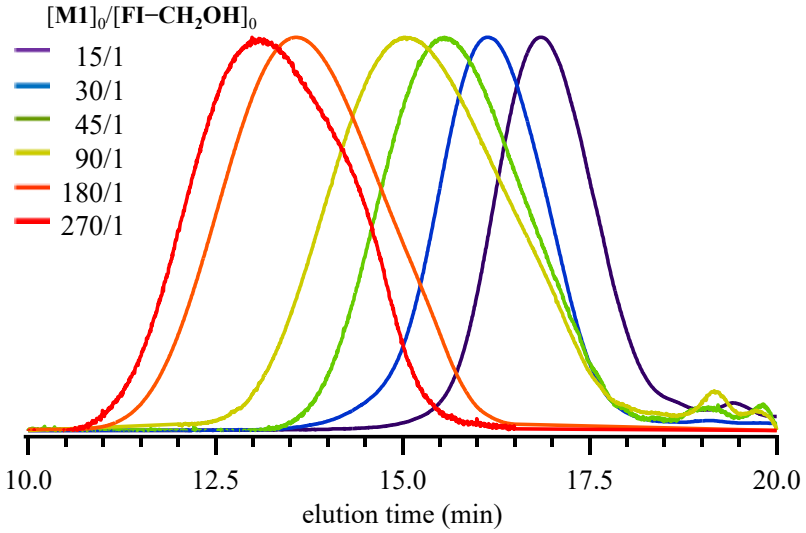

Figure 2-4. SEC traces of PF obtained using different $[\mathbf{M1}]_0/[\mathbf{FI{-}CH_2OH}]_0$ ratios (purple line, 15/1; blue line, 30/1; green line, 45/1; yellow line, 90/1; orange line, 180/1; red line, 270/1) detected by RI detector (eluent, THF; flow rate, 1.0 mL min^{-1}).

2.2.4 Synthesis of α-and ω-chain end-functionalized PFs using functional initiators and terminators

To make the present polymerization more useful and versatile as a general synthetic tool for producing PFs, it is quite important to achieve end functionalization, which is useful for block copolymer synthesis and grafting to solid surfaces or nanoparticles. Thus, author first performed the SCTP of **M1** using a variety of functional iodobenzene derivatives (**FI−CH$_3$**, **FI−OH**, **FI−NH$_2$**, **FI−CHO**, **FI−COCH$_3$**, **FI−COOEt**, **FI−CH=CH$_2$**, and **FI−C≡C−TMS**) as the initiator under the optimized reaction conditions ([**FI−R^1**]$_0$/[**M1**]$_0$ ratio of 1/15, in THF/H_2O = 10/1 (v/v), at −10 °C), leading to *α*-end-functionalized PFs (Table 2-2). All the polymerizations proceeded homogeneously and were quenched by adding 12 mol L^{-1} HCl. The $M_{n,SEC}$ and $Đ_M$ of the obtained PFs were 4400–7800 g mol^{-1} and 1.25–1.37 (Figure 2-5). In the ^{1}H NMR spectrum of the PF obtained using **FI−CH$_3$** (run 12), a characteristic signal appeared at 2.45 ppm due to the methyl protons of the tolyl group (proton **F**) along with major signals for the PF backbone (Figure 2-6). Similarly, ^{1}H NMR signals originating from the initiator residues were confirmed together with the those for the main chain of PF for the other products; the signals at 10.11 ppm (proton **G**) were due to the aldehyde proton of **FI−CHO**; those at 3.51 ppm (**H**) were due to the methyl protons of **FI−COCH$_3$**; those at 4.45 ppm (**I**) and 1.45 ppm (**J**) were due to the methylene and methyl protons of **FI−COOEt**; the ones at 5.93, 5.29, and 4.74 ppm (**K**, **L**, and **M**) were due to the olefin protons of **FI−CH=CH$_2$**; and those at 0.08 ppm (**N**) were due to the methyl protons of **FI−C≡C−TMS**, as seen in Figure 2-6.

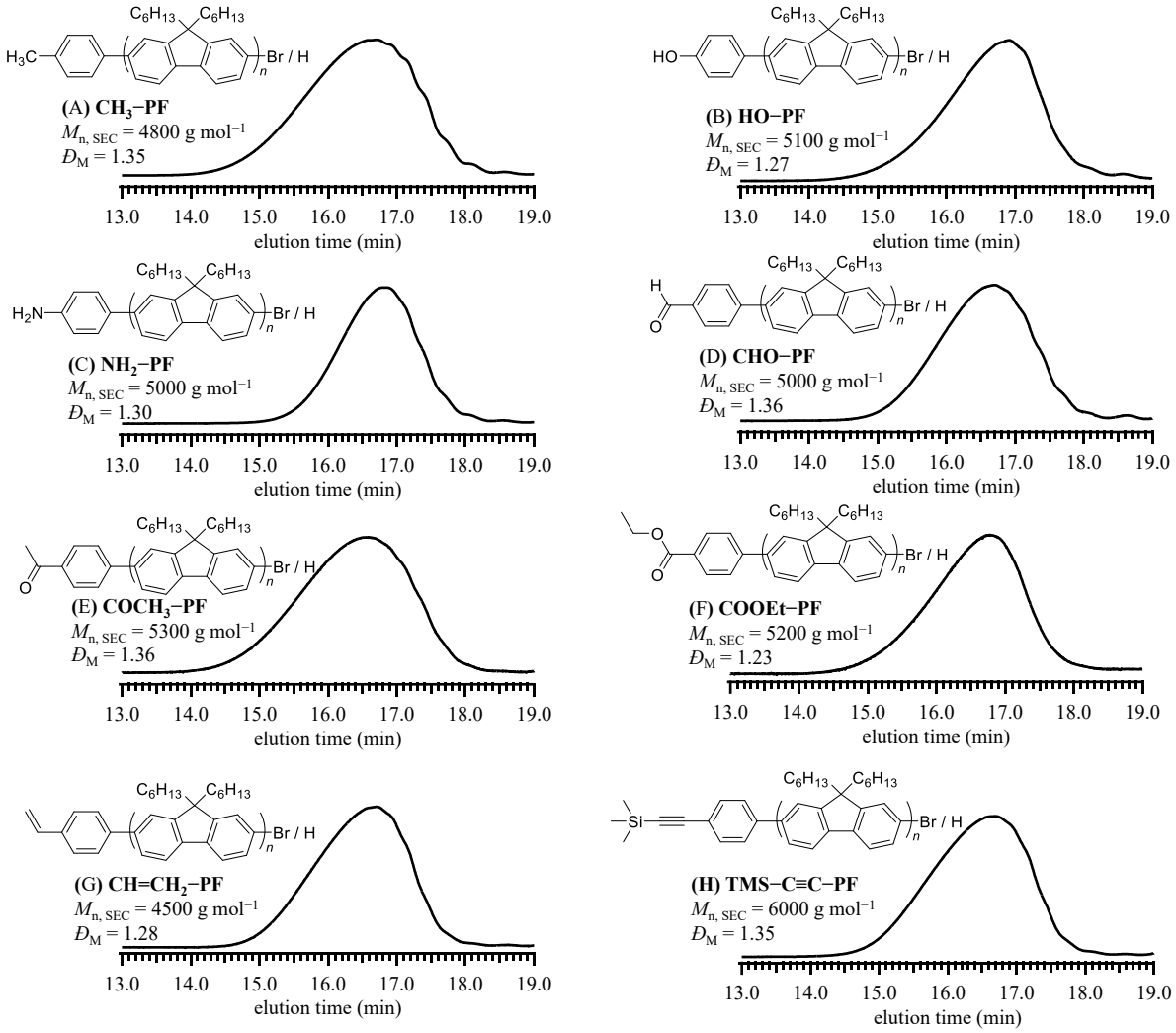

Figure 2-5. SEC traces of (A) **CH₃−PF**, (B)**HO−PF**, (C) **H₂N−PF**, (D) **OHC−PF**, (E) **CH₃CO−PF**, (F) **EtCOO−PF**, (G) **CH₂=CH−PF**, and (H) **TMS−C≡C−PF** (runs 12-19 in Table 2-2), detected by RI detector (eluent, THF; flow rate 1.0 mL min^{-1}).

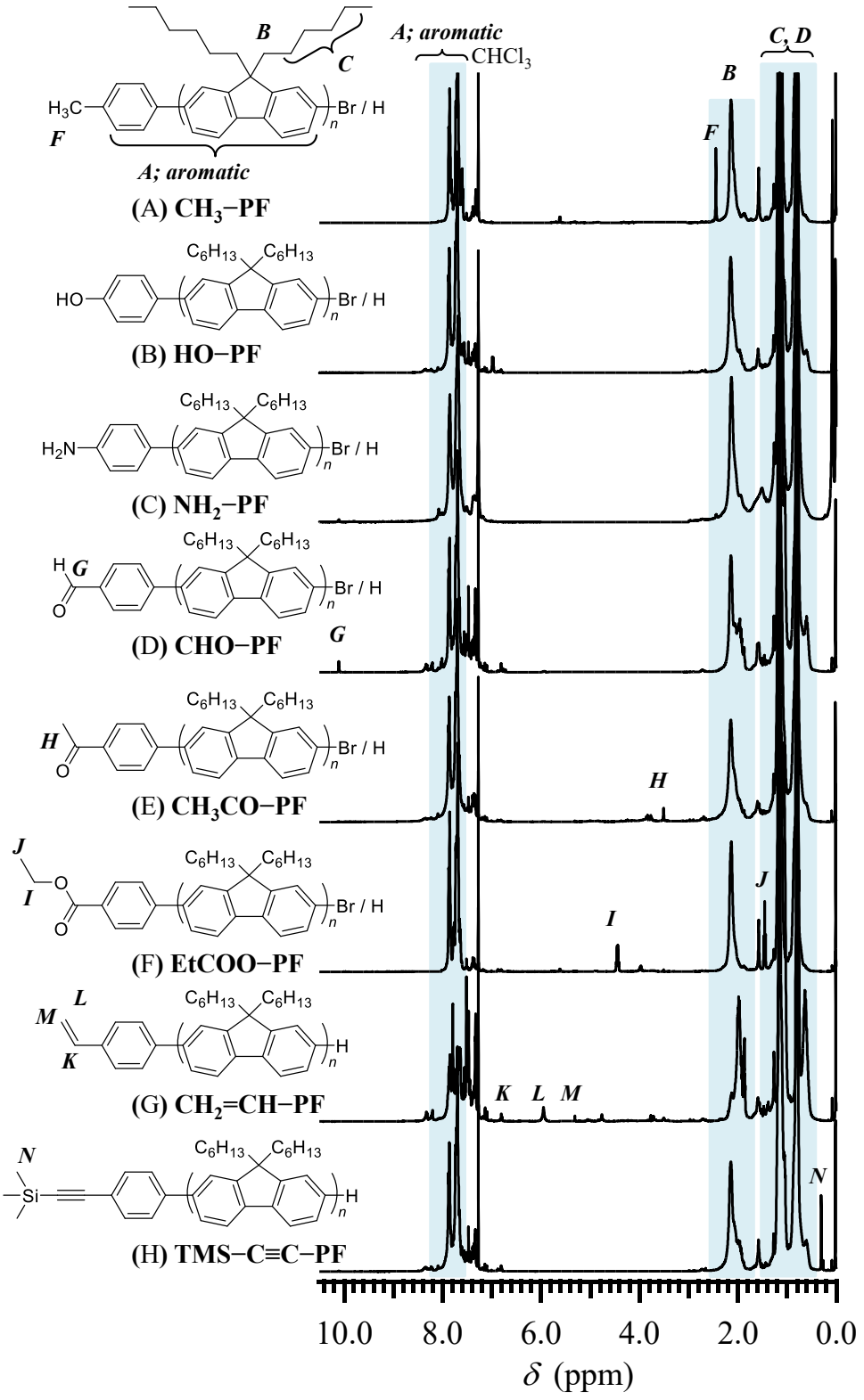

Figure 2-6. ^{1}H NMR spectra of (A) **CH_3−PF**, (B) **HO−PF**, (C) **H_2N−PF**, (D) **OHC−PF**, (E) **CH_3CO−PF**, (F) **EtCOO−PF**, (G) **CH_2=CH−PF**, and (H) **TMS−C≡C−PF** (runs 12-19 in Table 2-2) in $CDCl_3$.

In order to confirm the end group fidelity, author employed MALDI-TOF MS analysis. For the PF obtained using **FI−CH$_3$**, the MALDI-TOF MS spectrum exhibited two series of peaks with a regular interval of 333.11 Da (Figure 2-7A). The observed peaks denoted by closed circles were assigned to the expected chemical structure of **CH$_3$−PF** having a tolyl moiety at the *α*-chain end and a proton at the *ω*-chain end, since the peak at 2085.54 Da matched well with the calculated mass for the 6-mer of **CH$_3$−PF** ($[M+H]^+$ = 2085.57 Da). Although peaks due to the **CH$_3$−PF** with a bromine atom at the *α*-chain end were also observed (denoted by open circles), a tolyl group was always incorporated at the *α*-chain end. In the MALDI-TOF MS spectrum of the PFs obtained using **FI−OH**, **FI−NH$_2$**, **FI−CHO**, **FI−COCH$_3$**, **FI−COOEt**, **FI−CH=CH$_2$**, and **FI−C≡C−TMS** as the initiator, the peak for the 6-mer was observed at 20872.62, 2087.52, 2098.59, 2113.56, 2143.65, 2097.54, and 2168.60 respectively, all of which agreed well with the *m*/*z* values calculated for the corresponding 6-mer PF with a −OH, −CH_3, −NH_2, −CHO, −$COCH_3$, −COOEt, −$CH=CH_2$, and −C≡C−TMS group at the *α*-chain end (Figure 2-7). The MALDI-TOF MS analysis undoubtedly demonstrated that the obtained PFs were indeed the desired *α*-chain end tolyl-, phenol-, aniline-, aldehyde-, acetyl-, ethyl ester-, vinyl-, and trimethylsilylethynyl-functionalized PFs (**CH$_3$−PF**, **HO−PF**, **H$_2$N−PF**, **OHC−PF**, **CH$_3$CO−PF**, **EtCOO−PF**, **CH$_2$=CH−PF**, and **TMS−C≡C−PF**, respectively). More importantly, these results demonstrated the good functional group tolerance of the proposed SCTP process.

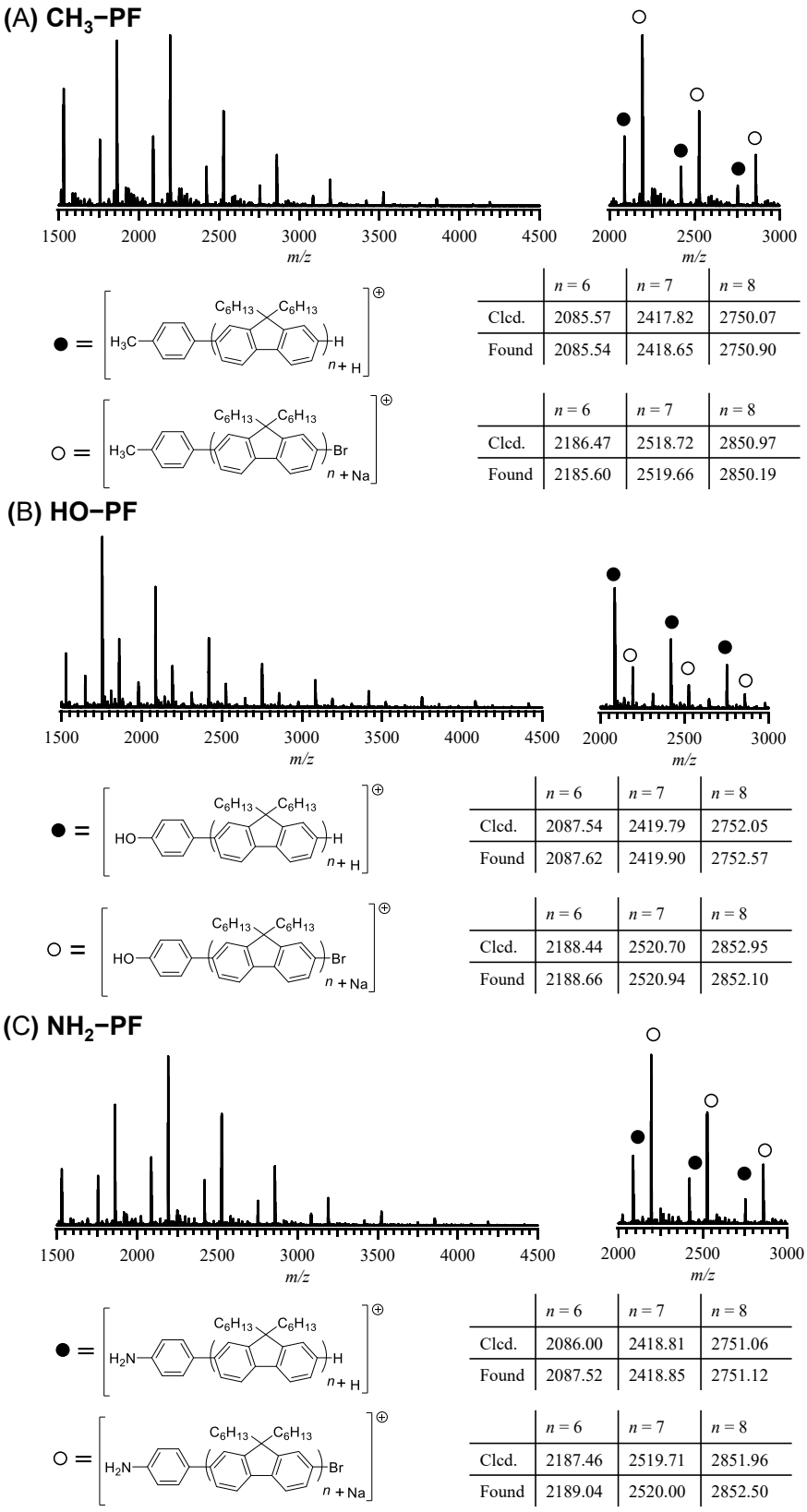

	n = 6	*n* = 7	*n* = 8
Clcd.	2085.57	2417.82	2750.07
Found	2085.54	2418.65	2750.90

	n = 6	*n* = 7	*n* = 8
Clcd.	2186.47	2518.72	2850.97
Found	2185.60	2519.66	2850.19

	n = 6	*n* = 7	*n* = 8
Clcd.	2087.54	2419.79	2752.05
Found	2087.62	2419.90	2752.57

	n = 6	*n* = 7	*n* = 8
Clcd.	2188.44	2520.70	2852.95
Found	2188.66	2520.94	2852.10

	n = 6	*n* = 7	*n* = 8
Clcd.	2086.00	2418.81	2751.06
Found	2087.52	2418.85	2751.12

	n = 6	*n* = 7	*n* = 8
Clcd.	2187.46	2519.71	2851.96
Found	2189.04	2520.00	2852.50

Figure 2-7 (continue)

(D) OHC−PF

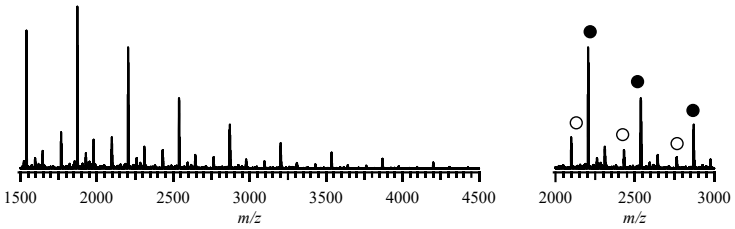

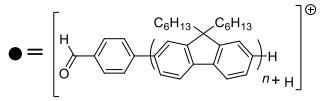

	n = 6	*n* = 7	*n* = 8
Clcd.	2098.57	2431.79	2764.05
Found	2098.59	2431.72	2763.29

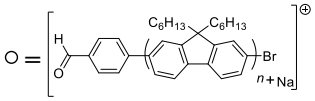

	n = 6	*n* = 7	*n* = 8
Clcd.	2200.44	2532.70	2864.68
Found	2201.53	2533.99	2865.03

(E) CH_3CO−PF

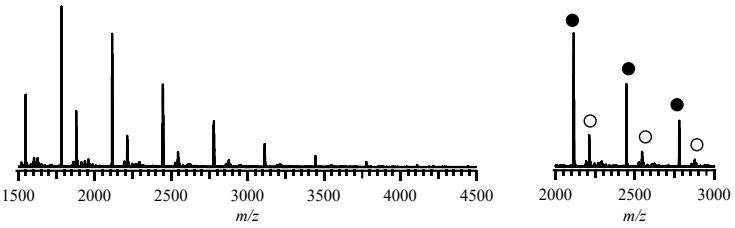

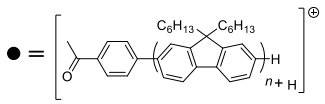

	n = 6	*n* = 7	*n* = 8
Clcd.	2113.56	2445.81	2778.06
Found	2113.56	2445.76	2778.14

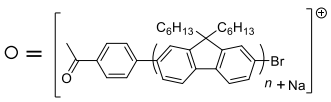

	n = 6	*n* = 7	*n* = 8
Clcd.	2211.78	2543.97	2875.65
Found	2211.46	2544.71	2876.96

(F) EtOOC−PF

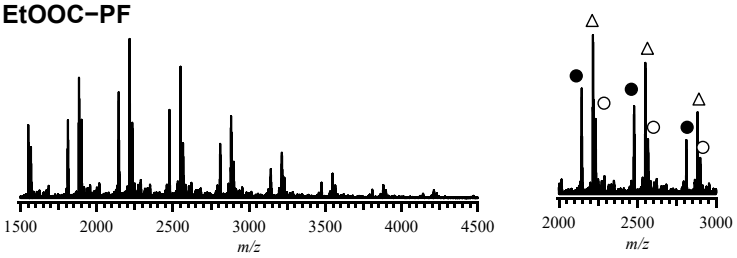

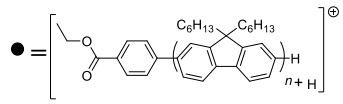

	n = 6	*n* = 7	*n* = 8
Clcd.	2097.57	2429.82	2762.07
Found	2097.54	2429.81	2762.10

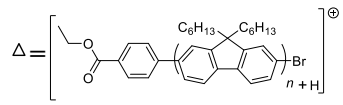

	n = 6	*n* = 7	*n* = 8
Clcd.	2221.48	2553.73	2885.98
Found	2222.66	2552.93	2886.27

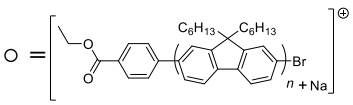

	n = 6	*n* = 7	*n* = 8
Clcd.	2244.47	2576.72	2908.97
Found	2242.87	2575.09	2899.45

Figure 2-7 (continue)

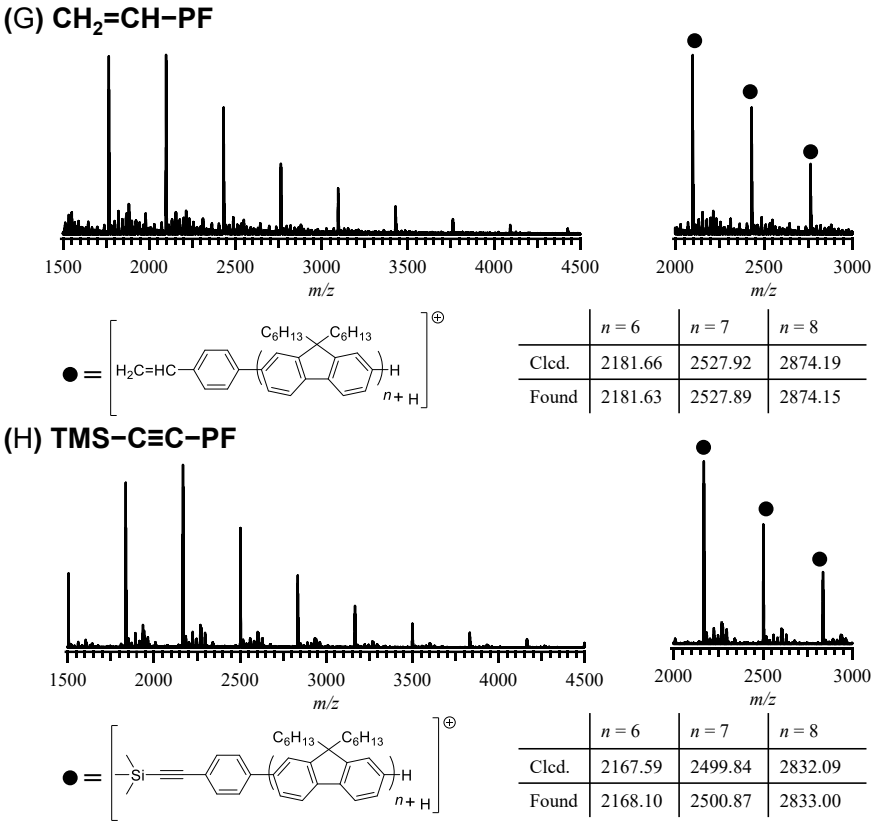

Figure 2-7. MALDI-TOF MS spectra of (A) **CH_3−PF**, (B) **HO−PF**, (B) **H_2N−PF**, (D) **OHC−PF**, (E) **CH_3CO**−PF, (F) **EtCOO**−PF, (G) **CH_2=CH**−PF, and (H) **TMS−C≡C−PF** (runs 12-19 in Table 2-2).

Table 2-2. Synthesis of *α*,*ω*-end-functionalized PFs via SCTP using various initiators and terminators[a]

run	R^1	R^2	$M_{n,SEC}$[b] (g mol^{-1})	$M_{n,NMR}$[c] (g mol^{-1})	$Đ_M$[b]	yield[d] (%)	*ω*-functionality[e](%)
12	CH_3	—	4800	4400	1.35	86.8	—
13	OH	—	5100	5300	1.27	85.8	—
14	NH_2	—	5000	5100	1.19	73.0	—
15	CHO	—	5000	7800	1.30	88.4	—
16	$COCH_3$	—	5300	5700	1.36	83.3	—
17	COOEt	—	5200	4100	1.23	81.7	—
18	$CH{=}CH_2$	—	4500	4100	1.28	80.8	—
19	C≡C−TMS	—	6000	7700	1.35	82.8	—
20	CH_2OH	CH_2OH	6100	5800	1.25	78.2	94.7
21	CH_2OH	C≡C−TMS	6600	5600	1.31	88.8	92.6
22	C≡C−TMS	C≡C−TMS	8750	6800	1.36	83.6	91.6

[a]THF/water (v/v) = 10/1; $[\mathbf{M1}]_0$ = 10 mmol L^{-1}; $[\mathbf{M1}]_0/[\mathbf{FI{-}R^1}]_0/[Pd_2(dba)_3{\bullet}CHCl_3]/[t\text{-}Bu_3P]/[K_3PO_4]/[\mathbf{FT{-}R^2}]_0$ = 15/1/0.3/2.2/1.5/10. [b]Determined by SEC (PSt standards, THF, 40 °C). [c]Determined by ^{1}H NMR spectrum in $CDCl_3$. [d]Isolated yields. [e]Determined by ^{1}H NMR.

Next, the author investigated *ω*-chain end functionalization by the termination reaction with functional triolborate salt-type terminators, i.e., potassium 4-hydroxymethylphenyltriolborate and potassium 4-trimetylsilylethynylphenyltriolborate (**FT−CH$_2$OH** and **FT−C≡C−TMS**, respectively). Under the optimized conditions, the SCTP of **M1** was first carried out in the presence of **FI-CH$_2$OH** and **FI−C≡C−TMS** as the initiators with a [**FI−R^1**]$_0$/[**M1**]$_0$ ratio of 15/1. After 12 min, 10 equivalents of the terminator (**FT−CH$_2$OH** or **FT−C≡C−TMS**) with respect to the initiator was injected to the polymerization mixture (runs 20, 21, and 22 in Table 2-2). All the polymerizations produced well-defined PFs with predicted $M_{n,SEC}$s and narrow $Đ_M$s (Figure 2-8). The ^{1}H NMR spectra of the products exhibited signals due to both the initiator and terminator moieties (Figure 2-9). For example, for the PF obtained from run 21, ^{1}H NMR signals attributable to the benzyl protons (proton **E**) were seen at 4.79 ppm for the initiator residue and those arising from the methyl protons (proton **N**) were seen at 0.08 ppm for the terminator residue. Furthermore, the MALDI-TOF MS analysis provided more direct evidence of the successful *ω*-chain end functionalization (Figure 2-10). The major series of peaks observed in the MALDI-TOF MS spectra for the products were assignable to the expected structures, i.e., **HOCH$_2$−PF−CH$_2$OH** (run 20), **HOCH$_2$−PF−C≡C−TMS** (run 21), and **TMS−C≡C−PF−C≡C−TMS** (run 22). For example, the peak observed at *m*/*z* of 2274.68 in the spectrum of **HOCH$_2$−PF−C≡C−TMS** matched with the calculated mass for the 6-mer having the expected chain end group structures. Such *α*,*ω*-difunctional PFs are of interest in the synthesis of ABA-type triblock copolymers and ABC-type triblock terpolymers, where the B block is PF. Overall, these results demonstrated that the present polymerization system is quite useful for the precise synthesis of end-functionalized PFs.

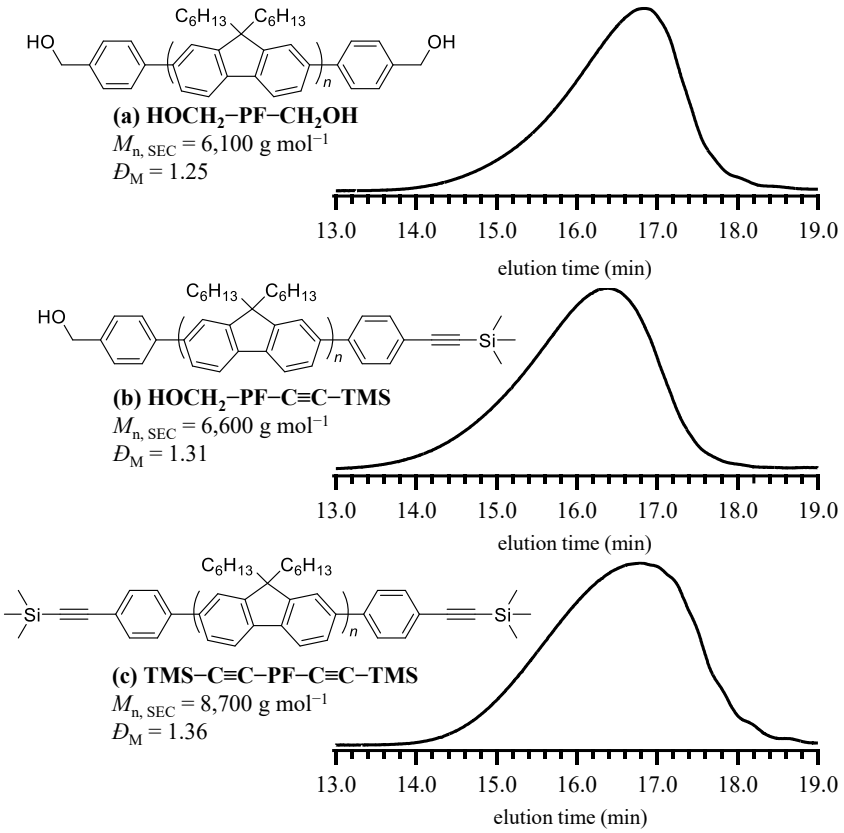

Figure 2-8. SEC traces of (A) **HOCH₂−PF−CH₂OH** (B) **HOCH₂−PF−C≡C−TMS**, and (C) **TMS−C≡C−PF−C≡C−TMS** (runs 20-22 in Table 2-2), detected by RI detector (eluent, THF; flow rate 1.0 mL min^{-1}).

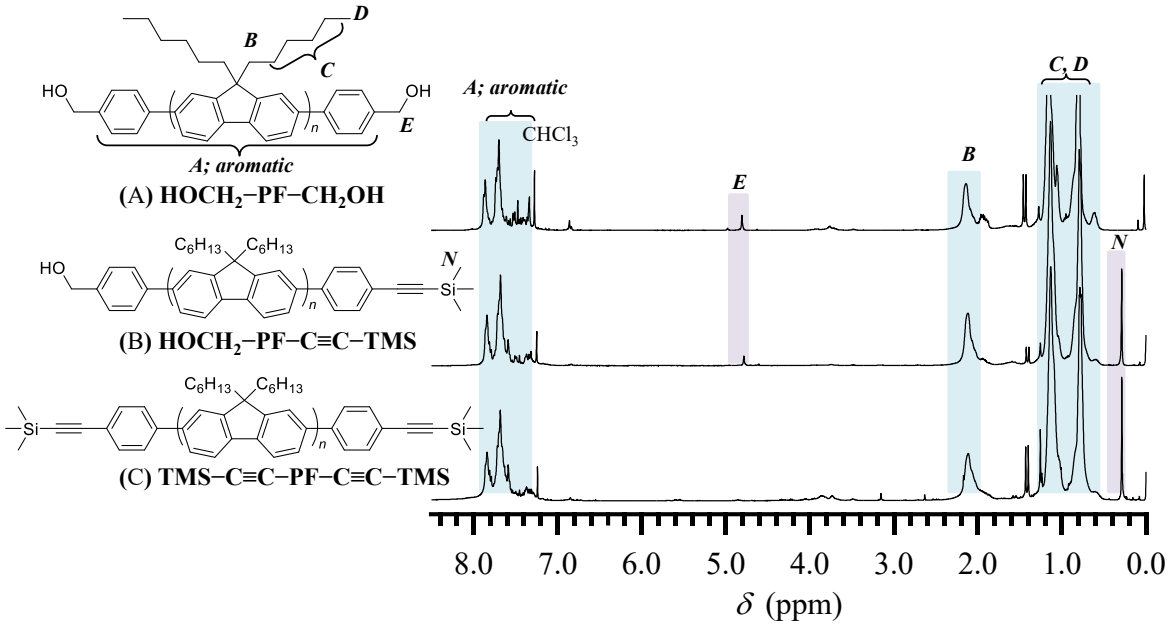

Figure 2-9. ^{1}H NMR spectra of (A) **HOCH₂−PF−CH₂OH** (B) **HOCH₂−PF−C≡C−TMS**, and (C) **TMS−C≡C−PF−C≡C−TMS** (runs 20-22 in Table 2-2) in $CDCl_3$.

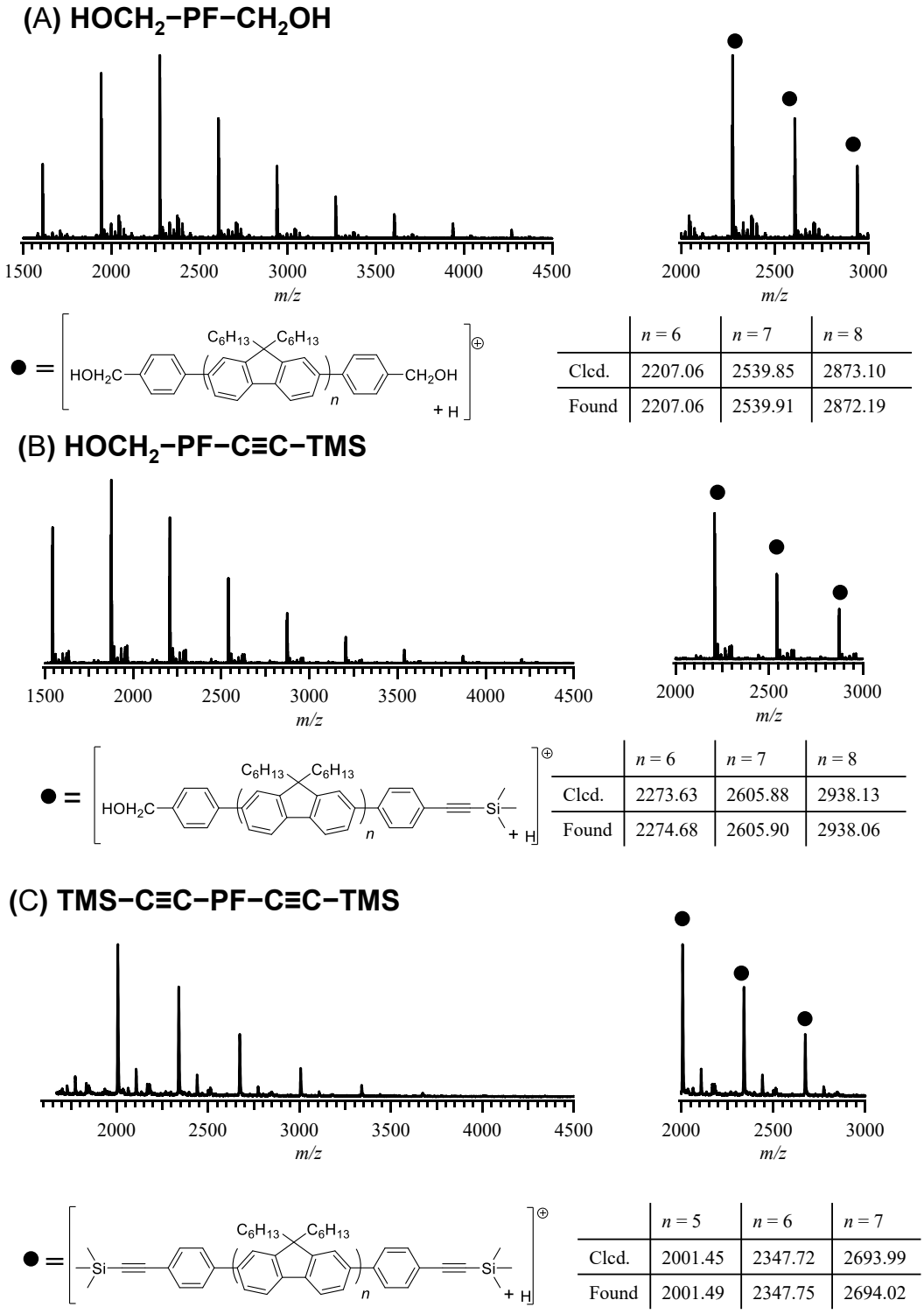

	n = 6	*n* = 7	*n* = 8
Clcd.	2207.06	2539.85	2873.10
Found	2207.06	2539.91	2872.19

	n = 6	*n* = 7	*n* = 8
Clcd.	2273.63	2605.88	2938.13
Found	2274.68	2605.90	2938.06

	n = 5	*n* = 6	*n* = 7
Clcd.	2001.45	2347.72	2693.99
Found	2001.49	2347.75	2694.02

Figure 2-10. MALDI-TOF MS spectra of (A) **HOCH₂−PF−CH₂OH** (B) **HOCH₂−PF−C≡C−TMS**, and (C) **TMS−C≡C−PF−C≡C−TMS** (runs 20-22 in Table 2-2).

2.2.5 Synthesis of PF-containing block and graft copolymers using macroinitiator

Given the good functional group tolerance and the well-controlled nature of the polymerization system described herein, a variety of polymers should be applied as the macroinitiator. Such an approach can be effective for the synthesis of PF-containing block and graft copolymers. It should be noted that the utility of the combination of the macroinitiator approach and catalyst-transfer polycondensation was very recently disclosed in the synthesized polythiophene-containing BCPs.[50] Thus, author investigated the SCTP of **M1** using various iodobenzene-functionalized macroinitiators to produce PF-containing block and graft copolymers. Notably, the water content in the solvent was reduced as much as possible to avoid possible precipitation of the macroinitiator. As summarized in Table 2-3, the water content in the solvent did not affect the polymerization properties, and author found that the SCTP of **M1** proceeds smoothly even in the THF/water (5000/1, v/v) solvent system.

Table 2-3. Effect of **M1** SCTP on varying water content in solvent[a]

THF/H_2O (v/v)	$M_{n,SEC}$[b] (g mol^{-1})	$M_{n,NMR}$[c] (g mol^{-1})	$Đ_M$[b]	yield[d] (%)
10/1	12,300	12,600	1.24	83.2
100/1	11,400	12,400	1.22	85.2
1000/1	11,100	12,000	1.22	84.3
5000/1[e]	10,500	11,900	1.20	84.3

[a]Polymerization conditions: Ar atmosphere; temperature, −10 °C; $[\mathbf{M1}]_0$ = 10 mmol L^{-1}; $[\mathbf{FI{-}CH_2OH}]_0/[\mathbf{M1}]_0/[Pd_2(dba)_3{\bullet}CHCl_3]/[t\text{-}Bu_3P]/[K_3PO_4]$ = 1/30/0.3/2.2/1.5. [b]Determined by SEC (PSt standards, THF, 40 °C). [c]Determined by ^1H NMR spectrum in $CDCl_3$. [d]Isolated yields. [e]Saturated aqueous solution of K_3PO_4.

Scheme 2-2. Syntheses of PSt-*b*-PF, PLA-*b*-PF, PCL-*b*-PF, and PEO-*b*-PF by SCTP using PSt−I, PLA−I, PCL−I, and PEO−I, respectively

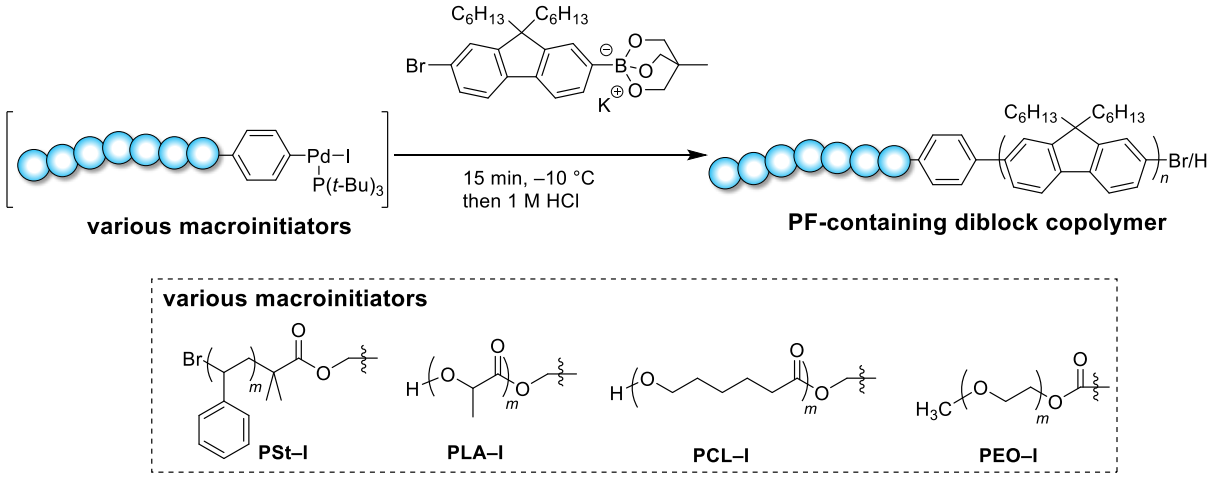

With this information in hand, author attempted the SCTP of **M1** with the iodobenzene-terminated polystyrene (**PSt−I**; $M_{n,NMR}$ = 2,150 g mol^{-1}, $Đ_M$ = 1.17, run 19) as the macroinitiator under the optimized polymerization conditions ([**PSt−I**]$_0$/[**M1**]$_0$ = 1/30; THF/water (v/v) = 5000/1; Table 2-3), producing **PSt-*b*-PF** diblock copolymer in one step (Scheme 2-2). SEC analysis revealed that **M1** polymerization indeed proceeded from **PSt−I**, as evidenced by a clear shift in the elution peak toward the higher-molecular-weight region with virtually no tailing (Figure 2-11A). In addition, the ^{1}H NMR spectrum of the product showed signals attributed to both the PF and PSt main chain (Figure 2-12), demonstrating the successful formation of **PSt-*b*-PF**. The $M_{n,NMR}$ for the PF block was determined to be 12,700 g mol^{-1}. To further verify the formation of the BCP, author employed diffusion-order NMR spectroscopy (DOSY). In the DOSY spectrum (Figure 2-13), only a single diffusion coefficient (D = 2.23 mm^2 s^{-1}) was observed for all the ^{1}H NMR signals due to both the blocks, evidencing the covalent attachment between the PF and PSt blocks. These results clearly demonstrated the success in the PF-containing BCP synthesis using the macroinitiator method.

Table 2-4. Polymerization of triolborate salt-type fluorene monomer using various macroinitiators[a]

run	macroinitiator			copolymer		yield [d]
		$M_{n,NMR}$[c] (g mol^{-1})	$Đ_M$[b]	$M_{n,NMR}$[c] (g mol^{-1})	$Đ_M$[b]	(%)
19	PSt−I	2150	1.17	12,700	1.20	87.0
20	PLA−I	6000	1.06	15,700	1.19	90.0
21	PCL−I	6700	1.07	16,000	1.11	85.0
22	PEO−I	5300	1.25	14,200	1.50	67.3

[a]Polymerization conditions: Ar atmosphere; solvent, THF/water (v/v) = 5000/1; [**M1**]$_0$ = 10 mmol L^{-1}; [**M1**]$_0$/[macroinitiator]$_0$/[$Pd_2(dba)_3$•$CHCl_3$]/[*t*-Bu_3P]/[K_3PO_4] = 30/1/0.5/2.2/1.5. [b] Determined by SEC (PSt standards, THF, 40 °C). [c] Determined by ^{1}H NMR spectrum in $CDCl_3$.[d] Isolated yield was calculated based on the mass recovery of the product.

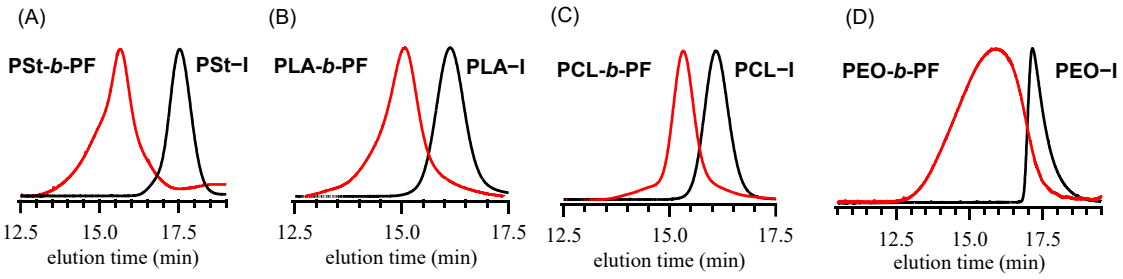

Figure 2-11. SEC traces of PF-containing block and graft copolymers (red curves: A, **PSt-*b*-PF**; B, **PLA-*b*-PF**; C, **PCL-*b*-PF**; and D, **PEO-*b*-PF)** and the corresponding macroinitiators (black curves: A, **PSt−I**; B, **PLA−I**; C, **PCL−I**; and D, **PEO−I**) detected by RI detector (eluent, THF; flow rate, 1.0 mL min^{-1}).

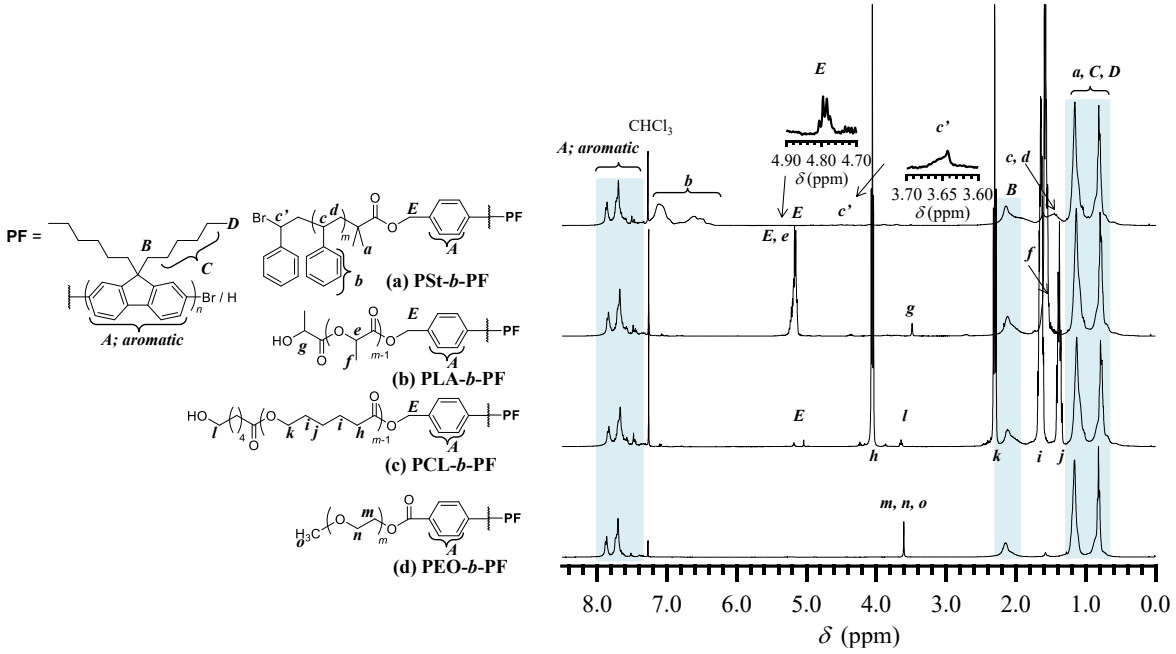

Figure 2-12. ^{1}H NMR spectra of (A) **PSt-*b*-PF**, (B) **PLA-*b*-PF**, (C) **PCL-*b*-PF**, and (D) **PEO-*b*-PF** (solvent, $CDCl_3$).

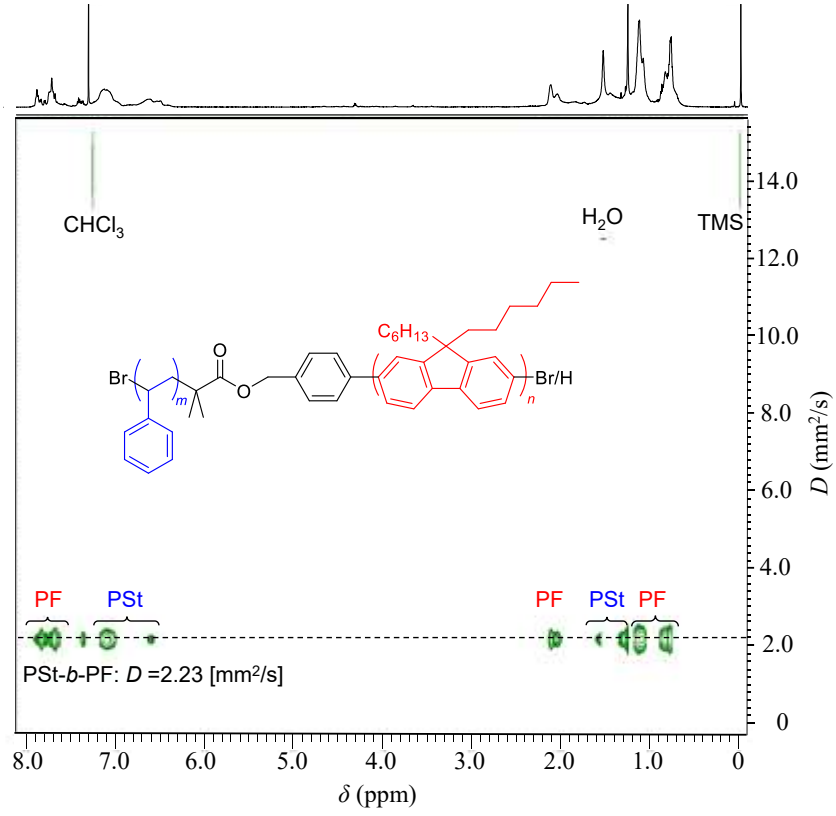

Figure 2-13. DOSY NMR spectrum of **PSt-*b*-PF** (run 1, Table 2-4) in $CDCl_3$ (600 MHz).

One of the key factors for the successful BCP synthesis should be the reduced water content in the solvent. To test this hypothesis, author examined the polymerization of **M1** with **PSt−I** in the THF/water (10/1, v/v) solvent system. As expected, the product was a mixture of the diblock copolymer and the unreacted macroinitiator (Figure 2-14). The increased water content in the polymerization medium likely induced precipitation/aggregation of the macroinitiators, as evidenced by the cloudy polymerization mixture. This is in clear contrast to the result obtained by following the SCTP approach described herein: the polymerization system was homogeneous due to good solubility in the solvent with a minimal amount of water. To further verify the advantage of using the triolborate salt-type monomer, author performed BCP synthesis using **M2** with **PSt−I** in THF/water (10/1 and 5000/1, v/v; Table 2-5). However, in both cases, SEC analysis of the products revealed the formation of a trace amount of the BCP (Figure 2-14), demonstrating that the combination of the triolborate salt-type monomer and reduced water content in the solvent is essential for successful BCP synthesis.

Table 2-5. SCTP of **M1** or **M2**[a]

run	[THF]/[H_2O] = v/v	monomer	$M_{n,SEC}$[b] (g mol^{-1})	$M_{n,NMR}$[c] (g mol^{-1})	$Đ_M$[b]	yield[d] (%)
23	10/1	**M2**	—	—	—	—
24	5000/1	**M1**	12,700	12,700	1.20	87.0

[a] Polymerization conditions: Ar atmosphere; solvent, THF/water (5000/1); [**M1**]$_0$ = 10 mmol L^{-1}; [macroinitiator]$_0$/[**M1**]$_0$/[$Pd_2(dba)_3$•$CHCl_3$]/[*t*-Bu_3P]/[K_3PO_4] = 1/15/0.3/2.2/1.5. [b] Determined by SEC (PSt standards, THF, 40 °C). [c] Determined by ^1H NMR spectrum in $CDCl_3$. [d] Isolated yields.

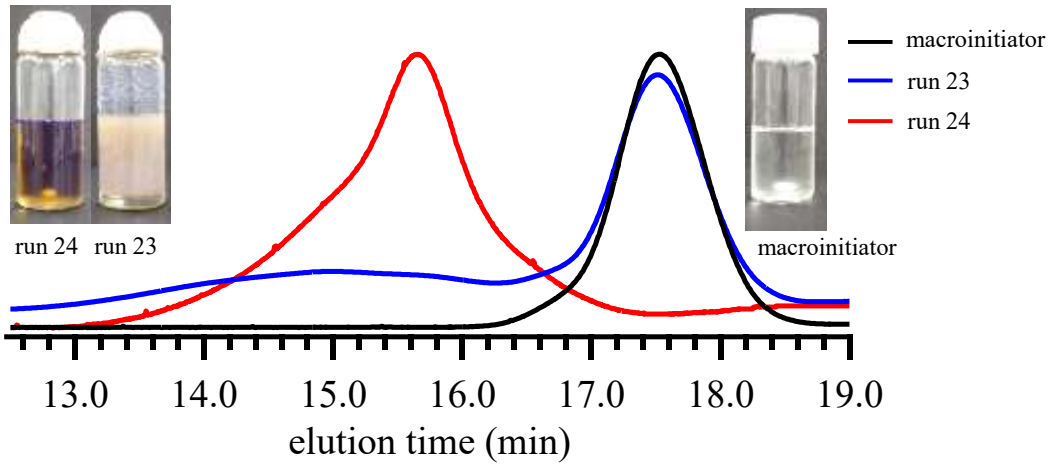

Figure 2-14. SEC traces of BCPs (blue line; run 23, red line; run 24 in Table 2-5) and the corresponding macroinitiator (black line) detected by RI detector (eluent, THF; flow rate, 1.0 mL min^{-1}).

The versatility of the presented BCP synthesis was further demonstrated by conducting SCTP with a variety of iodobenzene-terminated macroinitiators, such as linear poly(*rac*-lactide) (**PLA−I**; $M_{n,NMR}$ = 6000 g mol^{-1}, $Đ_M$ = 1.06, run 20 in Table 2-4), poly(ε-caprolactone) (**PCL−I**; $M_{n,NMR}$ = 6700 g mol^{-1}, $Đ_M$ = 1.07, run 21), and poly(ethylene oxide) (**PEO−I**; $M_{n,NMR}$ = 5300 g mol^{-1}, $Đ_M$ = 1.25, run 22) in THF/water (5000/1, v/v; [macroinitiator]$_0$/[**M1**]$_0$ = 1:30) (Scheme 2-3A). Table 2-4 summarizes the polymerization results. All the polymerizations proceeded homogeneously and gave the corresponding diblock copolymers, i.e., **PLA-*b*-PF**, **PCL-*b*-PF**, and **PEO-*b*-PF** with $Đ_M$ values in the range 1.11–1.50, in good yields. Figure 2-11 shows the SEC traces of the obtained BCPs and the corresponding macroinitiators. The elution peak of the macroinitiator shifted to the higher-molecular-weight region after the SCTP of **M1**, indicating that the SCTP was initiated from the corresponding macroinitiators. The ^{1}H NMR spectra of the obtained BCPs exhibited characteristic signals due to the macroinitiator block, as well as those arising from the PF block (Figure 2-12), which further confirmed the successful BCP synthesis.

To further expand this approach, author examined macroinitiators possessing multiple iodobenzene initiating sites (Scheme 2-3).

Scheme 2-3. Syntheses of PF-*b*-PCL-*b*-PF, (PCL-*b*-PF)$_3$, and PBA-*g*-PF by SCTP using (PCL−I)$_2$, (PCL−I)$_3$, and P(BA$_{50}$-*co*-BzI$_4$), respectively

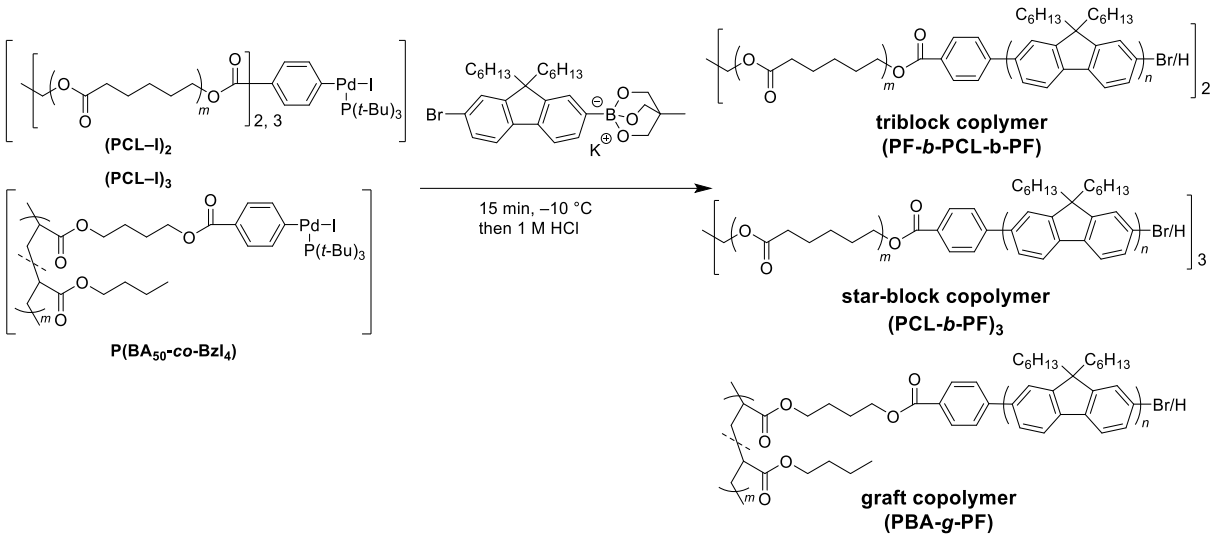

Thus, the SCTP of **M1** was conducted using linear (**(PCL−I)$_2$**; $M_{n,NMR}$ = 7900 g mol^{-1}, $Đ_M$ = 1.05, [**(PCL−I)$_2$**]$_0$/[**M1**]$_0$ = 1/30; run 25, in Table 2-6) and three-armed star-shaped PCLs having an iodobenzene at each chain end (**(PCL−I)$_3$**; $M_{n,NMR}$ = 7300 g mol^{-1}, $Đ_M$ = 1.05, [**(PCL−I)$_3$**]$_0$/[**M1**]$_0$ = 1/30; run 26 in in Table 2-6) as the macroinitiators to produce a **PF-*b*-PCL-*b*-PF** triblock copolymer and **(PCL-*b*-PF)$_3$** three-armed star-block copolymers. In addition, poly(*n*-butyl acrylate) having multiple iodobenzene moieties on the side chain (**P(BA$_{50}$-*co*-BzI$_4$)**; $M_{n,NMR}$ = 8100 g mol^{-1}, $Đ_M$ = 1.09, [**P(BA$_{50}$-*co*-BzI$_4$)**]$_0$/[**M1**]$_0$ = 1/40; run 27 in Table 2-6) was employed as the macroinitiator to produce a PF-containing graft copolymer (**PBA-*g*-PF**). The ^{1}H NMR and SEC analyses confirmed the successful synthesis of the targeted triblock, star-block, and graft copolymers **(**Figures 2-15 and 2-16).

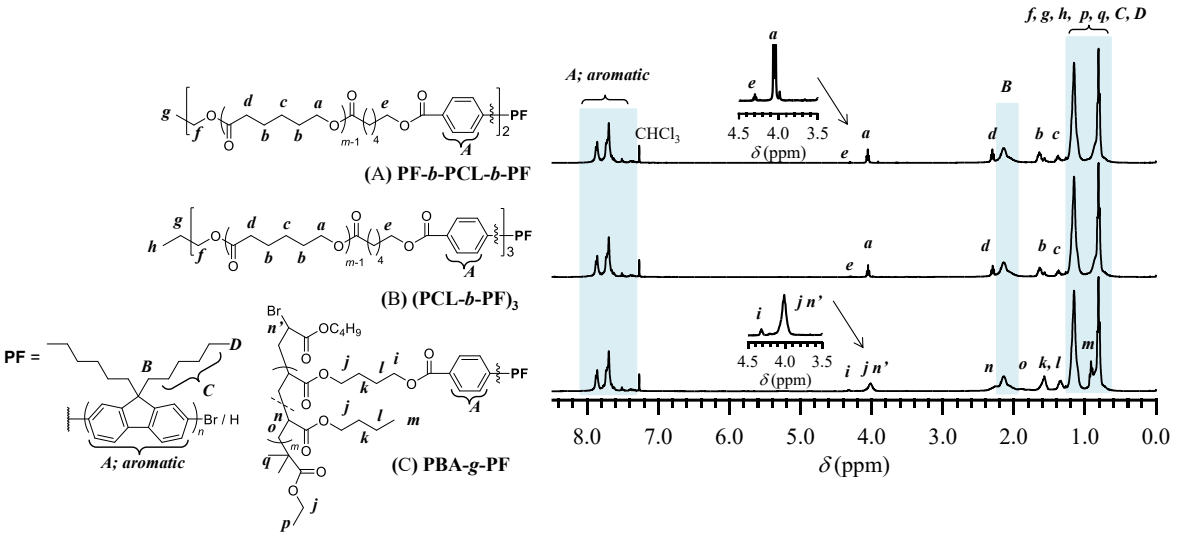

Figure 2-15. ^{1}H NMR spectra of (A) **PF-*b*-PCL-*b*-PF**, (B) **(PCL-*b*-PF)$_3$**, and (C) **PBA-*g*-PF** (solvent, $CDCl_3$).

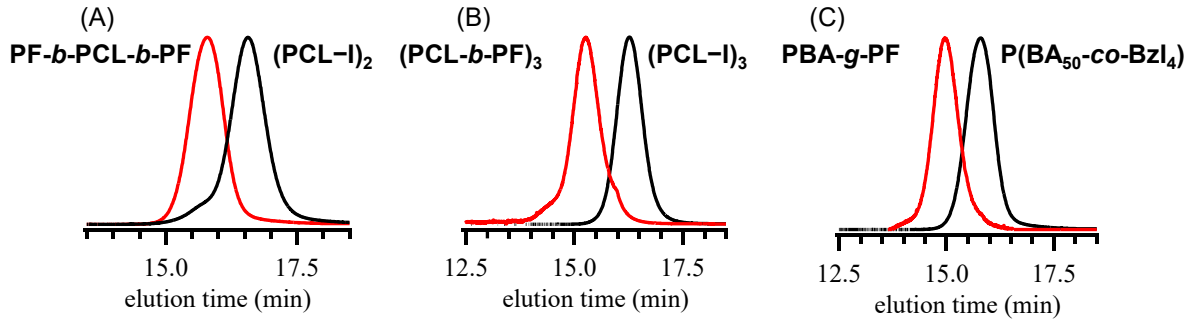

Figure 2-16. SEC traces of PF-containing block and graft copolymers (red curves: A, **PF-*b*-PCL-*b*-PF**; B, **(PCL-*b*-PF)$_3$**; and C, **PBA-*g*-PF)** and the corresponding macroinitiators (black curves: A, **(PCL−I)$_2$**; B, **(PCL−I)$_3$**; and C, **P(BA$_{50}$-*co*-BzI$_4$)**) detected by RI detector (eluent, THF; flow rate, 1.0 mL min^{-1}).

Table 2-6. Polymerization of triolborate salt-type fluorene monomer using macroinitiators possessing multiple iodobenzene initiating sites[a]

run	macroinitiator			copolymer		yield [d]
		$M_{n,NMR}$[c] (g mol^{-1})	$Đ_M$[b]	$M_{n,NMR}$[c] (g mol^{-1})	$Đ_M$[b]	(%)
25[e]	(PCL−I)$_2$	7,900	1.05	17,800	1.10	88.5
26[f]	(PCL−I)$_3$	7,300	1.05	17,100	1.07	82.6
27[g]	P(BA$_{50}$-*co*-BzI$_4$)	8,100	1.09	21,300	1.08	76.3

[a]Polymerization conditions: Ar atmosphere; solvent, THF/water (v/v) = 5000/1; [**M1**]$_0$ = 10 mmol L^{-1}; [**M1**]$_0$/[macroinitiator]$_0$/[$Pd_2(dba)_3$•$CHCl_3$]/[*t*-Bu_3P]/[K_3PO_4] = 30/1/0.5/2.2/1.5. [b] Determined by SEC (PSt standards, THF, 40 °C). [c] Determined by ^{1}H NMR spectrum in $CDCl_3$. [d] Isolated yield was calculated based on the mass recovery of the product. [e] [**M1**]$_0$/[macroinitiator]$_0$/[$Pd_2(dba)_3$•$CHCl_3$]/[*t*-Bu_3P]/[K_3PO_4] = 30/1/4.4/3.0. [f] [**M1**]$_0$/[macroinitiator]$_0$/[$Pd_2(dba)_3$•$CHCl_3$]/[*t*-Bu_3P]/[K_3PO_4] = 30/1/1.5/6.6/4.5. [g] [**M1**]$_0$/[macroinitiator]$_0$/[$Pd_2(dba)_3$•$CHCl_3$]/[*t*-Bu_3P]/[K_3PO_4] = 40/1/2.0/8.8/6.0.

2.3 Conclusions

In conclusion, the author successfully demonstrated that the SCTP of the triolborate salt-type fluorene monomer can be an efficient and versatile approach to the precise synthesis of high-molecular-weight and end-functionalized PFs with narrow dispersity. Kinetic and post-polymerization experiments revealed that the SCTP proceeded rapidly through the chain growth and controlled/living polymerization route. Use of the triolborate salt-type fluorene monomer suppressed the side reactions, which is key to the successful synthesis of high-molecular-weight PFs as well as achieving α,ω-chain end-functionalized PFs. In addition, the well-controlled polymerization allowed direct access to PF-containing block and graft copolymers by combining with various macroinitiators by SCTP. One of the key factors for the successful block, triblock, star-block, and graft copolymers syntheses is the reduced water content in the polymerization medium, which suppressed the potential precipitation/aggregation of the macroinitiators. Therefore, the SCTP of the triolborate salt-type fluorene monomer offers the advantage of achieving precise polymerization in a simpler reaction system and affords well-defined PFs with various functionalities at the chain ends.

2.4 Experimental Section

Materials

2-(7-Bromo-9,9-dihexyl-9*H*-fluorene-2-yl)4,4,5,5-tetramethyl-1,2,3dioxaborolane[51] and tris(dibenzylideneacetone)dipalladium(0)-chloroform adduct ($Pd_2(dba)_3$•$CHCl_3$),[52] were prepared according to reported methods.

Benzoic acid, 2-bromoisobutyryl bromide, *n*-butyl acrylate, *ε*-caprolactone, 18-crown-6, 1,8-diazabicyclo[5.4.0]-undec-7-ene (DBU), 4-(dimethylamino)pyridine (DMAP), *trans*,*trans*-1,5-diphenyl-1,4-pentadien-3-one, diphenyl phosphate, ethyl 2-bromoisobutyrate, ethyl 4-iodobenzoate, 4-hydroxybutyl acrylate, 4'-iodoacetophenone, 4-iodoaniline, 4-iodobenzaldehyde, 4-iodobenzoyl chloride, 4-iodobenzyl alcohol, 4-iodotoluene, *rac*-Lactide (*rac*-LA), *N*,*N*,*N*',*N*'',*N*''-pentamethyldiethylenetriamine (PMDETA), styrene, *trans*-2-[3-(4-*tert*-butylphenyl)-2-methyl-2-propylidene]malononitrile, triisopropyl borate, and trimethylolethane were purchased from Tokyo Chemical Industry Co., Ltd. (TCI), and used as received.

n-Butyllithium (*n*-BuLi; in *n*-hexane as 1.6 mol L^{-1} solution) 2,7-dibromo-9,9-dihexylfluorene, potassium hydroxide (KOH), and triethylamine (TEA) were purchased from Kanto Chemical Co., Inc., and used as received.

4-Hydroxymethylphenylboronic acid, 4-iodostyrene, tri(*t*-butyl)phosphine, and tripotassium phosphate (K_3PO_4) were purchased from Fujifilm Wako Pure Chemical Co. and used as received.

4-Iodophenol was purchased from Manac Co., Inc., and used as received.

Copper(I) bromide (CuBr), (4-iodophenylethynyl)trimethylsilane, poly(ethylene oxide) monomethyl ether ($M_{n,NMR}$ = 5,000 g mol^{-1}), and 4-trimetylsilylethynylphenylboronic acid were purchased from Sigma-Aldrich Chemicals Co. and used as received.

rac-Lactide (*rac*-LA; TCI, >98%) was purified by recrystallization (twice) from dry toluene and stored in a glovebox.

DBU, ε-CL, and styrene were purified by distillation over CaH_2 under reduced pressure and stored in a glovebox.

Commercially-available dry CH_2Cl_2 (Kanto Chemical Co., Inc., >99.5%, water content, <0.001%) was further purified by an MBRAUN MB SPS Compact solvent purification system equipped with a MB-KOL-C column and a MB-KOL-A column, which was then directly used for the polymerizations. Commercially-available dry THF and dry toluene (Kanto Chemical Co., Inc., >99.5%, water content, <0.001%) was further purified by an MBRAUN MB SPS Compact solvent purification system equipped with a MB-KOL-C column and a MB-KOL-A column, which was then directly used for the polymerizations. Commercially-available dry toluene was further purified by MBRAUN solvent purification system (MB SPS COMPACT) equipped with a column of an activated alumina and a column of an activated copper catalyst.

Instruments

Polymerization was carried out in an MBRAUN stainless steel glovebox equipped with a gas purification system (molecular sieves and a copper catalyst) under a dry argon atmosphere (H_2O, O_2 <0.1 ppm). The moisture and oxygen contents in the glovebox were monitored by an MB-MO-SE 1 moisture sensor and an MB-OX-SE 1 oxygen sensor, respectively.

^1H (400 MHz) and ^{13}C NMR (100 MHz) spectra were obtained using a JEOL JNM-ECS400 instrument at 25 °C.

DOSY NMR measurement was performed at 30 °C on a JEOL JNM-ECZ600R NMR spectrometer operating at 600 MHz and equipped with a ROYAL probe (NM100006) capable of producing gradients in the z direction with strength 90 G cm^{-1}. The pulse sequence used was stimulated-echo and longitudinal eddy current delay. The gradient strength was logarithmically incremented in 16 steps from 50 mT up to 200 mT of the maximum gradient strength. The gradient duration was 2 ms and the diffusion delay was 0.1 s. The spectra were collected with a spectral window from −2.5 to 12.5 ppm in 8 transients and with 4 dummy transients in the beginning, with an acquisition time of 3 s and relaxation delay of 15 s.

Size exclusion chromatography (SEC) was performed at 40 °C using a Jasco high-performance liquid chromatography system (PU-2080Plus Intelligent HPLC pump, CO-2065Plus Column oven, RI-2031Plus Intelligent RI detector, and Shodex DG-2080-54) equipped with a Shodex KF-G guard column (4.6 mm × 10 mm; particle size, 8 μm) and two Shodex KF-804 columns (linear; particle size, 7 μm; 8.0 mm × 300 mm; exclusion limit, 4 × 10^5) in THF at a flow rate of 1.0 mL min^{-1}. The number-average molecular weight ($M_{n,SEC}$) and dispersity ($Đ_M$) of the polymer were calculated on the basis of a polystyrene calibration.

Matrix-assisted laser desorption ionization time-of-flight mass spectrometry (MALDI-TOF MS) measurement of the polymer was carried out in the reflector mode using an ABSCIEX TOF/TOF/5800 equipped with a 337 nm nitrogen laser (3 ns pulse width). The MALDI-TOF MS samples were prepared by depositing a mixture of the polymer and matrix in THF onto a sample plate. A 1/80 (v/v) ratio of [PF (1.0 g L^{-1} in THF)]/[*trans*-2-[3-(4-tert-butylphenyl)-2-methyl-2-propylidene]malononitrile (10 g L^{-1} in THF)] was used.

Synthesis of potassium 2-(7-bromo-9,9-dihexyl-9*H*-fluorene-2-yl)triolborate

Scheme 2-4. Synthesis of triolborate salt-type fluorene monomer

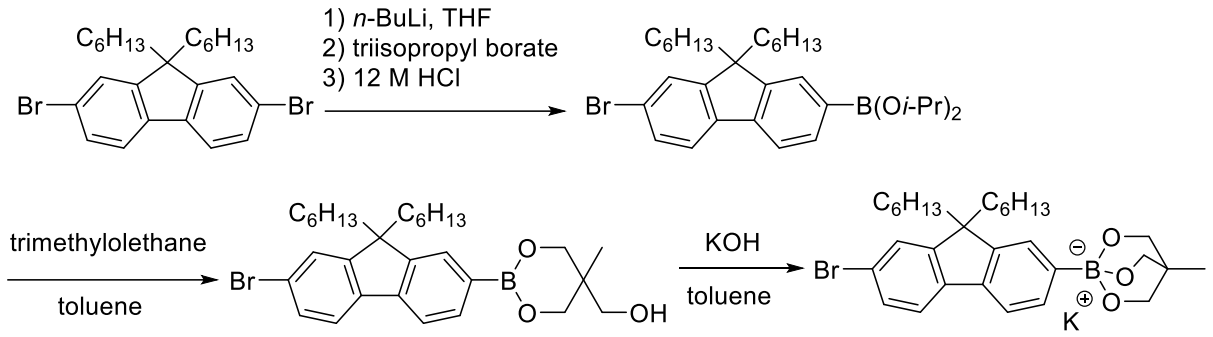

To a 500 mL three-necked round bottom flask, 2,7-dibromo-9,9-dihexylfluorene (40.0 g, 81.2 mmol) was added and dried under vacuum at room temperature for 6 h. Dry-THF (320 mL) was introduced to this flask and cooled to −78 °C. *n*-BuLi (50.8 mL,81.2 mmol, 1.6 M in hexane) was injected slowly via a syringe, and the whole mixture was stirred for 1.5 h under argon atmosphere. Triisopropyl borate (28.0 mL, 121.9 mmol) was then added to this reaction mixture. The mixture was gradually brought back to room temperature and stirred for 9 h under argon atmosphere. The reaction was quenched by the addition of 12 mol L^{-1} HCl (30 mL). The solvent was removed by evaporation, and the residue was dissolved in CH_2Cl_2 and washed with brine. The organic layer was dried over Na_2SO_4 and evaporated completely. The residue was purified by silica gel column chromatography (*n*-hexane → MeOH) to give 2-(7-bromo-9,9-dihexyl-9*H*-fluorene-2-yl)diisopropyl boronate (41.7 g, yield; 90.5%) as a white powder.

2-(7-Bromo-9,9-dihexyl-9*H*-fluorene-2-yl)diisopropyl boronate (30.0 g, 55.4 mmol) and trimethylolethane (6.7 g, 55.4 mmol) were then dissolved in toluene (150 ml). Isopropanol was removed by azeotropic distillation for 4 h by a Dean-Stark apparatus. Then, KOH (3.1 g, 55.4 mmol) was added, and the mixture was refluxed for 4 h. The precipitate was collected by filtration, washed with cyclohexane, and dried under reduced pressure to give 2-(7-bromo-9,9-

dihexyl-9*H*-fluorene-2-yl)triolborate (25.7 g, 44.3 mmol, 80% yield) was yellow solid.

^{1}H NMR (400 MHz, DMSO-d_6): δ (ppm) 7.93–7.77 (m, Ar–*H*), 7.75–7.57 (m, Ar–*H*), 7.50 (d, Ar–*H*), 3.56 (s, –O(C*H*$_2$)$_3$CCH$_3$), 2.12 (br, –C*H*$_2$(CH$_2$)$_4$CH$_3$), 1.36–0.66 (m, –CH$_2$(C*H*$_2$)$_4$C*H*$_3$), 0.47 (s, –O(CH$_2$)$_3$CC*H*$_3$).

^{13}C NMR (100 MHz, DMSO-d_6): δ (ppm) 150, 147.8, 141.0, 140, 137.9, 134.8, 133.5, 131.4, 130.6, 129.6, 128.4, 122.5, 69.1, 52.6, 43.9, 32.9, 31.8, 29.9, 24.4, 22.7, 14.9, 14.1.

HRMS (ESI): *m*/*z* calcd for $C_{30}H_{41}BO_3Br^-$: 538.23739; found: 538.23782.

Synthesis of potassium aryltriolborates

Scheme 2-5. Synthesis of terminators

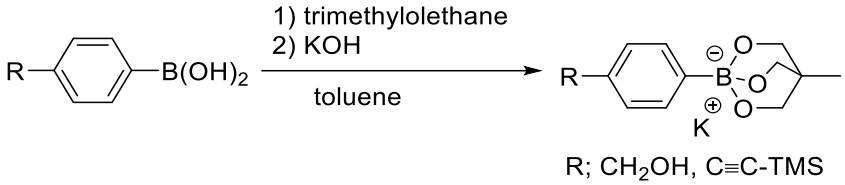

Arylboronic acid (65.8 mmol, 1.0 eq.) and trimethylolethane (65.8 mmol, 1.0 eq.) were dissolved in toluene (150 mL). Water was removed by azeotropic distillation for 4 h by a Dean-Stark apparatus. Then, KOH (65.8 mmol, 1.0 eq.) was added, and the mixture was refluxed for 4 h. The precipitate was collected by filtration, washed with *n*-hexane, and dried under reduced pressure to give the corresponding potassium aryltriolborate.

Potassium 4-hydroxymethylphenyltriolborate

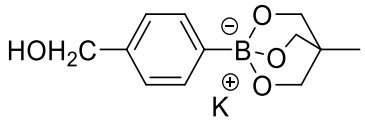

14.4 g, 80% yield: White solid

^{1}H NMR (400 MHz, DMSO-d_6): δ (ppm) 7.30 (d, J = 6.8 Hz, Ar–*H*), 6.98–6.88 (m, Ar–*H*), 4.79 (d, –C*H*$_2$OH), 3.56 (s, –O(C*H*$_2$)$_3$CCH$_3$), 0.47 (s, –O(CH$_2$)$_3$CC*H*$_3$)

^{13}C NMR (100 MHz, DMSO-d_6): δ (ppm) 141.2, 137.4, 133.6, 127.1, 69.1, 64.7, 32.9, 14.9.

HRMS (ESI): m/z calcd for $C_{12}H_{16}BO_4^-$: 234.11858; found: 234.1183

Potassium 4-trimetylsilylethynylphenyltriolborate

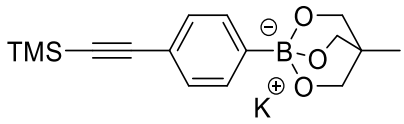

18.3 g, 82% yield: White solid

^{1}H NMR (400 MHz, DMSO-d_6): δ (ppm) 7.30 (d, J = 6.8 Hz, Ar–*H*), 6.98-6.88 (m, Ar–*H*), 3.56 (s, –O(C*H*$_2$)$_3$CCH$_3$), 0.47 (s, –O(CH$_2$)$_3$CC*H*$_3$), 0.08 (s, –Si(C*H*$_3$)$_3$)

^{13}C NMR (100 MHz, DMSO-d_6): δ (ppm) 141.2, 133.6, 127.1, 69.1, 64.7, 32.9, 14.9.

HRMS (ESI): *m*/*z* calcd for $C_{16}H_{22}BO_3Si^-$: 300.14731; found: 300.14758.

Synthesis of 4-iodobenzyl 2-bromo-2-methylpropanoate

Scheme 2-6. Synthesis of initiator

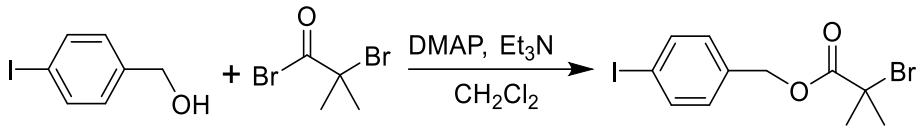

4-iodobenzyl alcohol (10 g, 42.7 mmol) and Et_3N (7.7 mL, 55.5 mmol) in dry-CH_2Cl_2 was added 2-bromo-2-dimethylpropionyl bromide (6.3 mL, 51.3 mmol). After stirring at room temperature for 2 h the reaction mature was filtered and extracted with Na_2CO_3 and 1M HCl solutions. The combined organic layers were then dried, evaporated to dryness (13.1 g, 80% yield).

^{1}H NMR ($CDCl_3$, 400 MHz): δ (ppm) 7.22-7.49 (m, Ar–*H*), 5.13 (s, 2H, –C*H*$_2$O–), 1.92 (s, 6H, –C*H*$_3$).

^{13}C NMR ($CDCl_3$, 100 MHz): δ (ppm) 171.3, 134.4, 131.8, 129.6, 122.4, 66.75, 55.50, 30.74.

HRMS (EI): *m*/*z* calcd for $C_{11}H_{12}O_2BrI$: 381.90610; found: 381.90653

Synthesis of iodobenzene-terminated poly(*rac*-lactide)

Scheme 2-7. Synthesis of poly(*rac*-lactide) as macroinitiator

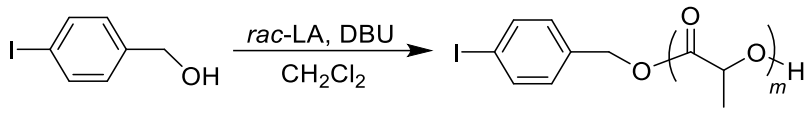

In a glovebox, DBU (51.9 μL, 347 μmol, 1.0 eq.) was added to a stirred solution of the 4-iodobenzyl alcohol (81.2 mg, 347 mmol, 1.0 eq.) and *rac*-LA (2.50 g, 17.35, 50 eq.) in dry-CH_2Cl_2 (25 mL). After 10 min, an excess of benzoic acid (ca. 500 mg) was added to the reaction mixture to terminate the polymerization. The mixture was purified by reprecipitation using THF as a good solvent and cold MeOH as a poor solvent to give iodobenzene-terminated poly(*rac*-lactide) as a white powder.10.4 g, 72.6% yield: white powder.

$M_{n,SEC}$ = 5800 g mol^{-1} (THF); $M_{n,NMR}$ = 6000 g mol^{-1} ($CDCl_3$), $Đ_M$ = 1.06.

^{1}H NMR (400 MHz, $CDCl_3$): δ (ppm) 7.75 (m, Ar–*H*), 5.19 (m, –C*H*$_2$O–, –C(=O)C*H*CH$_3$O–), 4.40–4.25 (m, –C(=O)C*H*CH$_3$OH), 1.58 (m, –C(=O)CHC*H*$_3$O–).

Synthesis of iodobenzene-terminated poly(ε-caprolactone)

Scheme 2-8. Synthesis of poly(ε-caprolactone) as macroinitiator

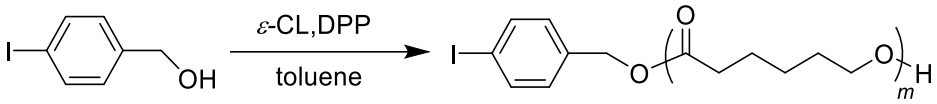

In a glovebox, DPP (73.1 mg, 292 μmol, 0.8 eq.) was added to a stirred solution of the 4-iodobenzyl alcohol (85.4 mg, 365 μmol, 1.0 eq.) and ε-CL (2.50 g, 21.9 mmol, 60 eq.) in dry-toluene (25 mL). After 6 h, an excess of Amberlyst® A21 was added to the reaction mixture to terminate the polymerization. The mixture was purified by reprecipitation using THF as a good solvent and cold MeOH as a poor solvent to give iodobenzene-terminated poly(ε-caprolactone) as a white powder. 1.91 g, 76.5%: white powder.

$M_{n,SEC}$ = 6500 g mol^{-1} (THF); $M_{n,NMR}$ = 6700 g mol^{-1} ($CDCl_3$), $Đ_M$ = 1.07.

^{1}H NMR (400 MHz, $CDCl_3$): δ (ppm) 7.75 (m, Ar–*H*), 5.19 (s, –C*H*$_2$O–), 4.06 (t, –COCH$_2$–), 3.65 (m, –C*H*$_2$OH), 2.31 (t, –C(=O)C*H*$_2$–), 1.60–1.70 (m, –C(=O)CH$_2$C*H*$_2$CH$_2$C*H*$_2$CH$_2$O–), 1.37 (m, –CO(CH$_2$)$_2$C*H*$_2$(CH$_2$)$_2$O–).

Synthesis of iodobenzene-terminated polystyrene

Scheme 2-9. Synthesis of polystyrene as macroinitiator

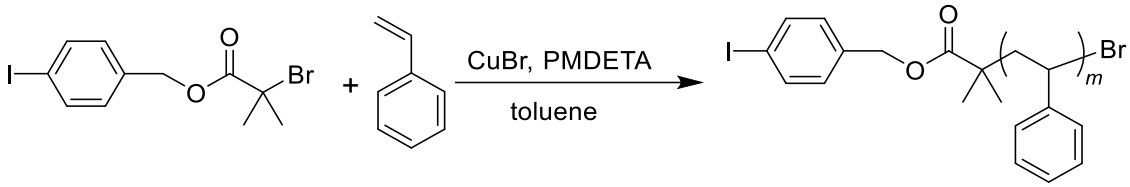

The preparation of iodobenzene-terminated polystyrene under the typical procedure is as follows: CuBr (230 mg, 1.60 mmol, 1.0 eq.) was evacuated for 30 min in a Schlenk flask and backfilled with argon. Styrene monomer was passed basic Al_2O_3 column firstly in order to remove the inhibitor. A mixture of styrene monomer (5.0 g, 48.0 mmol, 30 eq.), PMDETA (334 μL, 1.60 mmol, 1.0 eq.), and 4-iodobenzyl 2-bromo-2-methylpropanoate (613 mg, 1.60 mmol, 1.0 eq.) were then mixed in anhydrous toluene was prepared and then removed gas by three freeze-pump-thaw cycles were applied for further purifying the mixture. Next, the liquid mixture was transferred to a flask including CuBr for the polymerization. The polymerization, which was performed in a preheated oil bath at 50 °C and the monomer conversion was monitored by ^{1}H NMR at different polymerization time interval. The polymerization was terminated by bubbling air into the solution. The crude product was passed through a neutral Al_2O_3 column and eluted with THF to remove the catalyst. The mixture was purified by reprecipitation using THF as a good solvent and cold MeOH as a poor solvent to give iodobenzene-terminated polystyrene as white powder. 2.70 g, 53.9%.

$M_{n,SEC}$ = 2500 g mol^{-1} (THF); $M_{n,NMR}$ = 2150 g mol^{-1} ($CDCl_3$), $Đ_M$ = 1.17.

^{1}H NMR ($CDCl_3$, 400 MHz): δ (ppm) 7.22–7.49 (m, Ar–*H*), 6.49–6.39 (m, Ar–*H*), 5.13 (s, 2H, –C*H*$_2$O–), 2.00–1.54 (s, 2H, Ar−C*H*$_2$−), 1.92 (s, 6H, –C*H*$_3$).

Synthesis of iodobenzene-terminated polymers

Scheme 2-10. Synthesis of macroinitiator

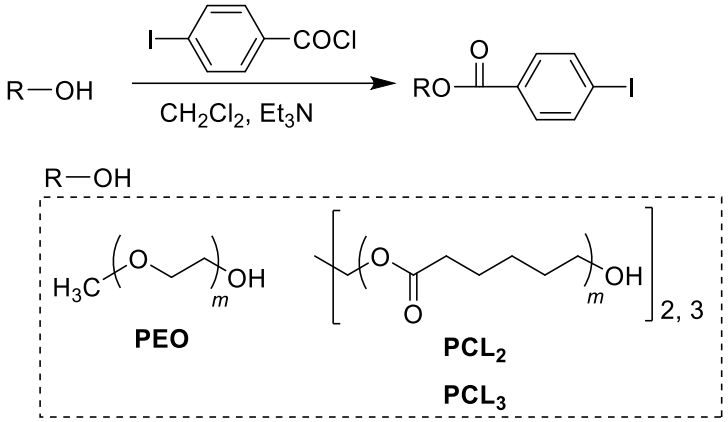

Polymer (PEO; $M_{n,NMR}$ = 5000 g mol^{-1} , PCL_2; $M_{n,NMR}$ = 7460 g mol^{-1} , PCL_3; $M_{n,NMR}$ = 6600 g mol^{-1}, 2.0 mmol) was added to a 200 mL three-necked flask and was dried under vacuum at room temperature for 9 h. The solution of 4-iodobenzoyl chloride (600 mg, 2.4 mmol), triethylamine (1.0 mL, 7.2 mmol), and dry CH_2Cl_2 (50 mL) was degassed by bubbling with Ar gas for 30 min and was then transferred to the three-necked flask using a cannula. The reaction mixture was stirred at room temperature for 24 h. The solvent was removed by rotary evaporation, and the residue was precipitated using THF as a good solvent and cold *n*-hexane as a poor solvent to give iodobenzene-terminated polymer as a white powder.

I−PEO

10.4 g, 99.5% yield: white powder. $M_{n,SEC}$ = 3100 g mol^{-1} (THF); $M_{n,NMR}$ = 5300 g mol^{-1} ($CDCl_3$), $Đ_M$ = 1.25.

^{1}H NMR (400 MHz, $CDCl_3$): δ (ppm) 7.90–7.66 (m, Ar–*H*), 3.67–3.56 (m, –C*H*$_2$C*H*$_2$–, –C*H*$_3$).

(I−PCL)$_2$

9.4 g, 93.9% yield: white powder. $M_{n,SEC}$ = 9400 g mol^{-1} (THF); $M_{n,NMR}$ = 7920 g mol^{-1} ($CDCl_3$), $Đ_M$ = 1.05.

^{1}H NMR (400 MHz, $CDCl_3$): δ (ppm) 7.94–7.74 (m, Ar–*H*), 4.32 (t, –C*H*$_2$OBz–I), 4.07 (t, –

$COCH_2$–), 2.32 (t, –C(=O)C*H*$_2$–), 1.70–1.60 (m, –C(=O)CH_2C*H*$_2$$CH_2$C*H*$_2$$CH_2$O–), 1.43–1.35 (m, –CO($CH_2$)$_2$C*H*$_2$($CH_2$)$_2$O–, –C*H*$_2$$CH_3$), 0.84 (s, –C*H*$_3$).

(I−PCL)$_3$

9.3 g, 93% yield: white powder. $M_{n,SEC}$ = 12,350 g mol^{-1} (THF); $M_{n,NMR}$ = 7290 g mol^{-1} ($CDCl_3$), $Đ_M$ = 1.05.

^{1}H NMR (400 MHz, $CDCl_3$): δ (ppm) 7.94–7.74 (m, Ar–*H*), 4.30 (t, –C*H*$_2$OBz–I), 4.06 (t, –$COCH_2$–), 2.31 (t, –C(=O)C*H*$_2$–), 1.89–1.55 (m, –C(=O)CH_2C*H*$_2$$CH_2$C*H*$_2$$CH_2$O–), 1.38 (m, –CO($CH_2$)$_2$C*H*$_2$($CH_2$)$_2$O–), 1.00 (s, –C*H*$_3$).

Synthesis of poly(*n*-butyl acrylate) having iodobenzene at the side chain

Scheme 2-11. Synthesis of macroinitiator

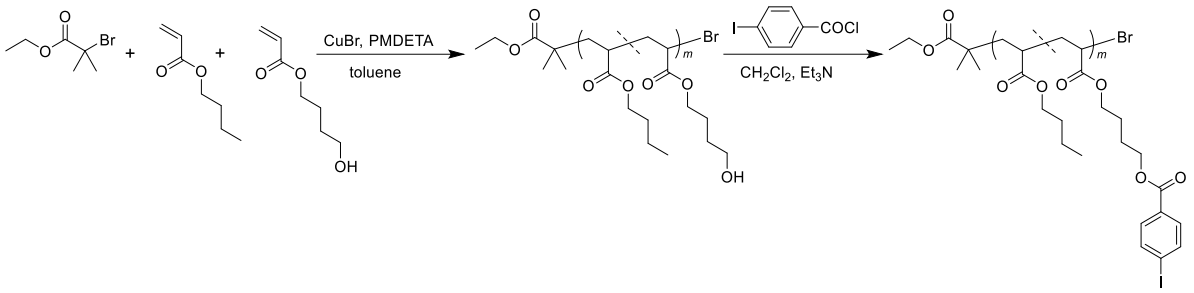

The preparation of poly(*n*-butyl acrylate) having iodobenzene at the side chain under the typical procedure is as follows: CuBr (336 mg, 2.34 mmol, 1.0 eq.) was evacuated for 30 min in a Schlenk flask and backfilled with argon. *n*-Butyl acrylate and 4-hydroxybutyl acrylate were passed basic Al_2O_3 column firstly in order to remove the inhibitor. A mixture of *n*-butyl acrylate (15 g, 117 mmol, 50 eq.), 4-hydroxybutyl acrylate (1.69 g, 2.34 mmol, 5 eq.), PMDETA (489 μL, 2.34 mmol, 1.0 eq.), and ethyl 2-bromoisobutyrate (457 mg, 2.34 mmol, 1.0 eq.) were then mixed in anhydrous toluene was prepared and then removed gas by three freeze-pump-thaw cycles were applied for further purifying the mixture. Next, the liquid mixture was transferred to a flask including CuBr for the polymerization. The polymerization, which was performed in a preheated oil bath at 50 °C and the monomer conversion was monitored by ^{1}H NMR at different polymerization time interval. The reaction mixture was quenched in liquid nitrogen and allowed to warm to room temperature. After the remaining *n*-butyl acrylate and 4-hydroxy acrylate were removed under reduced pressure, 4-iodobenzoyl chloride (600 mg, 2.08 mmol), triethylamine (1.64 mL, 3.12 mmol), and dry CH_2Cl_2 (50 mL) were added to the residue, and the solution was stirred at room temperature for 24 h. The solvent was removed by rotary evaporation, and the residue was precipitated using THF as a good solvent and cold *n*-hexane as a poor solvent to give poly(*n*-butyl acrylate) having iodobenzene at the side chain as a yellow viscous liquid. 6.67 g, 40.0%.

$M_{n,SEC}$ = 7630 g mol^{-1} (THF); $M_{n,NMR}$ = 8130 g mol^{-1} ($CDCl_3$), $Đ_M$ = 1.09.

^{1}H NMR ($CDCl_3$, 400 MHz): δ (ppm) 7.94–7.74 (m, Ar–*H*), 4.35 (t, –C*H*$_2$OBz–I), 4.04 (t, –C(=O)OC*H*$_2$CH$_2$–), 2.28 (br, –C*H*$_2$CH–), 1.92 (br, –CH$_2$C*H*–), 1.60–1.38 (m, –(C*H*$_2$)$_2$–), 1.24 (t, –CH$_2$C*H*$_3$), 1.09 (d, –C(=O)C(C*H*$_3$)$_2$–), 0.94 (t, –C*H*$_3$).

Polymerization of potassium 2-(7-bromo-9,9-dihexyl-9*H*-fluorene-2-yl)triolborate

Scheme 2-12. Polymerization of triolborate salt-type fluorene monomer

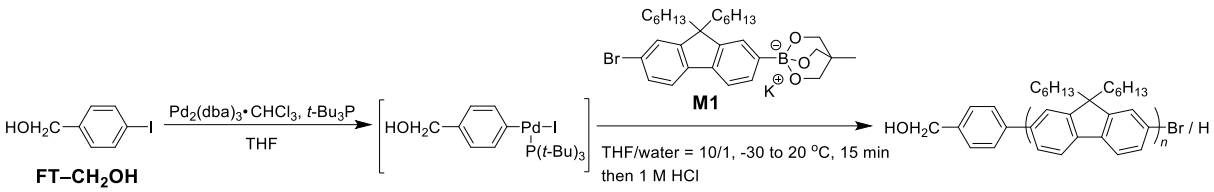

In the glovebox, 4-iodobenzyl alcohol (**FI−CH$_2$OH**; 115 μL, 57.5 μmol, as 0.50 mol L^{-1} stock solution in THF), $Pd_2(dba)_3$•$CHCl_3$ (17.9 mg, 17.2 μmol), and *t*-Bu_3P (253 μL, 127 μmol, as 0.5 mol L^{-1} stock solution in THF) were placed in a vial and dissolved in THF (5 mL). After stirring for 1 h at room temperature, the mixture was passed through a 0.45 μm PTFE filter to produce a Pd-initiator solution. The vial containing the stock solution of the Pd-initiator was sealed and taken out from the glovebox. In a 300 mL recovery flask, a mixture of THF (86 mL) and deionized water (8.6 mL) was deoxygenated by argon bubbling at least for 1 h. The stock solution of the Pd-initiator was transferred to the flask using a cannula under an argon atmosphere, and the entire mixture was cooled to −10 °C. Potassium 2-(7-bromo-9,9-dihexyl-9*H*-fluorene-2-yl)triolborate (**M1**; 3.45 mL, 0.86 mmol, as 0.25 mol L^{-1} stock solution in THF) was quickly added to the mixture under an argon atmosphere, and the entire mixture was vigorously stirred for 15 min at −10 °C. To the reaction mixture, 1 mol L^{-1} HCl (5 mL) was added to terminate the polymerization. The solvent was removed by evaporation, and the residue was dissolved in CH_2Cl_2 and washed with brine. The organic layer was dried over Na_2SO_4 and concentrated. The mixture was filtered, and the filtrate was evaporated under reduced pressure. The resulting solution was concentrated and precipitated using THF as a good solvent and cold acetone as a poor solvent to give **HOCH$_2$−PF**. The polymerization results are listed in Table 2-7.

Table 2-7. SCTP of **M1** under various conditions [a]

temp (°C)	$M_{n,SEC}$ [b] (g mol^{-1})	$M_{n,NMR}$ [c] (g mol^{-1})	$Đ_M$ [b]	yield [d] (%)	yield (mg)
20	8500	9500	1.36	80.3	230
0	8300	9200	1.33	85.2	244
−10	5700	5800	1.18	84.3	241
−30	—	—	—	—	—

[a] Polymerization condition: Ar atmosphere; solvent, THF/water (v/v) = 10/1; [**M1**]$_0$ = 10 mmol L^{-1}; [**M1**]$_0$/[**FI−CH$_2$OH**]$_0$/[$Pd_2(dba)_3$•$CHCl_3$]/[*t*-Bu_3P] = 15/1/0.3/2.2. [b] Determined by SEC (PSt standards, THF, 40 °C). [c] Determined by ^{1}H NMR spectrum in $CDCl_3$. [d] Isolated yields.

Evaluation of the living nature of the SCTP of triolborate salt-type monomer

Scheme 2-13. Post-polymerization experiment for the SCTP

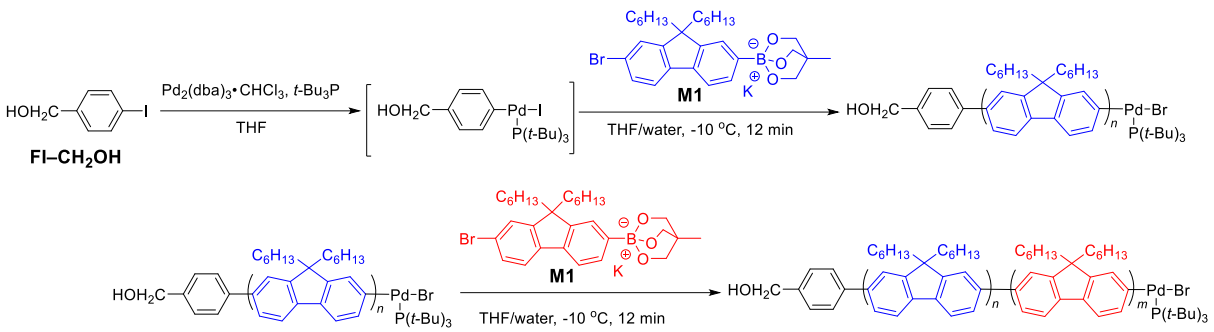

In the glovebox, **FI−CH$_2$OH** (1.15 mL, 0.58 mmol, as 0.5 mol L^{-1} stock solution in THF), $Pd_2(dba)_3$•$CHCl_3$ (178.6 mg, 0.173mmol), and *t*-Bu_3P (2.53 mL, 1.27 mmol, as 0.5 mol L^{-1} stock solution in THF) were placed in a vial and dissolved in THF (15 mL). After stirring for 1 h at room temperature, the mixture was passed through a 0.45 μm PTFE filter to produce a Pd-initiator solution. The vial containing the stock solution of the Pd-initiator was sealed and taken out from the glovebox. In a 1000 mL recovery flask, a mixture of THF (860 mL) and water (86 mL) was deoxygenated by argon bubbling at least for 1 h. The stock solution of the Pd-initiator was transferred to the flask using a cannula under an argon atmosphere, and the entire mixture was cooled to −10 °C. **M1** (34.5 mL, 8.63 mmol, as 0.25 mol L^{-1} stock solution in THF) was quickly added to the mixture under an argon atmosphere, and the entire mixture was vigorously stirred for 12 min at −10 °C. Then, **M1** (34.5 mL, 8.63 mmol, as 0.25 mol L^{-1} stock solution in THF) was added. A small aliquot (0.3 mL) of the reaction mixture was collected at 0.5, 1.0, 2.0, 5.0, 10, 12.5, 13, 14, 17, and 24 min. Each aliquot was quenched with 1 mol L^{-1} HCl solution and extracted with CH_2Cl_2. The separated organic layer was evaporated under reduced pressure to get a residue. Half of the residue was dissolved in $CDCl_3$ to determine the conversion of monomer by ^{1}H NMR (conversions of 31%, 39%, 65%, 85%, 99%, 119%, 146%, 161%, 176%, and 199% were observed for 0.5, 1.0, 2.0, 5.0, 10, 12.5, 13, 14, 17, and 24 min, respectively). The other half of the residue was dissolved in THF, and the solution was

filtered. The filtrate was analyzed by SEC to determine the M_n and $Đ_M$ values of the polymers. The $M_{n,SEC}$ ($Đ_M$) values of each polymer initiated by $Pd_2(dba)_3$•$CHCl_3$/*t*-Bu_3P/**FI−CH₂OH** for 0.5, 1.0, 2.0, 5.0, 10, 12.5, 13, 14, 17, and 24 min were 1960 (1.22), 2400 (1.22), 3860 (1.23), 4970 (1.23), 5760 (1.23), 6940 (1.25), 8450 (1.25), 9280 (1.26), 9850 (1.27), and 11460 g mol^{-1} (1.28) respectively. The polymerization results are listed in Table 2-8.

Table 2-8. Monomer conversion, molecular weight, and dispersity at each reaction time[a]

reaction time (min)	conversion (%)	$M_{n,SEC}$[b] (g mol^{-1})	$Đ_M$[b]	$M_{n,NMR}$[c] (g mol^{-1})
0.5	31	2100	1.22	1960
1.0	39	2500	1.22	2400
2.0	65	3700	1.23	3860
5.0	85	5000	1.23	4970
10.0	99	6100	1.24	5760
12.5	119	7100	1.25	6940
13.0	146	8600	1.25	8450
14.0	161	9400	1.26	9280
17.0	176	10,000	1.27	9850
24.0	199	12,000	1.28	11,460

[a] Polymerization conditions: Ar atmosphere; solvent, THF/water (v/v) = 10/1; [**M1**]$_0$ = 10 mmol L^{-1}; [**M1**]$_0$/[**FI−CH₂OH**]$_0$/[$Pd_2(dba)_3$•$CHCl_3$]/[*t*-Bu_3P] = 15/1/0.3/2.2. [b] Determined by SEC (PSt standards, THF, 40 °C). [c] Determined by ^{1}H NMR spectrum in $CDCl_3$.

Molecular weight control

Scheme 2-14. Molecular weight control of PF

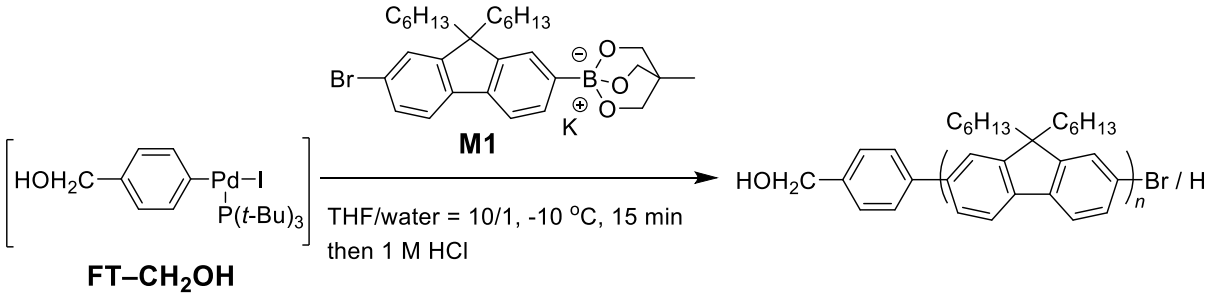

A polymerization of **M1** was conducted with the optimized condition while varying the [**M1**]$_0$/[**FI−CH$_2$OH**]$_0$ ratio (30/1, 45/1, 90/1, 180/1 and 270/1) for aiming at synthesizing the higher molecular weight PFs. The final product of **HOCH$_2$−PF** was obtained as a yellow solid. The polymerization results are listed in Table 2-9.

Table 2-9. Synthesis of PFs with varied molecular weights[a]

[**M1**]$_0$/[**FI−CH$_2$OH**]$_0$	degree of polymerization[b]	$M_{n,SEC}$ [b] (g mol^{-1})	$Đ_M$[b]	$M_{n,NMR}$ [c] (g mol^{-1})	yield[d] (%)
15	17	5700	1.18	5800	84.3
30	37	10,000	1.24	12,600	83.2
45	53	14,200	1.25	17,800	84.3
90	88	25,700	1.28	29,400	85.4
180	205	44,700	1.37	68,300	82.6
270	250	69,400	1.38	83,300	88.9

[a] Polymerization conditions: temperature, −10 °C; Ar atmosphere; solvent, THF/water (v/v) = 10/1; [**M1**]$_0$ = 10 mmol L^{-1}; [**FI−CH$_2$OH**]$_0$/[Pd$_2$(dba)$_3$•CHCl$_3$]/[*t*-Bu$_3$P]/[K$_3$PO$_4$] = 1/0.3/2.2/1.5. [b] Determined by SEC (PSt standards, THF, 40 °C). [c] Determined by ^{1}H NMR spectrum in CDCl$_3$. [d] Isolated yields.

Synthesis of *α*-end-functionalized PFs using functional initiators

Scheme 2-15. Polymerization with various initiators

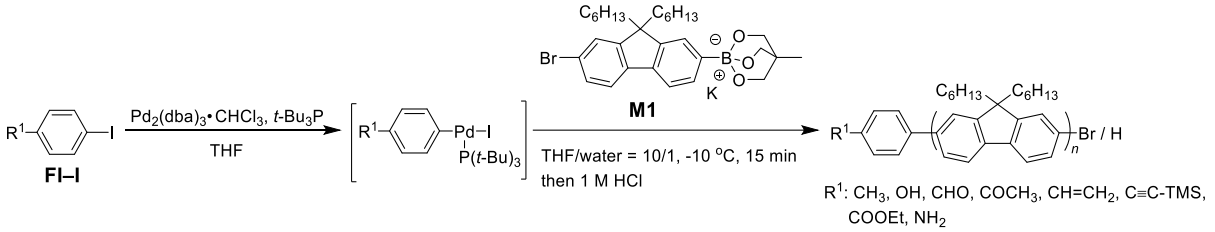

The *α*-end-functionalized PF was synthesized by the SCTP of **M1** (3.45 mL, 0.86 mmol, as 0.25 mol L^{-1} stock solution in THF) with aryl halide (**FI−R^1**; 115 μL, 57.5 μmol, as 0.50 mol L^{-1} stock solution in THF), $Pd_2(dba)_3$•$CHCl_3$ (17.9 mg, 17.2 μmol), *t*-Bu_3P (253 μL, 127 μmol, as 0.5 mol L^{-1} stock solution in THF) in a mixture of THF (86 mL), K_3PO_4 (18.3 mg, 86.3 μmol), and deionized water (8.6μL). The final products of *α*-end-functionalized PF was obtained as a yellow solid.

α-Methyl-functionalized poly(9,9-dihexyl-2,7-fluorene)

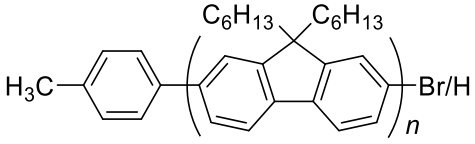

248 mg, 86.8% yield: Yellow solid. $M_{n,SEC}$ = 4800 g mol^{-1} (THF); $M_{n,NMR}$ = 4400 g mol^{-1} ($CDCl_3$), $Đ_M$ = 1.35.

^{1}H NMR (400 MHz, $CDCl_3$): *δ* (ppm) 7.93–7.77 (m, Ar–*H*), 7.75–7.57 (m, Ar–*H*), 7.50 (d, Ar–*H*), 2.45 (s, –C*H*$_3$), 2.12 (br, –C*H*$_2$(CH_2)$_4$$CH_3$), 1.36–0.66 (m, –$CH_2$(C*H*$_2$)$_4$C*H*$_3$).

α-Hydroxyl-functionalized poly(9,9-dihexyl-2,7-fluorene)

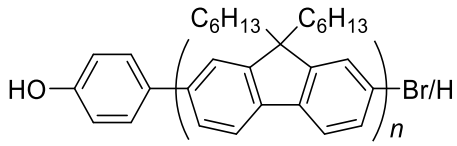

245 mg, 85.8% yield: Yellow solid. $M_{n,SEC}$ = 5100 g mol^{-1} (THF); $M_{n,NMR}$ = 5300 g mol^{-1} ($CDCl_3$), $Đ_M$ = 1.27.

^{1}H NMR (400 MHz, $CDCl_3$): δ (ppm) 7.93–7.77 (m, Ar–*H*), 7.75–7.57 (m, Ar–*H*), 7.50 (d, Ar–*H*), 2.12 (br, –C*H*$_2$(CH$_2$)$_4$CH$_3$), 1.36–0.66 (m, –CH$_2$(C*H*$_2$)$_4$C*H*$_3$).

α-Amino-functionalized poly(9,9-dihexyl-2,7-fluorene)

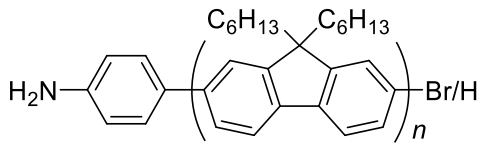

208 mg, 73.0% yield: Yellow solid. $M_{n,SEC}$ = 5000 g mol^{-1} (THF); $M_{n,NMR}$ = 5100 g mol^{-1} ($CDCl_3$), $Đ_M$ = 1.19.

^{1}H NMR (400 MHz, $CDCl_3$): δ (ppm) 7.93–7.77 (m, Ar–*H*), 7.75–7.57 (m, Ar–*H*), 7.50 (d, Ar–*H*), 2.37 (s, -C*H*$_3$), 2.12 (br, –C*H*$_2$(CH$_2$)$_4$CH$_3$), 1.36–0.66 (m, –CH$_2$(C*H*$_2$)$_4$C*H*$_3$).

α-Aldehyde-functionalized poly(9,9-dihexyl-2,7-fluorene)

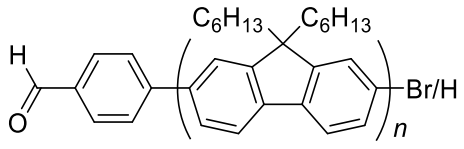

253 mg, 88.4% yield: Yellow solid. $M_{n,SEC}$ = 5000 g mol^{-1} (THF); $M_{n,NMR}$ = 7800 g mol^{-1} ($CDCl_3$), $Đ_M$ = 1.30.

^{1}H NMR (400 MHz, $CDCl_3$): δ (ppm) 10.11 (–C*H*O), 7.93–7.77 (m, Ar–*H*), 7.75–7.57 (m, Ar–*H*), 7.50 (d, Ar–*H*) , 2.37 (s, -C*H*$_3$), 2.12 (br, –C*H*$_2$(CH$_2$)$_4$CH$_3$), 1.36–0.66 (m, –CH$_2$(C*H*$_2$)$_4$C*H*$_3$).

α-Acetyl-functionalized poly(9,9-dihexyl-2,7-fluorene)

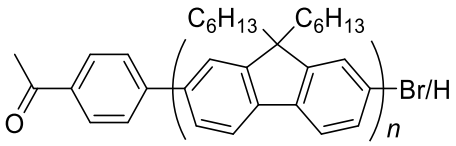

238 mg, 83.3% yield: Yellow solid. $M_{n,SEC}$ = 5300 g mol^{-1} (THF); $M_{n,NMR}$ = 5700 g mol^{-1} ($CDCl_3$), $Đ_M$ = 1.36.

^{1}H NMR (400 MHz, $CDCl_3$): δ (ppm) 7.93–7.77 (m, Ar–*H*), 7.75–7.57 (m, Ar–*H*), 7.50 (d, Ar–*H*), 3.51 (d, –COC*H*$_3$), 2.12 (br, –C*H*$_2$(CH$_2$)$_4$CH$_3$), 1.36–0.66 (m, –CH$_2$(C*H*$_2$)$_4$C*H*$_3$).

α-Ethyl ester-functionalized poly(9,9-dihexyl-2,7-fluorene)

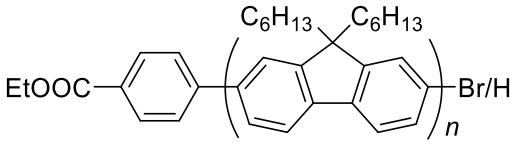

234 mg, 81.7% yield: Yellow solid. $M_{n,SEC}$ = 5200 g mol^{-1} (THF); $M_{n,NMR}$ = 4100 g mol^{-1} ($CDCl_3$), $Đ_M$ = 1.23.

^{1}H NMR (400 MHz, $CDCl_3$): δ (ppm) 7.93–7.77 (m, Ar–*H*), 7.75–7.57 (m, Ar–*H*), 7.50 (d, Ar–*H*), 4.45 (m, –C*H*$_2$CH$_3$), 2.12 (br, –C*H*$_2$(CH$_2$)$_4$CH$_3$), 1.45 (–C*H*$_3$), 1.36–0.66 (m, –CH$_2$(C*H*$_2$)$_4$C*H*$_3$).

α-Vinyl-functionalized poly(9,9-dihexyl-2,7-fluorene)

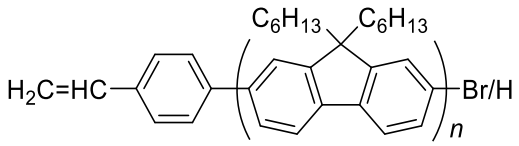

231 mg, 80.8% yield: Yellow solid. $M_{n,SEC}$ = 4,500 g mol^{-1} (THF); $M_{n,NMR}$ = 4,100 g mol^{-1} ($CDCl_3$), $Đ_M$ = 1.28.

^{1}H NMR (400 MHz, $CDCl_3$): δ (ppm) 7.93–7.77 (m, Ar–*H*), 7.75–7.57 (m, Ar–*H*), 7.50 (d, Ar–*H*), 5.93 m, (–C*H*=CH_2), 5.29, 4.74 (–CH=C*H*$_2$), 2.12 (br, –C*H*$_2$(CH_2)$_4$$CH_3$), 1.36–0.66 (m, –$CH_2$(C*H*$_2$)$_4$C*H*$_3$).

α-Trimethylsilylethynyl-functionalized poly(9,9-dihexyl-2,7-fluorene)

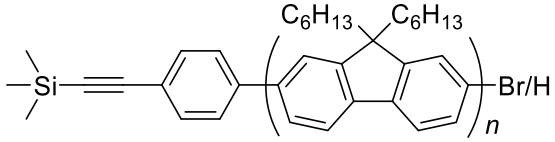

237 mg, 82.8% yield: Yellow solid. $M_{n,SEC}$ = 6000 g mol^{-1} (THF); $M_{n,NMR}$ = 7700 g mol^{-1} ($CDCl_3$), $Đ_M$ = 1.35.

^{1}H NMR (400 MHz, $CDCl_3$): δ (ppm) 7.93–7.77 (m, Ar–*H*), 7.75–7.57 (m, Ar–*H*), 7.50 (d, Ar–*H*), 2.12 (br, –C*H*$_2$(CH_2)$_4$$CH_3$), 1.36–0.66 (m, –$CH_2$(C*H*$_2$)$_4$C*H*$_3$), 0.8 (–Si–C≡C–(C*H*$_3$)$_3$).

Synthesis of *ω*-end-functionalized PF using functional terminators

Scheme 2-16. Polymerization with various terminators

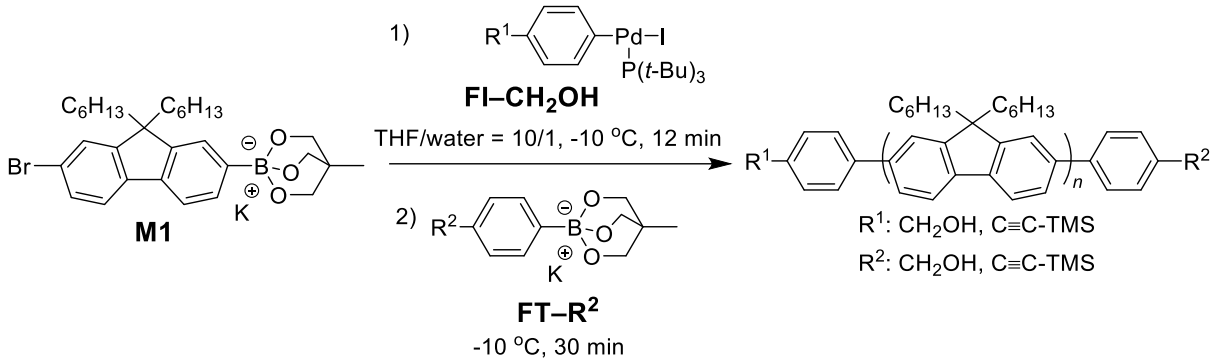

In the glovebox, **FI−CH$_2$OH** (115 μL, 57.5 μmol, as 0.50 mol L^{-1} stock solution in THF), $Pd_2(dba)_3$•$CHCl_3$ (17.9 mg, 17.2 μmol), and *t*-Bu_3P (253 μL, 127 μmol, as 0.5 mol L^{-1} stock solution in THF) were placed in a vial and dissolved in THF (5 mL). After stirring for 1 h at room temperature, the mixture was passed through a 0.45 mm PTFE filter to produce a Pd-initiator solution. The vial containing the stock solution of the Pd-initiator was sealed and taken out of the glovebox. In a 100 mL recovery flask, THF (86 mL), K_3PO_4 (18.3 mg, 86.3 μmol), and deionized water (8.6μL) were deoxygenated by argon bubbling at least for 1 h. The stock solution of the Pd-initiator was transferred to the flask using a cannula under an argon atmosphere, and the entire mixture was cooled to −10 °C. **M1** (3.45 mL, 0.86 mmol, as 0.25 mol L^{-1} stock solution in THF) was quickly added to the mixture under an argon atmosphere, and the entire mixture was vigorously stirred for 12 min at −10 °C. The reaction was quenched by injecting potassium aryltriolborate (**FT−R^2**; 2.30 mL, 575 μmol, as 0.25 mol L^{-1} stock solution in THF) and stirred for 30 min. The solvent was removed by evaporation, and the residue was dissolved in CH_2Cl_2 and washed with brine. The organic layer was dried over Na_2SO_4 and concentrated. The mixture was filtered and the filtrate was evaporated under reduced pressure. The resulting solution was concentrated and precipitated using THF as a good solvent and cold acetone as a poor solvent to give the *ω*-end-functionalized PF.

α,*ω*-Dihydroxymethyl-functionalized poly(9,9-dihexyl-2,7-fluorene)

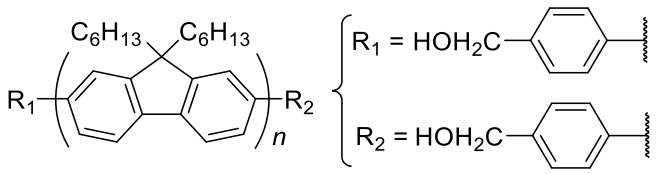

224 mg, 78.2% yield: Yellow solid. $M_{n,SEC}$ = 6100 g mol^{-1} (THF); $M_{n,NMR}$ = 5600 g mol^{-1} ($CDCl_3$), $Đ_M$ = 1.25.

^{1}H NMR (400 MHz, $CDCl_3$): δ (ppm) 7.93–7.77 (m, Ar–*H*), 7.75–7.57 (m, Ar–*H*), 7.50 (d, Ar–*H*), 4.97 (s, –C*H*$_2$OH), 2.12 (br, –C*H*$_2$(CH$_2$)$_4$CH$_3$), 1.36–0.66 (m, –CH$_2$(C*H*$_2$)$_4$C*H*$_3$).

α-Hydroxymethyl,*ω*-trimethylsilylethynyl-functionalized poly(9,9-dihexyl-2,7-fluorene)

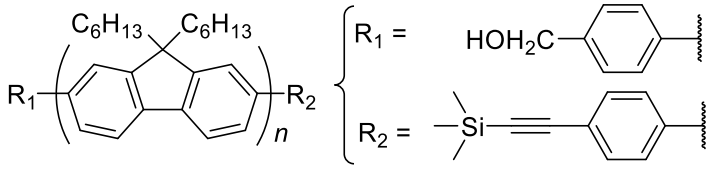

252 mg, 88.0% yield: Yellow solid. $M_{n,SEC}$ = 6600 g mol^{-1} (THF); $M_{n,NMR}$ = 5600 g mol^{-1} ($CDCl_3$), $Đ_M$ = 1.31.

^{1}H NMR (400 MHz, $CDCl_3$): δ (ppm) 7.93–7.77 (m, Ar–*H*), 7.75–7.57 (m, Ar–*H*), 7.50 (d, Ar–*H*), 4.97 (s, –C*H*$_2$OH), 2.12 (br, –C*H*$_2$(CH$_2$)$_4$CH$_3$), 1.36–0.66 (m, –CH$_2$(C*H*$_2$)$_4$C*H*$_3$) , 0.8 (–Si–C≡C–(C*H*$_3$)$_3$).

α, *ω*-Bistrimethylsilylethynyl-functionalized poly(9,9-dihexyl-2,7-fluorene)

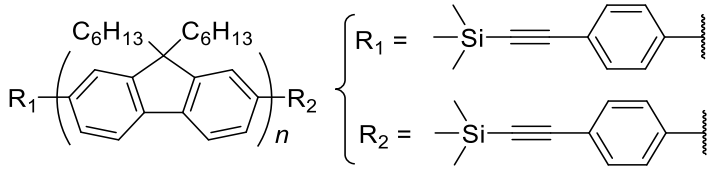

252 mg, 88.0% yield: Yellow solid. $M_{n,SEC}$ = 8700 g mol^{-1} (THF); $M_{n,NMR}$ = 6800 g mol^{-1} ($CDCl_3$), $Đ_M$ = 1.36.

^{1}H NMR (400 MHz, $CDCl_3$): δ (ppm) 7.93–7.77 (m, Ar–*H*), 7.75–7.57 (m, Ar–*H*), 7.50 (d, Ar–*H*), 4.97 (s, –C*H*$_2$OH), 2.12 (br, –C*H*$_2$(CH$_2$)$_4$CH$_3$), 1.36–0.66 (m, –CH$_2$(C*H*$_2$)$_4$C*H*$_3$) , 0.8 (–Si–C≡C–(C*H*$_3$)$_3$).

Effect of water content in the solvent on the polymerization properties

Scheme 2-17. Polymerization in THF/water cosolvent with varied water content

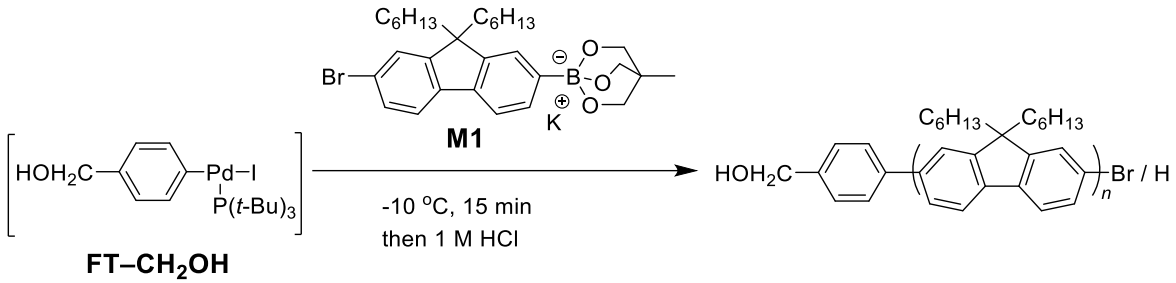

In order to elucidate the effect of water content in the solvent on the polymerization properties, the SCTP of **M1** was performed with varying the THF/water ratio (THF/water (v/v) = 10/1, 100/1, 1000/1, 5000/1, and without water). The final product of **HOCH₂−PF** was obtained as a yellow solid.

The effect on water on polymerization

Scheme 2-18. The effect of water on SCTP

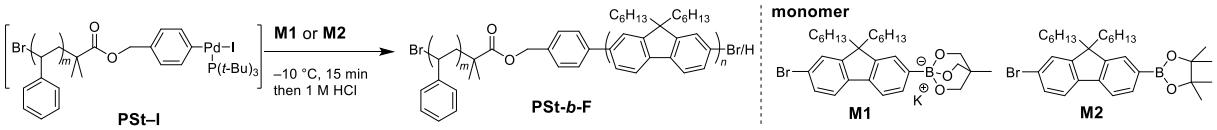

In order to adjust the polymerization effect of water in the solvent, **M1** or **M2** polymerization was performed while varying the [THF]/[water] ratio (10/1 and 5000/1). The final product of **HOCH$_2$−PF** was obtained as a yellow solid. The polymerization results are listed in Table 2-5.

Synthesis of PF-containing block copolymers using macroinitiators

Scheme 2-19. Synthesis of PF-containing block copolymers by SCTP with various macroinitiators

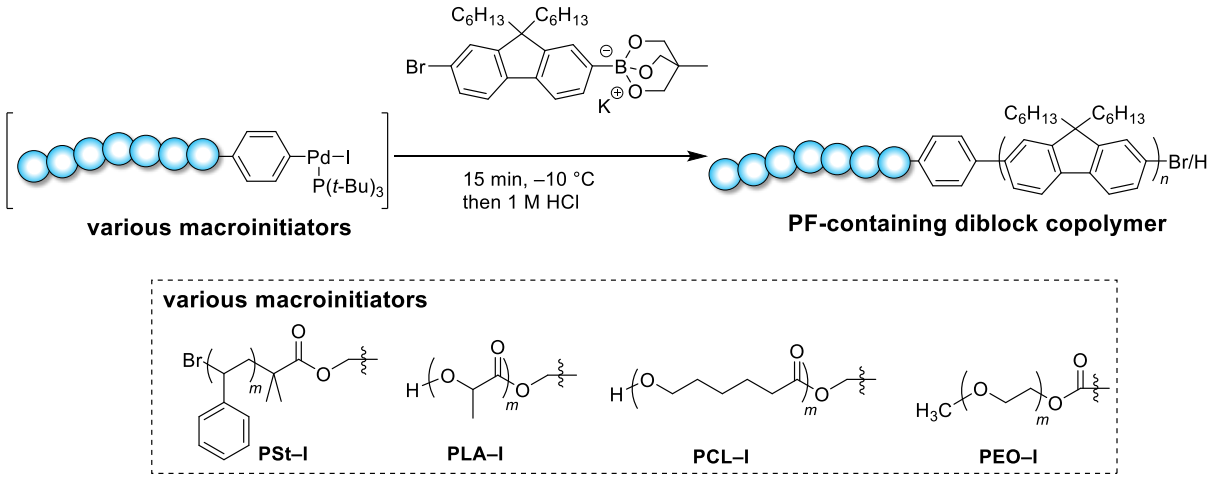

The PF-containing block copolymers were synthesized by the SCTP of **M1** (10.4 mL, 2.59 mmol, as 0.25 mol L^{-1} stock solution in THF) with the macroinitiators (**I−St**; $M_{n,\,NMR}$; 11,300, $Đ_M$; 1.10, **I−PLA**; $M_{n,\,NMR}$; 9500, $Đ_M$; 1.06, **I−PCL**; $M_{n,\,NMR}$; 11,300, $Đ_M$; 1.10, **I−PEO**; $M_{n,\,NMR}$; 11,300, $Đ_M$; 1.10, 86.3 μmol, 1.0 eq.), $Pd_2(dba)_3$•$CHCl_3$ (26.8 mg, 25.9 μmol, 0.5 eq.), *t*-Bu_3P (380 μL, 190 μmol, as 0.5 mol L^{-1} stock solution in THF, 2.2 eq.) in a mixture of THF (248 mL), K_3PO_4 (2.7 mg, 130 μmol, 1.5 eq.), and deionized water (25 μL, 60 eq.). The final products were obtained as a yellow solid.

PF-*b*-PSt

0.93 g, 87.0% yield: Yellow solid. $M_{n,SEC}$ = 12,700 g mol^{-1} (THF); $M_{n,NMR}$ = 12,700 g mol^{-1} ($CDCl_3$), $Đ_M$ = 1.20.

^{1}H NMR (400 MHz, $CDCl_3$): δ (ppm) 7.93–7.77 (m, Ar–*H*), 7.75–7.57 (m, Ar–*H*), 7.50 (d, Ar–*H*), 7.30–6.30 (m, Ar–*H*), 2.12 (br, –C*H*$_2$(CH_2)$_4$$CH_3$), 2.00–1.54 (m, –C*H*C*H*$_2$–), 1.36–0.66 (m, –CH_2(C*H*$_2$)$_4$C*H*$_3$).

PF-*b*-PLA

1.30 g, 90.0% yield: Yellow solid. $M_{n,SEC}$ = 16,800 g mol^{-1} (THF); $M_{n,NMR}$ = 15,700 g mol^{-1} ($CDCl_3$), $Đ_M$ = 1.19.

^{1}H NMR (400 MHz, $CDCl_3$): δ (ppm) 7.93–7.77 (m, Ar–*H*), 7.75–7.57 (m, Ar–*H*), 7.50 (d, Ar–*H*), 5.29-5.11 (m, –COC*H*(CH_3)O–), 1.66-1.43 (m, –COCH(C*H*$_3$)O–), 2.12 (br, –C*H*$_2$(CH_2)$_4$$CH_3$), 1.36–0.66 (m, –$CH_2$(C*H*$_2$)$_4$C*H*$_3$).

PF-*b*-PCL

1.33 g, 85.0% yield: Yellow solid. $M_{n,SEC}$ = 17,700 g mol^{-1} (THF); $M_{n,NMR}$ = 16,000 g mol^{-1} ($CDCl_3$), $Đ_M$ = 1.11.

^{1}H NMR (400 MHz, $CDCl_3$): δ (ppm) 7.93–7.77 (m, Ar–*H*), 7.75–7.57 (m, Ar–*H*), 7.50 (d, Ar–*H*), 4.06 (t, –COC*H*$_2$–), 3.65 (m, –C*H*$_2$OH), 2.31 (t, –COOC*H*$_2$–), 2.12 (br, –C*H*$_2$(CH_2)$_4$$CH_3$), 1.60-1.70 (m, –COCH$_2$C*H*$_2$($CH_2$)$_2$$CH_2$$CH_2$O–),1.37 (m, –CO($CH_2$)$_2$C*H*$_2$($CH_2$)$_2$O–), 1.36–0.66 (m, –$CH_2$(C*H*$_2$)$_4$C*H*$_3$).

PF-*b*-PEO

1.04 g, 67.3% yield: Yellow solid. $M_{n,SEC}$ = 10,300 g mol^{-1} (THF); $M_{n,NMR}$ = 14,200 g mol^{-1} ($CDCl_3$), $Đ_M$ = 1.50.

^{1}H NMR (400 MHz, $CDCl_3$): δ (ppm) 7.93–7.77 (m, Ar–*H*), 7.75–7.57 (m, Ar–*H*), 7.50 (d, Ar–*H*), 3.67-3.55 (m, –OC*H*$_2$C*H*$_2$–, –OC*H*$_3$), 2.12 (br, –C*H*$_2$(CH_2)$_4$$CH_3$), 2.00–1.54 (m, –C*H*C*H*$_2$–), 1.36–0.66 (m, –CH_2(C*H*$_2$)$_4$C*H*$_3$).

Synthesis of PF-containing diblock copolymer using multiple initiating sites

Scheme 2-20. Synthesis of PF-containing diblock copolymer by SCTP with multiple initiating sites

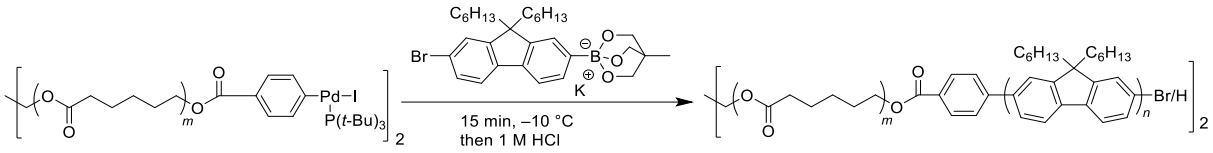

The PF-containing block copolymers were synthesized by the SCTP of **M1** (10.4 mL, 2.59 mmol, as 0.25 mol L^{-1} stock solution in THF) with the macroinitiators (**(I−PCL)2**; $M_{n,NMR}$ = 7900 g mol^{-1}, $Đ_M$ = 1.05, 68.3 mg, 86.3 μmol, 1.0 eq.), $Pd_2(dba)_3$•$CHCl_3$ (8.9 mg, 8.63 μmol, 1.0 eq.), *t*-Bu_3P (76 μL, 38 μmol, as 0.5 mol L^{-1} stock solution in THF, 4.4 eq.) in a mixture of THF (248 mL), K_3PO_4 (5.5 mg, 26 μmol, 3.0, eq.), and deionized water (25 μL, 60 eq.). The final products were obtained as a yellow solid.

PF-*b*-PCL-*b*-PF

96.6 mg, 88.5% yield: Yellow solid. $M_{n,SEC}$ = 15,800 g mol^{-1} (THF); $M_{n,NMR}$ = 17,800 g mol^{-1} ($CDCl_3$), $Đ_M$ = 1.10.

^{1}H NMR (400 MHz, $CDCl_3$): δ (ppm) 7.94–7.74 (m, Ar–*H*), 7.75–7.57 (m, Ar–*H*), 7.50 (d, Ar–*H*), 4.32 (t, –C*H*$_2$OBz–I), 4.07 (t, –COC*H*$_2$-), 2.32 (t, –COOC*H*$_2$–), 1.70–1.60 (m, –C(=O)CH$_2$C*H*$_2$CH$_2$C*H*$_2$CH$_2$O–), 2.12 (br, –C*H*$_2$(CH$_2$)$_4$CH$_3$), 1.70–1.60 (m, –COCH$_2$C*H*$_2$(CH$_2$)$_2$CH$_2$CH$_2$O–),1.43–1.35 (m, –CO(CH$_2$)$_2$C*H*$_2$(CH$_2$)$_2$O–), 1.36–0.66 (m, –CH$_2$(C*H*$_2$)$_4$C*H*$_3$, –C*H*$_3$).

Synthesis of PF-containing star-block copolymer using multiple initiating sites

Scheme 2-21. Synthesis of PF-containing star-block copolymer by SCTP with multiple initiating sites

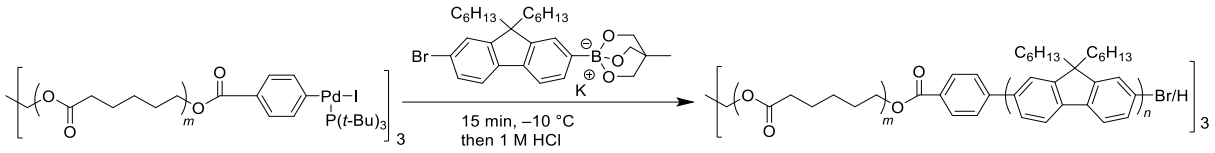

The PF-containing block copolymers were synthesized by the SCTP of **M1** (10.4 mL, 2.59 mmol, as 0.25 mol L^{-1} stock solution in THF) with the macroinitiators (**(I−PCL)$_3$**; $M_{n,NMR}$ = 7900 g mol^{-1}, $Đ_M$ = 1.05, 62.9 mg, 86.3 μmol, 1.0e.q), $Pd_2(dba)_3$•$CHCl_3$ (13.4 mg, 13 μmol, 1.5 e.q), *t*-Bu_3P (114 μL, 57 μmol, as 0.5 mol L^{-1} stock solution in THF, 6.6 e.q) in a mixture of THF (248 mL), K_3PO_4 (8.2 mg, 39 μmol, 4.5 e.q), and deionized water (25 μL, 60 eq.). The final products were obtained as a yellow solid.

(PCL-*b*-PF)$_3$

87.9 mg,82.6% yield: Yellow solid. $M_{n,SEC}$ = 15,300 g mol^{-1} (THF); $M_{n,NMR}$ = 17,100 g mol^{-1} ($CDCl_3$), $Đ_M$ = 1.07.

^{1}H NMR (400 MHz, $CDCl_3$): δ (ppm) 7.93–7.74 (m, Ar–*H*), 7.75–7.57 (m, Ar–*H*), 7.50 (d, Ar–*H*), 4.30 (t, –C*H*$_2$OBz–I), 4.06 (t, –COC*H*$_2$–), 2.31 (t, –C(=O)C*H*$_2$–), 1.89–1.55 (m, –C(=O)CH$_2$C*H*$_2$CH$_2$C*H*$_2$CH$_2$O–), 2.12 (br, –C*H*$_2$(CH$_2$)$_4$CH$_3$), 1.60–1.70 (m, –COCH$_2$C*H*$_2$(CH$_2$)$_2$CH$_2$CH$_2$O–), 1.38 (m, –CO(CH$_2$)$_2$C*H*$_2$(CH$_2$)$_2$O–, –C*H*$_3$), 1.36–0.66 (m, –CH$_2$(C*H*$_2$)$_4$C*H*$_3$).

Synthesis of PF-containing graft copolymer using multiple initiating sites

Scheme 2-22. Synthesis of PF-containing graft copolymer by SCTP with using multiple initiating sites

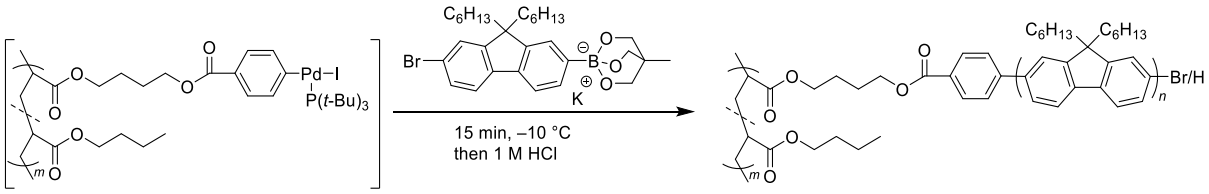

The PF-containing block copolymers were synthesized by the SCTP of **M1** (10.4 mL, 2.59 mmol, as 0.25 mol L^{-1} stock solution in THF) with the macroinitiators (**P(BA$_x$-*co*-BzI$_y$)**; $M_{n,NMR}$ = 8100 g mol^{-1}, $Đ_M$ = 1.09, 52.6 mg, 86.3 μmol, 1.0 e.q.), $Pd_2(dba)_3$•$CHCl_3$ (21.4 mg, 20.7 μmol, 3.2 e.q.), *t*-Bu_3P (114 μL, 57 μmol, as 0.5 mol L^{-1} stock solution in THF, 8.8 e.q.) in a mixture of THF (248 mL), K_3PO_4 (8.2 mg, 39 μmol, 6.0 e.q.), and deionized water (25 μL, 60 eq.). The final products were obtained as a yellow solid.

PBA-*g*-PF

76.3 mg, 75.3% yield: Yellow solid. $M_{n,SEC}$ = 14,900 g mol^{-1} (THF); $M_{n,NMR}$ = 21,300 g mol^{-1} ($CDCl_3$), $Đ_M$ = 1.08.

^{1}H NMR (400 MHz, $CDCl_3$): δ (ppm) 7.93–7.74 (m, Ar–*H*), 7.75–7.57 (m, Ar–*H*), 7.50 (d, Ar–*H*), 4.06 (t, –COCH_2–), 4.35 (t, –CH_2OBz–), 4.04 (t, –C(=O)OC$H_2$$CH_2$–), 2.28 (br, –C$H_2$CH–), 2.12 (br, –C$H_2$($CH_2$)$_4$$CH_3$), 1.92 (br, –$CH_2$C*H*–), 1.60–1.38 (m, –(CH_2)$_2$–),1.36–0.66 (m, –CH_2(CH_2)$_4$CH_3, –CH_2CH_3, –CH_3).

2.5 References

1. J. H. Burroughes, D. D. C. Bardley, A. R. Brown, R. N. Marks, K. Mackay, R. H. Friend, P. L. Burns, and A. B. Holmes, *Nature* **1990**, *347*, 539−541.
2. M.-C. Choi, Y. Kim, and C.-S. Ha, *Prog. Polym. Sci*. **2008**, *33*, 581−630.
3. A. C. Grimsdale, K. L. Chan, R. E. Martin, P. G. Jokisz, and A. B. Holmes, *Chem. Rev*. **2009**, *109*, 897−1091.
4. D.-H. Jiang, S. Kobayashi, C.-C. Jao, Y. Mato, T. Isono, Y.-H. Fang, C.-C. Lin, T. Satoh, S.-H. Tung, and C.-C. Kuo, *Polymers* **2020**, *12*, 84−95.
5. B. S. Ong, Y. Wu, Y. Li, P. Liu, and H. Pan, *Chem. Eur. J*. **2008**, *14*, 4766−4778.
6. F. Cicoira, and C. Santato, *Adv. Funct. Mater*. **2007**, *17*, 3421−3434.
7. K. M. Coakley, and M. D. McGehee, *Chem. Mater*. **2004**, *16*, 4533−4542.
8. S. Gunes, H. Neugebauer, and N. S. Sariciftci, *Chem. Rev*., *2007*, *107*, 1324−11338.
9. G. Li, R. Zhu, and Y. Yang, *Photonics*. **2012**, *6*, 153−161.
10. Q.-D. Ling, D.-J. Liaw, C. Zhu, D. S.-H. Chan, E.-T. Kang, and K.-G. Neoh, *Prog. Polym. Sci*. **2008**, *33*, 917−978.
11. B. Cho, S. Song, Y. Ji, T.-W. Kim, and T. Lee, *Adv. Funct. Mater*. **2011**, *21*, 2806−2829.
12. Y.-C Chiu, C.-C. Shih, and W.-C. Chen, *J. Mater. Chem. C*. **2015**, *3*, 551−558.
13. J.-C. Hsu, A. Hirao, and W.-C. Chen, *J. Mater. Chem*. **2012**, *22*, 5820−5827.
14. D. Neher, *Macromol. Rapid Commun*. **2001**, *22*, 1365−1385.
15. U. Scherf, and E. J. W. List, *Adv. Mater*. **2002**, *14*, 477−487.
16. T. Yamamoto, *Macromol. Rapid Commun*. **2002**, *23*, 583−606.
17. F. Babudri, G. M. Farinola, and F. Naso, *J. Mater. Chem*. **2004**, *14*, 11−34.
18. G. Barbarella, M. Melucci, and G. Sotgiu, *Adv. Mater*., **2005**, *17*, 1581−1593.
19. A. Yokoyama, H. Suzuki, Y. Kubota, K. Ohuchi, H. Higashimura, and T. Yokozawa, *J. Am. Chem. Soc*. **2007**, *129*, 7236−7237.
20. T. Yokozawa, and A. Yokoyama, *Chem. Rev*. **2009**, *109*, 5595−5619.
21. K. Kosaka, T. Uchida, K. Mikami, Y. Ohta, and T. Yokozawa, *Macromolecules*,**2018**, *51*, 364−369.
22. H.-H. Zhang, C.-H. Xing, and Q.-S. Hu, *J. Am. Chem. Soc*. **2012**, *134*, 13156−13159.
23. H.-H. Zhang, C.-H. Xing, G. B. Tsemo, and Q.-S. Hu. *ACS Macro Lett*. **2013**, *2*, 10−13.
24. H.-H. Zhang, Q.-S. Hu, and K. Hong. *Chem. Commun*. **2015**, *51*, 14869−14872.
25. H.-H. Zhang, C.-H. Xing, Q.-S. Hu, and K. Hong, *Macromolecules* **2015**, *48*, 967−978.
26. H.-H. Zhang, W. Peng, J. Dong, and Q.-S. Hu. *ACS Macro Lett*. **2016**, *5*, 656−660.
27. J. Dong, H. Guo, and Q.-S. Hu. *ACS Macro Lett*. **2017**, *6*, 1301−1304.
28. Y. K. Kwon, and M. S. Kim, *Macromolecules* **2009**, *42*, 887−891.
29. H. H. Ahn and Y. K. Kwon, *Polymer,* **2013**, *54*, 4864−4872.
30. P. Chen, G. Yang, T. Liu, T. Li, M. Wang, and W. Huang, *Polym. Int*. **2006**, ***55***, 473−490.
31. Y.-C. Chiu, C.-C. Kuo, C.-J. Lin, and W.-C. Chen, *Soft Matter* **2011**, *7*, 9350−9358.
32. P. Leclere, M. Surin, and R. Lazzaroni, *Eur. Polym. J*. **2004**, *40*, 885−892.

33. Y.-C. Chiu, Y. Chen, C.-C. Kuo, S.-H. Tung, T. Kakuchi, and W.-C. Chen, *ACS Appl. Mater. Interfaces* **2012**, *4*, 7, 3387–3395.
34. H.-C. Hsieh, C.-C. Hung, K. Watanabe, J.-Y. Chen, Y.-C. Chiu, T. Isono, Y.-C. Chiang, R. R. Reghu, T. Satoh, and W.-C. Chen, *Polym. Chem*. **2018**, *9*, 3820−3831.
35. C. S. Fisher, M. C. Baier, and S. Mecking, *J. Am. Chem. Soc*. **2013**, *135*, 1148−1154.
36. J.-T. Wang, K. Saito, H.-C. Wu, H.-S. Sun, C.-C Hung, Y. Chen,T. Isono, T. Kakuchi, T. Satoh and W.-C. Chen, *NPG Asia Materials* **2016**, *8*, 1−11.
37. J.-J. Li, J.-J. Wang, Y.-N. Zhou, and Z.-H. Luo, *RSC Adv*. *2014*, 4, 19869−19877.
38. A. Bolonesi, F. Galeotti, U. Giovanella, F. Bertini, and S. Yunus, *Langmuir* **2009**, *25*, 533−5338.
39. S. Huber, and S. Mecking, *Macromolecules* **2019**, *52*, 5917−5924.
40. K. Saito, T. Isono, H.-S. Sun, T. Kakuchi, W.-C. Chen and T. Satoh, *Polym. Chem*. **2015**, *6*, 6959–6972.
41. A.-N. A.-Duong, C.-C Wu, Y.-T. Li, Y.-S. Huang, H.-Y. Cai, I J. Hai, Y.-H. Cheng, C.-C. Hu, J.-Y. Lai, C.-C. Kuo, and Y.-C. Chiu, *Macromolecules* **2020**, *53*, 4030−4037.
42. H.-S. Sun, Y.-C. Chiu, W.-Y. Lee, Y. Chen, A. Hirao, T. Satoh, T. Kakuchi, and W.-C. Chen, *Macromolecules* **2015**, *48*, 3907−3917.
43. (a) *Organic Synthesis via Boranes*, *Vol*. 2 (Eds.: H. C. Brown and M. Zaidlewicz), Aldrich, Milwaukee. 2001; (b) *Science of Synthesis, Houben-Weyl Methods of Molecular Transformations*, *Vol*. 6 (Eds.: D. E. Kaufmann and D. S. Matteson), Thieme, Stuttgart. 2005; (c) *Boronic Acids* (Ed.: D. G. Hall), Wiley-VCH, Weinheim. 2005.
44. (a) N. Miyaura, A. Suzuki, *Chem*. *Rev*., **1995**, *95*, 2457−2483; (b) N. Miyaura, Organoboron Compounds. *Top*. *Curr*. *Chem*. **2002**, *219*, 11−59; c) *Organic Synthesis via Boranes*, *Vol*. 3 (Eds.: A. Suzuki and H. C. Brown), Aldrich, Milwaukee. 2003; (d) *Metal-Catalyzed Cross-Coupling Reactions*, 2nd ed. (Eds.: A. Meijere and F. Diederich), Wiley-VCH, Weinheim. 2004, 41−123.
45. Y. Yamamoto, M. Takizawa, X.-Q. Yu, and N. Miyaura, *Angew*. *Chem*. *Int*. *Ed*. **2008**, *47*, 928−931.
46. G.-Q. Li, Y. Yamamoto, and N. Miyaura, *Tetrahedron* **2011**, *67*, 6804−6811.
47. S. Sakashita, M. Takizawa, J. Sugai, H. Ito, and Y. Yamamoto, *Org. Lett*. **2013**, *15*, 4308−4311.
48. K. Kosaka, Y. Ohta, and T. Yokozawa, *Macromol. Rapid Commun*. **2015**, *36*, 373−377.
49. C. Amatore, A. Jutans, and G. L. Duc, *Chem. Eur. J*. **2011**, *17*, 2492−2503.
50. H.-N. Choi, H.-S. Yang, J.-H. Chae, T.-L. Choi, and I.-H. Lee, *Macromolecules* **2020**, *53*, 5497–5503.
51. A. Yokoyama, H. Suzuki, Y. Kubota, K. Ohuchi, H. Higashimura, T. Yokozawa, *J*. *Am*. *Chem*. *Soc*. **2007**, *129*, 7236−7237.
52. S. S. Zalesskiy, and V. P. Ananikov, *Organometallics* **2012**, *31*, 2302−2309.

Chapter 3

Suzuki–Miyaura Catalyst-Transfer Polycondensation of Triolborate Salt-Type Carbazole Monomers

3.1 Introduction

Among the approaches to give π-conjugated polymers, catalyst transfer polymerization for polycarbazoles has not been extensively studied. Polycarbazoles can be distinguished based on the bonding positions of repeating units.[1] Poly(*N*-alkyl-3,6-carbazole)s (3,6-PCz), with an *m*-phenylene-like configuration, have been applied to organic light-emitting diodes (OLEDs), flash memory devices, and devices utilizing thermally activated delayed fluorescence.[2–6] In contrast, poly(*N*-alkyl-2,7-carbazole)s (2,7-PCz), possessing a *p*-phenylene-like configuration, have been used in OLEDs and organic photovoltaics (OPVs) devices.[7–12] Despite their promising potential in many applications, the synthesis of polycarbazoles relies on the polycondensation of symmetric bifunctional monomers (i.e., A−A + B−B type reaction, where the A and B mean complementary reactive groups).[13,14] However, there are only a few examples of chain-growth-type catalyst transfer polycondensation for synthesizing poly(*N*-alkyl-carbazole)s.[15] Tan et al. first reported the synthesis of poly(*N*-heptadecan-2,7-carbazole) and poly(*N*-octyl-3,6-carbazole) via Kumada–Tamao–Corriu catalyst-transfer polycondensation (KCTP).[16] However, the poor functional group tolerance of the Grignard-type monomers used in KCTP limited the application of functional initiators to introduce reactive functional groups on the chain end. In contrast, due to the good functional group tolerance of organoboron species, Suzuki–Miyaura catalyst-transfer polycondensation (SCTP) is highly attractive for the precise synthesis of poly(*N*-alkyl-carbazole)s with functional end groups. Jager et al. reported the synthesis of an end-functionalized poly(*N*-octyl-3,6-carbazole) via the SCTP of a pinacolboronate-type monomer.[17] However, a chain transfer reaction occurred during polymerization, leading to the formation of macrocyclic by-products and polymers with undesired end groups. To the best of author knowledge, the SCTP synthesis of 2,7-PCz has

never been reported. This offers room to further investigate control of the SCTP to precisely synthesize 3,6- and 2,7-PCzs with desired molecular weights, narrow dispersity ($Đ_M$), and end groups. Accordingly, author focused on triolborate salt-type monomers, which possess higher nucleophilicity than conventional pinacolboronate-type monomers. Triolborate salts are known to show higher reactivity than other organoboron reagents,[18,19] enabling reactions with heteroaromatic and alkyl compounds,[20,21,22] which are typically inactive in Suzuki–Miyaura coupling. In addition, triolborate salts show good solubility in common organic solvents and are air-/water-stable, and hence, they can be applied for Suzuki–Miyaura coupling without the addition of water and a base. By utilizing these characteristics, author summarized the SCTP of a triolborate salt-type fluorene monomer in Chapter 2, which successfully compensated for the shortcomings encountered in the SCTP of conventional pinacolboronate fluorene monomers.[23]

In this chapter, the author investigated the SCTP of triolborate salt-type carbazole monomers, i.e., potassium 3-(6-bromo-9-(2-octyldodecyl)-9*H*-carbazole-2-yl) triolborate (**M3**) and potassium 2-(7-bromo-9-(2-octyldodecyl)-9*H*-carbazole-2-yl) triolborate (**M4**), with the aim of establishing a synthetic approach for well-defined 3,6-PCzs and 2,7-PCzs. Author successfully achieved the selective synthesis of end-functionalized 3,6-PCz by the SCTP of **M3** at low temperatures to suppress the chain transfer reaction. The SCTP of **M4** proceeded in chain growth and a controlled/living polymerization mechanism to produce 2,7-PCzs with controlled molecular weights (5080–37,900 g mol^{-1}) and a relatively narrow $Đ_M$ (1.35–1.48). Using the established SCTP conditions, author successfully synthesized random copolymers of *N*-alkyl-3,6- and 2,7-carbazoles, random copolymers of *N*-alkyl-carbazole and 9,9-dialkylfluorene, and 2,7-PCz-containing block copolymers (BCPs).

3.2 Result and Discussion

3.2.1 SCTP of M3 to produce 3,6-PCz

The author first investigated the synthesis of end-functionalized poly[9-(2-octyldodecyl)-3,6-carbazole] (3,6-PCz) with a narrow $Đ_M$. Recently, Jager et al. demonstrated the synthesis of 3,6-PCzs by the SCTP of a pinacol boronate-type monomer, using bromobenzene derivative as the initiator.[17] However, a significant amount of macrocyclic byproduct was generated owing to the chain transfer reaction, in addition to the desired linear polymer obtained from the bromobenzene derivative. Author hypothesized that the chain transfer reaction can be suppressed by using triolborate salt-type monomers because of its high reactivity even at low temperatures, resulting in suppressed cyclization side reactions (Scheme 3-1).

Scheme 3-1. Synthetic scheme for the end-functionalized PCzs based on the SCTP of triolborate salt-type carbazole monomers

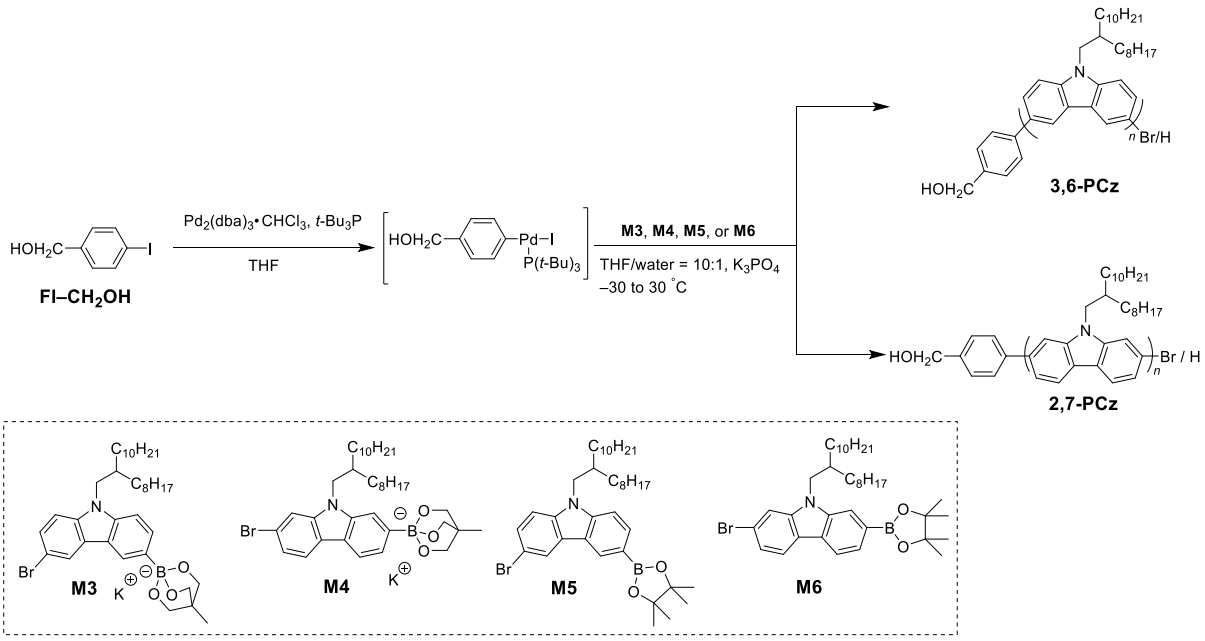

The author first attempted the polymerization of potassium 3-(6-bromo-9-(2-octyldodecyl)-9*H*-carbazole-2-yl)triolborate (**M3**) using an initiating system that consisted of **FI−CH$_2$OH**, $Pd_2(dba)_3$•$CHCl_3$, and *t*-Bu_3P, with an [**M3**]$_0$/[**FI−CH$_2$OH**]$_0$/[$Pd_2(dba)_3$•$CHCl_3$]/[*t*-Bu_3P]/[K_3PO_4] ratio of 15/1/0.3/2.2/1.5 at 30 °C in a mixture of THF/water (10/1; v/v, [**M3**]$_0$ = 10 mmol L^{-1}), based on the previously established conditions for polyfluorene synthesis in Chapter 2.[23] Although SCTP proceeded to afford 3,6-PCz ($M_{n,SEC}$ = 5500 g mol^{-1}), the SEC analysis revealed a bimodal distribution with a $Đ_M$ of 1.32 (run 1, Table 3-1, Figure 3-1). The structure of the 3,6-PCz was investigated using matrix-assisted laser desorption/ionization time-of-flight mass spectroscopy (MALDI-TOF MS). As shown in Figure 3-1 and 3-2, the MALDI-TOF mass spectrum exhibited six series of peaks with a regular interval of 445.47 Da, corresponding to 9-(2-octyldodecyl) carbazole repeating units. One of the observed series of peaks was assigned to $HOCH_2$−3,6-PCz with a phenylmethanol residue at the α-chain end and a bromine atom at the ω-chain end (BnOH/Br); for example, the peak of 1969.43 at *m*/*z* matched well with the theoretical mass for the 4-mer of $HOCH_2$−3,6-PCz ($[M + H]^+$ = 1971.46 Da). However, peaks corresponding to 3,6-PCz with hydrogen and bromine ends (Br/H; e.g., *m*/*z* of 1864.42 Da), bromine at both ends (Br/Br; e.g., *m*/*z* of 1942.31 Da), and cyclic 3,6-PCz (e.g., *m*/*z* = 1783.50 Da) were observed, revealing the uncontrolled polymerization nature.

Table 3-1. SCTP of triolborate salt-type carbazole monomers under various conditions[a]

run	monomer	[monomer]$_0$/[**FI−CH$_2$OH**]$_0$	temp (°C)	$M_{n,SEC}$ [b] (g mol^{-1})	$Đ_M$ [b]	conv. (%)	yield [c] (%)
1	M3	15/1	30	5500	1.32	83.2	80.6
2[d]	M3	15/1	30	5900	1.30	74.2	65.2
3	M3	15/1	−10	6300	1.19	65.3	60.1
4	M3	15/1	−30	—	—	—	—
5	M5	15/1	−10	—	—	—	—
6	M4	15/1	30	3700	1.23	99.2	74.8
7	M4	15/1	−30	—	—	—	—
8	M4	15/1	−10	—	—	—	—
9	M6	15/1	30	—	—	—	—
10	M4	30/1	30	8600	1.35	98.6	74.2
11	M4	60/1	30	16,400	1.45	97.6	75.6
12	M4	90/1	30	32,000	1.48	96.4	73.2

[a] Polymerization condition: atmosphere, Ar; solvent, THF/water (10/1, v/v); [monomer]$_0$ = 10 mmol L^{-1}; [**FI−CH$_2$OH**]$_0$/[$Pd_2(dba)_3$•$CHCl_3$]/[*t*-Bu_3P]/[K_3PO_4] = 1/0.3/2.2/1.5. [b] Determined by SEC using PSt standards. [c] Isolated yields. [d] *t*-Bu_3P (4.4 equiv.).

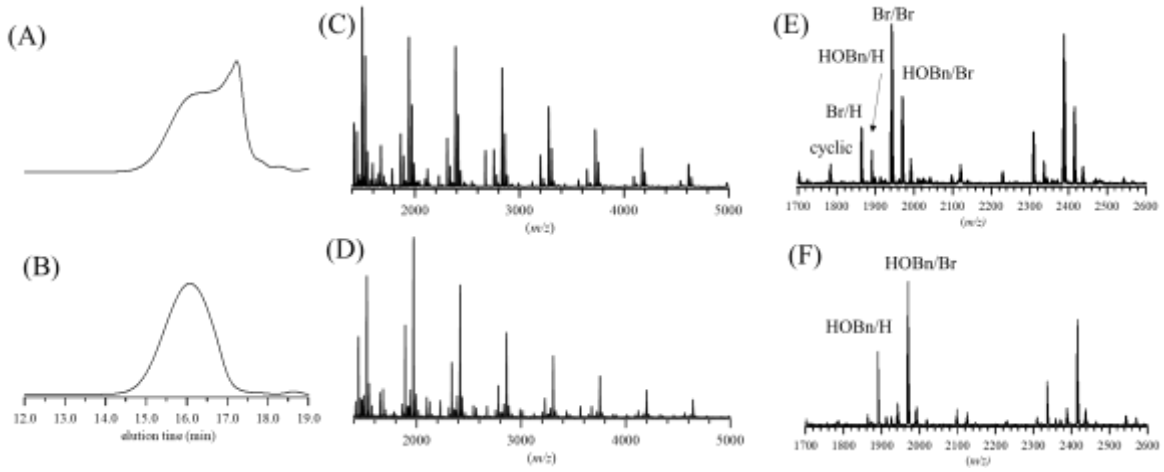

Figure 3-1. (A) SEC trace of 3,6-PCz (run 1, Table 3-1) detected by RI detector (eluent, THF; flow rate, 1.0 mL min^{-1}). (C and E) MALDI-TOF mass spectrum of 3,6-PCz obtained from run 1 (Table 3-1). (B, D and F) SEC trace and MALDI-TOF mass spectrum of 3,6-PCz obtained from run 1 after preparative SEC.

According to a report by Jager et al.,[17] the sharp SEC elution peaks observed in the lower-molecular-weight region and the relatively broad elution peak at high molecular weight in Figure 3-1 most likely arise from the cyclic by-product and linear polymer, respectively. The MALDI-TOF mass spectrum of the high-molecular-weight side, which was isolated by preparative SEC, predominantly showed peaks corresponding to 3,6-PCz, with a phenylmethanol residue at the end (Figure 3-1). Nevertheless, these results suggest that the chain transfer reaction occurred significantly, even with the triolborate salt-type monomer under this polymerization condition.

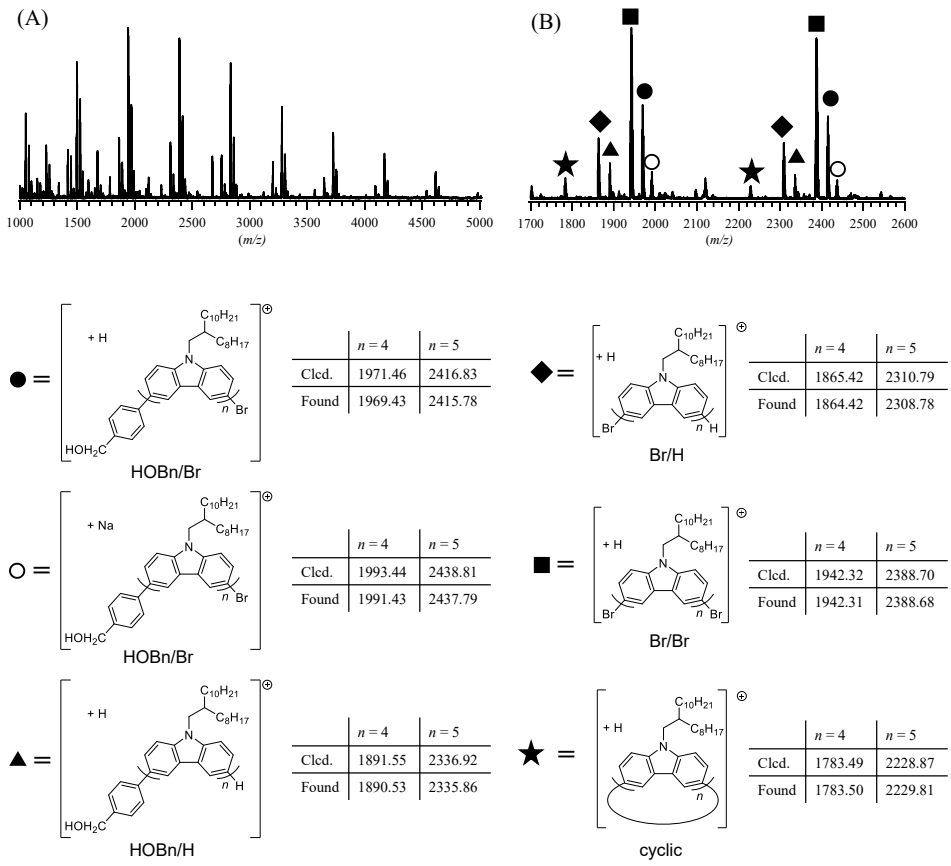

	●	◆	○	■	▲	★
	n = 4	*n* = 4	*n* = 4	*n* = 4	*n* = 4	*n* = 4
Clcd.	1971.46	1865.42	1993.44	1942.32	1891.55	1783.49
Found	1969.43	1864.42	1991.43	1942.31	1890.53	1783.50
	n = 5	*n* = 5	*n* = 5	*n* = 5	*n* = 5	*n* = 5
Clcd.	2416.83	2310.79	2438.81	2388.70	2336.92	2228.87
Found	2415.78	2308.78	2437.79	2388.68	2335.86	2229.81

Figure 3-2. MALDI-TOF mass spectral analysis of **$HOCH_2$−3,6-PCz** obtained from run 1 (Table 3-1). (A) MALDI-TOF mass spectrum. (B) Expanded spectrum ranging from 1700 to 2600 Da.

To inhibit the chain transfer reaction, author optimized the polymerization conditions for **M3**. Hong et al. reported the synthesis of polyfluorene with a narrow $Đ_M$ by SCTP with the addition of extra *t*-Bu_3P.[24] Therefore, author conducted the polymerization of **M3** by adding 4.4 equiv. of *t*-Bu_3P with respect to **FI−CH$_2$OH**, without changing any other factors (run 2, Table 3-3). As a result, the SEC elution peak corresponding to the cyclic by-product was reduced compared to that in run 1, implying that the chain transfer reaction was suppressed to some extent (Figure 3-1). Next, polymerization was carried out by lowering the reaction temperature (−30 °C and −10 °C) to further reduce the unwanted chain transfer reaction. For polymerization at −30 °C (run 4), **M3** precipitated during SCTP. In contrast, the polymer given at −10 °C (run 3) exhibited a nearly monomodal SEC elution peak with a narrow dispersity of 1.19 (Figure 3-3). Consequently, lowering the reaction temperature was found to be an effective method to suppress the chain transfer reaction as well as cyclic by-product formation.

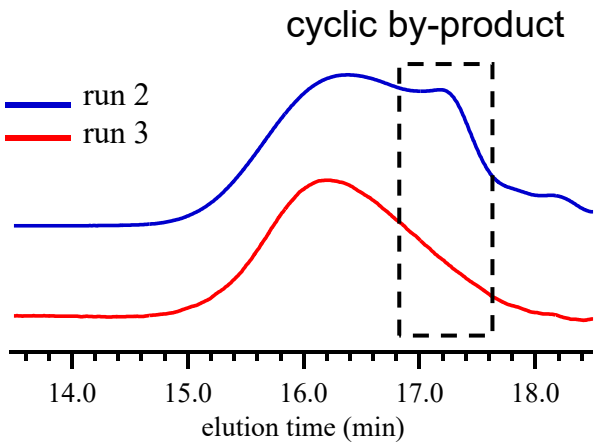

Figure 3-3. SEC traces of 3,6-PCzs obtained from runs 2, and 3 in Table 3-1.

For comparison, author examined the polymerization of a conventional pinacolboronate-type carbazole monomer, 3-(6-bromo-9-(2-octyldodecyl)-9*H*-carbazole-2-

yl)4,4,5,5-tetramethyl-1,2,3dioxaborolane (**M5**), under the same conditions as for **M3**. However, no polymerization was observed at −10 °C (run 5, Table 3-1, Figure 3-4). This result demonstrates that the SCTP of the triolborate salt-type monomer at low temperatures is essential for the controlled synthesis of 3,6-PCz.

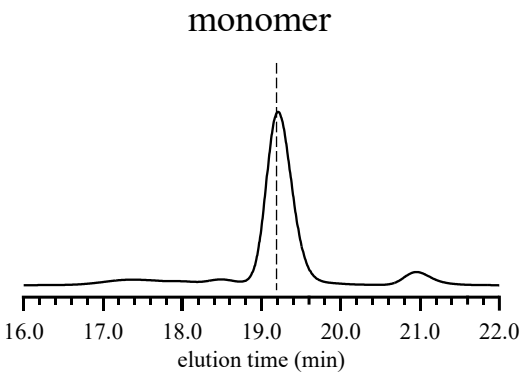

Figure 3-4. SEC traces of crude reaction mixture for the SCTP of **M5** (eluent, THF; flow rate, 1.0 mL min^{-1}).

The structure of 3,6-PCz obtained at −10 °C (run 3) was characterized in detail by NMR and mass spectral analyses. In the ^{1}H NMR spectrum (Figure 3-5A), the major signals were successfully assigned to the 3,6-PCz backbone (8.65–7.31 ppm: proton A) and 2-octyldodecyl side chain (2.11 ppm: proton B, 4.12 ppm: proton C, 1.82–0.75 ppm: proton D and E), which is consistent with the reported ^{1}H NMR data for poly[9-(2-octyl)-3,6-carbazole] synthesized via SCTP.[17] More importantly, a minor signal due to the benzyl proton (proton F) in the α-chain end group was observed at 4.75 ppm, indicating the initiation from **FI−CH$_2$OH**. Thus, the obtained product was identified as the expected poly[9-(2-octyldodecyl)-3,6-carbazole] possessing a phenylmethanol residue at the α-chain end (**HOCH$_2$−3,6-PCz**). The number-average molecular weight ($M_{n,NMR}$) of the **HOCH$_2$−3,6-PCz** (run 3), determined based

on end group analysis of the ^{1}H NMR spectrum, was 6,700 g mol^{-1}. In order to confirm the end-group fidelity, author performed MALDI-TOF MS analysis on this sample. The MALDI-TOF mass spectrum showed two series of peaks with a regular interval of 445.47 Da, corresponding to 9-(2-octyldodecyl) carbazole repeating units (Figure 3-5B). The peaks indicated by filled circles (●) were assignable to **HOCH$_2$−3,6-PCz** possessing a phenylmethanol residue at the α-chain end and a bromine atom at the ω-chain end (BnOH/Br); for example, the peak at m/z of 1970.40 showed good agreement with the theoretical mass for the 4-mer ($[M + H]^+$ = 1970.46 Da). The peaks indicated by filled triangles (▲) were assignable to **HOCH$_2$−3,6-PCz** possessing a phenylmethanol residue at the α-chain end and a hydrogen atom ω-chain end (BnOH/H). Overall, the SCTP of **M3** at low temperature enables better control, yielding narrowly dispersed 3,6-PCzs with sufficient end-group fidelity.

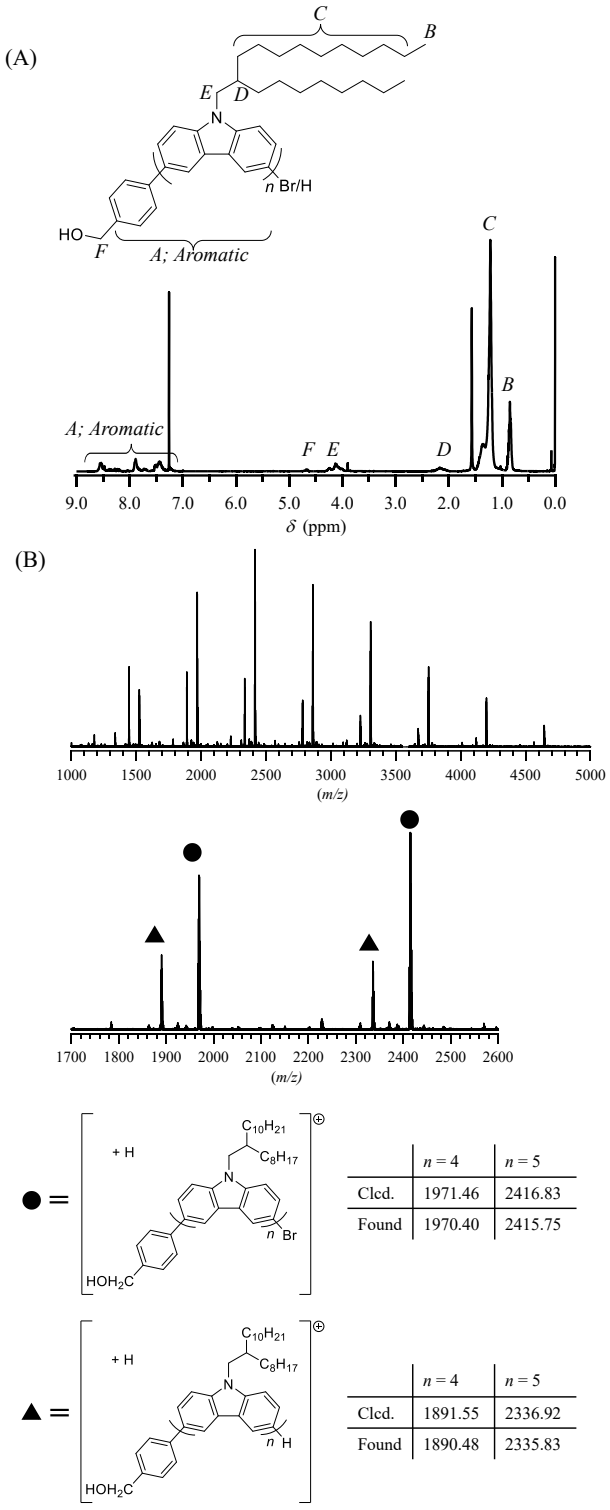

	n = 4	n = 5
Clcd.	1971.46	2416.83
Found	1970.40	2415.75

	n = 4	n = 5
Clcd.	1891.55	2336.92
Found	1890.48	2335.83

Figure 3-5. ^{1}H NMR and MALDI-TOF mass spectral analysis of **$HOCH_2$−3,6-PCz** obtained from run 3 (Table 3-1). (A) ^{1}H NMR in $CDCl_3$ (400 MHz). (B) MALDI-TOF mass spectrum with peak assignments.

To understand the polymerization properties of **M3**, author evaluated the time-dependent change of the reaction product via the SEC and MALDI-TOF MS analysis of the crude aliquot quenched by the addition of HCl (1 mol L^{-1}). It was expected for chain growth polycondensation, but SEC did not confirm an increase in molecular weight over time (Figure 3-6). This suggests that the polymerization of **M3** does not proceed in a perfect living fashion, even with the best polymerization conditions. It is reasonable to deduce that various side reactions occur in this polymerization system. MALDI-TOF MS analysis in Figure 3-7 revealed a complex polymerization behavior. From the beginning of polymerization to 5 h, 3,6-PCz with HOBn/Br (*m*/*z* of 1969.3 Da) and HOBn/H (*m*/*z* of 1969.3 Da) chain end structures were the major products, suggesting that polymerization was initiated from the palladium 4-iodobenzyl alcohol[tris(1,1-dimethylethyl)phosphine] (iodobenzyl alcohol-Pd) complex, as expected. However, when polymerization continued thereafter, the populations of 3,6-PCz with Br/Br (*m*/*z* of 1943.1 Da) and Br/H (*m*/*z* of 1863.3 Da) chain end structures increased over time (Figures 3-7).

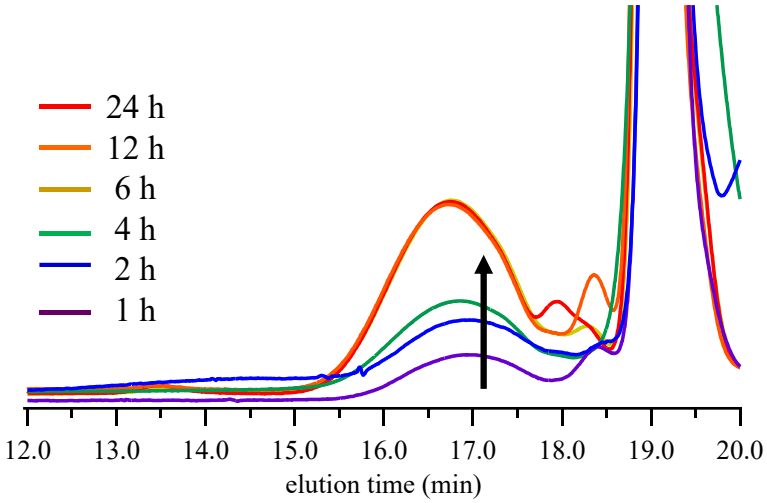

Figure 3-6. SEC traces of crude aliquot collected from the polymerization mixture of **M3** at selected times.

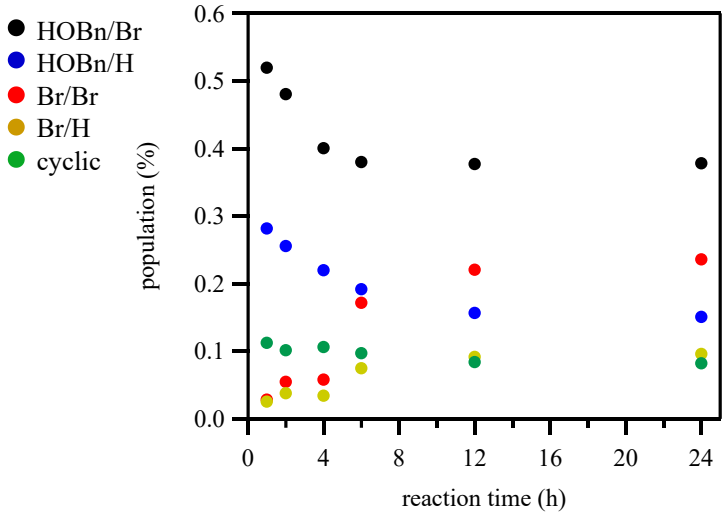

Figure 3-7. Evolution of 3,6-PCz species with different chain ends over time, as determined by MALDI-TOF MS analysis.

This complex polymerization behavior can be explained as shown in Scheme 3-2. The first step of polymerization involves the transmetallation between the initiator and monomer to yield the Pd complex (**i**) when the Pd(0) species, which are generated by reductive elimination, are intramolecularly shifted to the carbon–bromine bond at the end of the same molecule. Polymerization proceeds via chain growth from (**ii**), resulting in the formation of 3,6-PCz with a phenylmethanol residue at the initiation end (HOBn/Br or HOBn/H) (Scheme 3-2A). However, when the Pd(0) species does not shift to the bromine end in the same molecule but intramolecularly shifts to the new monomer, a new initiating species (**iii**) is generated.[25–28] The initiating species (**iii**) generates 3,6-PCz with a triolborate residue at the α-chain end and bromine atom at the ω-chain end, which results in the formation of the cyclic by-product though the intramolecular reaction. Meanwhile, when the Pd catalyst is oxidized by a trace amount of oxygen,[29,30] the homocoupling of two monomer molecules (**iv**) produces another initiating species, which results in the formation of 3,6-PCz at the brominated α-chain end (Br/Br and Br/H) (Scheme 3-2B).

Overall, even the polymerization of the triolborate salt-type monomer **M3** did not proceed in a perfect fashion. Nevertheless, author successfully obtained 3,6-PCz with the desired initiator residue virtually without contamination of the cyclic by-product, by optimizing the polymerization temperature and time.

Scheme 3-2. (A) Polymerization mechanism of 3,6-PCz. (B) Plausible mechanisms for the formation of 3,6-PCzs with different chain end structures and cyclic 3,6-PCz

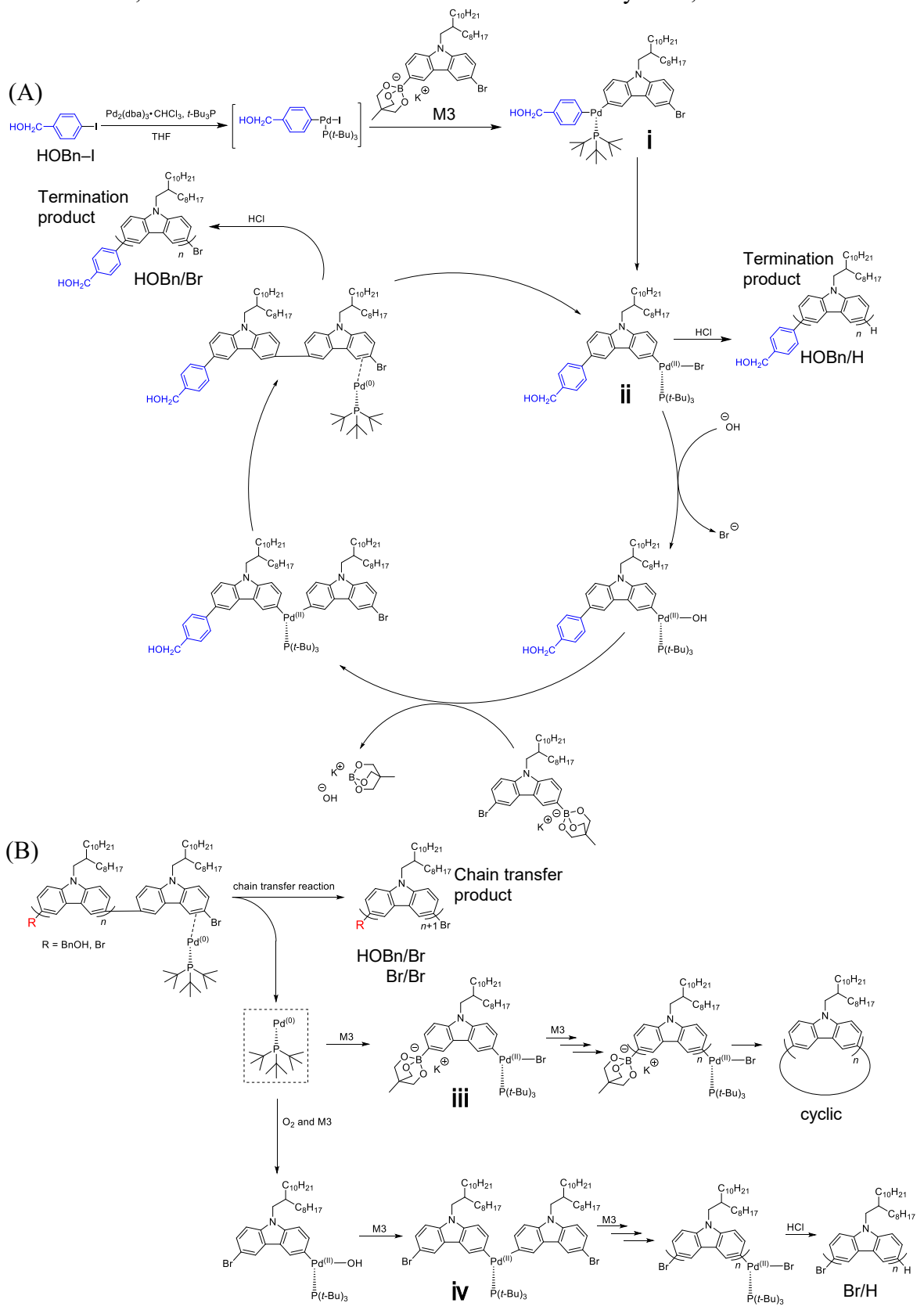

3.2.2 SCTP of M4 to produce 2,7-PCz

Next, the author investigated the polymerization of potassium 2-(7-bromo-9-(2-octyldodecyl)-9*H*-carbazole-2-yl)triolborate (**M4**). The initial attempt was carried out using an initiating system that consisted of **FI−CH$_2$OH**, $Pd_2(dba)_3$•$CHCl_3$, and *t*-Bu_3P with an [**M4**]$_0$/[**FI−CH$_2$OH**]$_0$/[$Pd_2(dba)_3$•$CHCl_3$]/[*t*-Bu_3P]/[K_3PO_4] ratio of 15/1/0.3/2.2/1.5 at 30 °C in a mixture of THF/water (10/1; v/v, [**M4**]$_0$ = 10 mmol L^{-1}) (Scheme 3-1; run 6 in Table 3-1), according to the best polymerization conditions for potassium 2-(7-bromo-9,9-dihexyl-9*H*-fluorene-2-yl)triolborate.[23] The SCTP of **M4** successfully proceeded to afford a polymer with $M_{n,SEC}$ = 3700 g mol^{-1} and $Đ_M$ = 1.23. To study the effect of the polymerization temperature, author carried out SCTP at −30 °C and −10 °C while fixing the other reaction parameters. At −30 °C (run 7), the monomer and product precipitated during the SCTP. Meanwhile, at −10 °C (run 8), a low monomer conversion was observed even after polymerization for 24 h. Consequently, it became apparent that **M4** should be performed at 30 °C. For comparison, author examined the SCTP of a conventional pinacolboronate-type monomer, i.e., 2-(7-bromo-9-(2-octyldodecyl)-9*H*-carbazole-2-yl)4,4,5,5-tetramethyl-1,2,3dioxaborolane (**M6**) under the comparable condition (run 9). As a result, no polymerization was observed even after 24 h. This result demonstrates the advantage of using a triolborate salt-type monomer for the synthesis of 2,7-PCz (Figure 3-8).

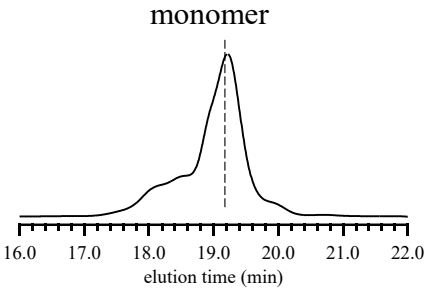

Figure 3-8. SEC traces of crude reaction mixture for the SCTP of **M6** (eluent, THF; flow rate, 1.0 mL min^{-1}).

Then, the structure of the obtained 2,7-PCz was characterized in detail by NMR and MALDI-TOF mass spectral analyses. Figure 3-9A shows the ^{1}H NMR spectrum of the product obtained from run 6. The major observed signals were reasonably assignable to the 2,7-PCz backbone (8.68–7.33 ppm: proton A) and 2-octyldodecyl side chain (2.12 ppm: proton B, 4.14 ppm: proton C, 1.82–0.73 ppm: proton D and E), which is consistent with the reported ^{1}H NMR data for poly[*N*-heptadecan-2,7-carbazole] synthesized via KCTP.[18] More importantly, a minor signal at 4.75 ppm was assigned to the benzyl proton at the α-chain end (proton E), which confirmed the successful installation of the functional end group. Therefore, the obtained product was ascribed to the expected poly[9-(2-octyldodecyl)-2,7-carbazole] possessing a phenylmethanol residue at the α-chain end (**HOCH$_2$−2,7-PCz**). The $M_{n,NMR}$ of **HOCH$_2$−2,7-PCz** (run 6) was calculated to be 5,080 g mol^{-1} by end-group analysis of the ^{1}H NMR spectrum. In order to further confirm the end-group fidelity, author performed MALDI-TOF MS analysis on the product from run 6. The MALDI-TOF mass spectrum mainly exhibited two series of peaks showing a regular interval of 445.4 Da corresponding to 9-(2-octyldodecyl) carbazole repeating units (Figure 3-9B). The peaks denoted by filled triangles (▲) were assignable to **HOCH$_2$−2,7-PCz** possessing a phenylmethanol residue at the α-chain end and a bromine atom at the ω-chain end. For example, the peak at m/z = 2415.75 matched with the theoretical mass for the 5-mer (BnOH/Br; $[M + H]^+$ = 2416.83 Da). The peaks denoted by filled circles (●) were assigned to **HOCH$_2$−2,7-PCz** possessing a phenylmethanol residue at the α-chain end and a hydrogen atom at the ω-chain end (BnOH/H; $[M + H]^+$ = 2336.92 Da). Overall, in contrast to the case of **M3**, the SCTP of **M4** proceeded in a controlled/living fashion to give narrowly dispersed 2,7-PCzs with good end-group fidelity.

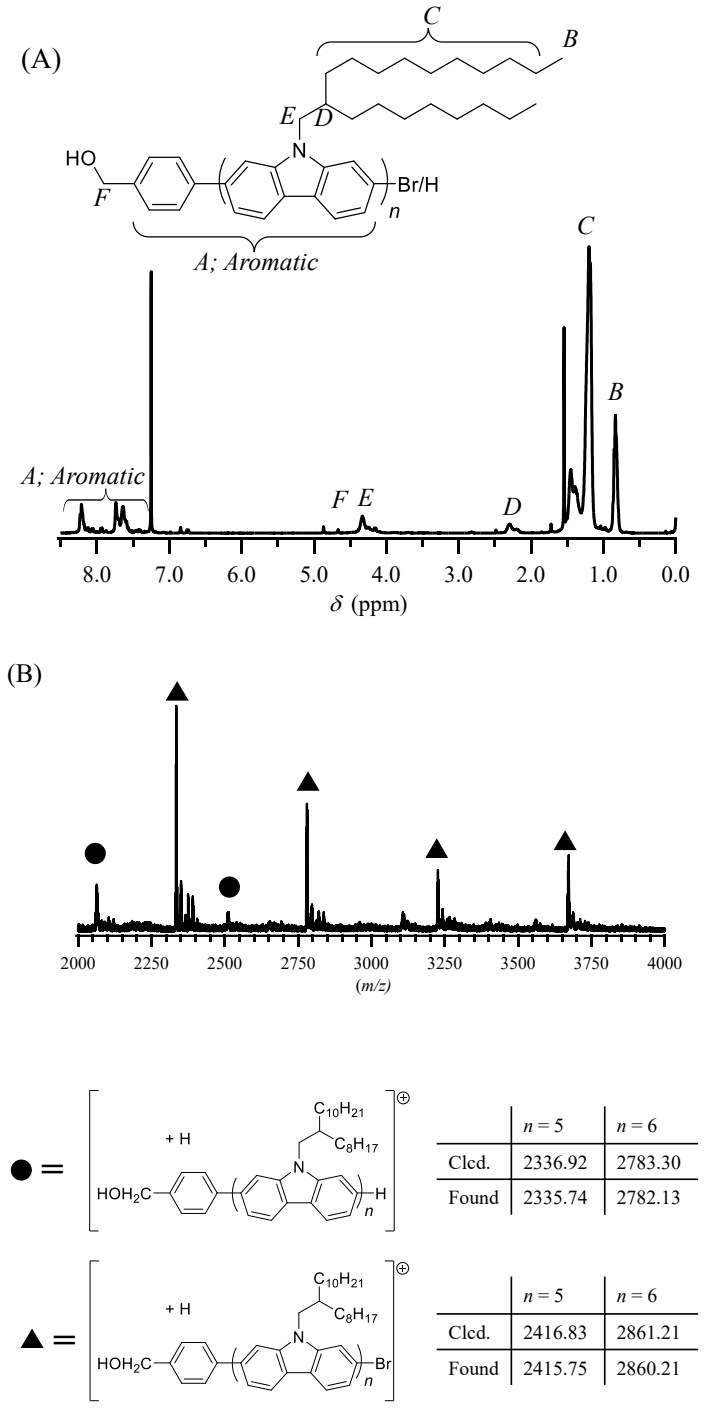

Figure 3-9. ^{1}H NMR and MALDI-TOF mass spectral analysis on **HOCH$_2$−2,7-PCz** obtained from run 6 (Table 3-1) (A) ^{1}H NMR in $CDCl_3$ (400 MHz). (B) MALDI-TOF mass spectrum with peak assignments.

In order to demonstrate the chain growth and controlled/living polymerization behaviors in the SCTP of **M4,** author carried out kinetic and block copolymerization experiments (Scheme 3-3). For the kinetic study, the polymerization of **M4** using **FI−CH$_2$OH** was performed in a mixture of THF/water (10/1, v/v, [**M4**]$_0$ = 10 mmol L^{-1}) at 30 °C with an [**M4**]$_0$/[**FI−CH$_2$OH**]$_0$/[Pd$_2$(dba)$_3$•CHCl$_3$]/[*t*-Bu$_3$P]/[K$_3$PO$_4$] ratio of 30/1/0.3/2.2/1.5. As shown in Figure 3-10A, polymerization proceeds smoothly, and >98% of the monomer is consumed within 12 h. Figure 3-10B reveals that the $M_{n,SEC}$ of the obtained 2,7-PCz linearly increases with the increase in the monomer conversion, while the $Đ_M$ values remain narrow ($Đ_M$ < 1.4). This is strong evidence for the chain-growth mechanism of the SCTP. The kinetic plot indicates a distinct first-order kinetic behavior for this polymerization system. According to slope of the kinetic plot, the rate constant was estimated to be 5.8×10^{-3} s^{-1} mol L^{-1} (Figure 3-10C). The rate constant of the **M4** was found to be smaller than that of the **M1** in Chapter 2 (0.42 s^{-1} mol L^{-1}). This is because the nitrogen of the carbazole ring is electron-donating, resulting in a lower π-electron density at the *m*-position (carbon at the 2,7-position) and a lower nucleophilicity of the triolborate. On the other hand, the π-electron density at the *p*-position (the 3,6-position carbon) is higher, so the nucleophilicity of the triolborate is stronger. Therefore, the reactivity of fluorene monomer and carbazole monomers increases in the order **M4**<**M1**<**M3** (Figure 3-11).

A block copolymerization experiment was further carried out to prove the controlled/living nature of the propagating end of 2,7-PCz. **M4** was first polymerized for 12 h with an [**M4**]$_0$/[**FI−CH$_2$OH**]$_0$/[Pd$_2$(dba)$_3$•CHCl$_3$]/[*t*-Bu$_3$P]/[K$_3$PO$_4$] ratio of 15/1/0.3/2.2/1.5, to yield an intermediate 2,7-PCz with an $M_{n,SEC}$ of 3700 g mol^{-1} and $Đ_M$ of 1.23. After confirming full monomer conversion, 15 equiv. of potassium 2-(7-bromo-9,9-dihexyl-9*H*-fluorene-2-yl)triolborate (**M1**) was added for chain extension, which afforded 2,7-PCz-*b*-PF with $M_{n,NMR}$

of 9400 g mol^{-1} and a $Đ_M$ of 1.38. The SEC traces of the products before and after block copolymerization are shown in Figure 3-10D, in which the SEC elution peak showed clear shift toward the high-molecular-weight side upon the addition of the second monomer. This result verified a truly controlled/living propagating end, which led to chain extension by the second monomer addition. Overall, the aforementioned results successfully support the chain-growth and controlled/living polymerization nature of the SCTP of **M4**.

Scheme 3-3. Block copolymerization experiment to confirm controlled/living nature in the SCTP of **M4**.

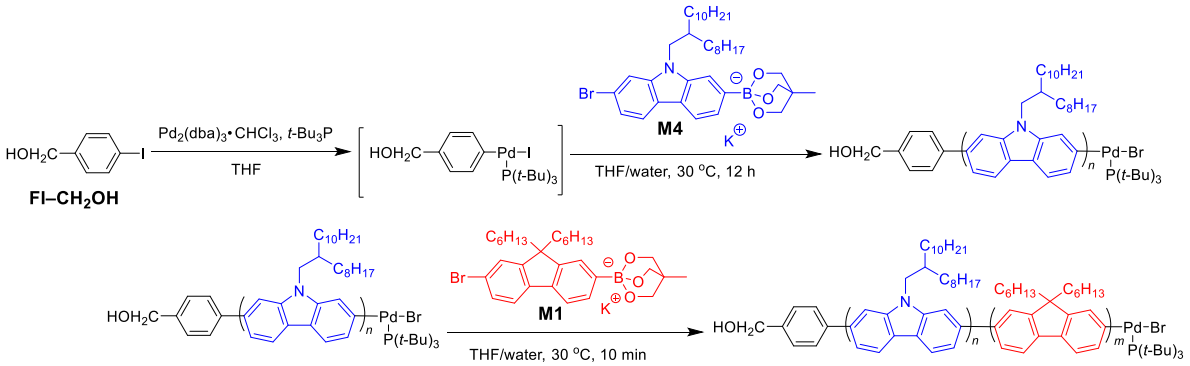

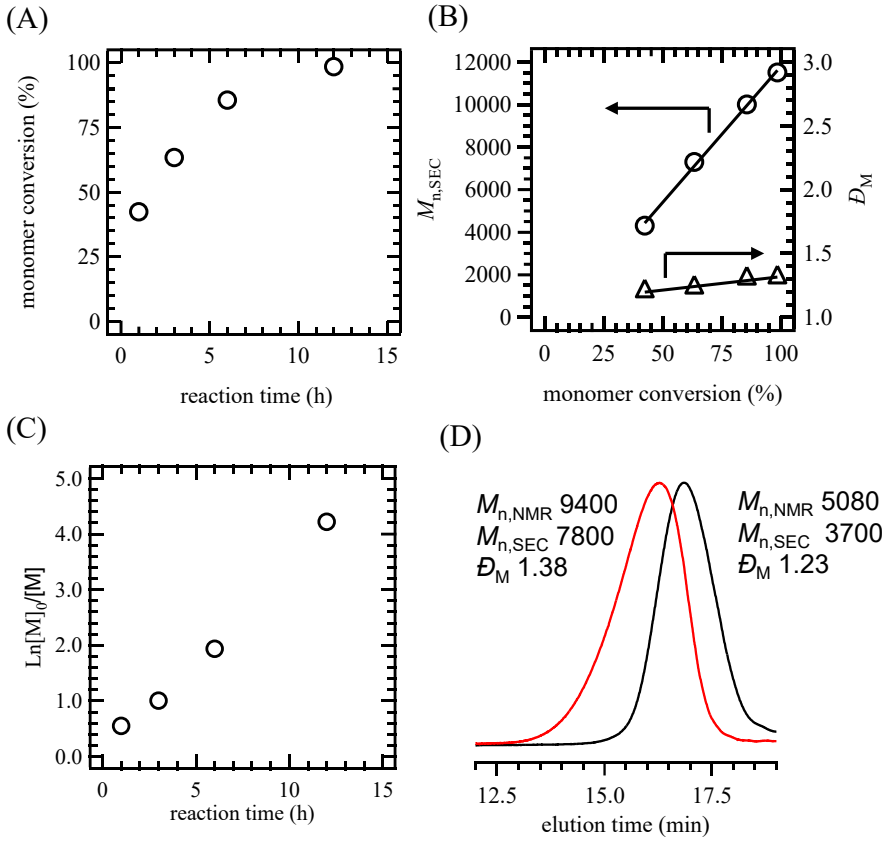

Figure 3-10. (A) Time-conversion plot in the SCTP of **M4** ([**M4**]$_0$/[**FI−CH$_2$OH**]$_0$/[$Pd_2(dba)_3$•$CHCl_3$]/[*t*-Bu_3P]/[K_3PO_4] = 15/1/0.3/2.2/1.5; solvent, THF/water (10/1, v/v); temp., 30 °C). (B) Dependence of $M_{n,SEC}$ and $Đ_M$ on the monomer conversion. (C) Kinetic plots for SCTP. (D) SEC traces of 2,7-PCz (black line) and 2,7-PCz-*b*-PF obtained after the second polymerization (red line).

With the optimized polymerization conditions, the SCTP of **M4** was performed with different [**M4**]$_0$/[**FI−CH$_2$OH**]$_0$ ratio (30/1 for run 10, 60/1 for run 11, and 90/1 for run 12) to synthesize 2,7-PCzs with different molecular weights. Thus, 2,7-PCzs with $M_{n,SEC}$ and $Đ_M$ values of 8600–32,000 g mol^{-1} and 1.35–1.48, respectively (runs 10–12, Table 3-1, $M_{n,NMR}$; 5080–37,900 g mol^{-1}) were successfully obtained (Figure 3-12). To the best of my knowledge, 2,7-PCz obtained from run 12 ($M_{n,SEC}$ of 37,900 g mol^{-1}) had the highest molecular weight among the poly[9-(2-octyldodecyl)-2,7-carbazoles] prepared by chain-growth polycondensation.

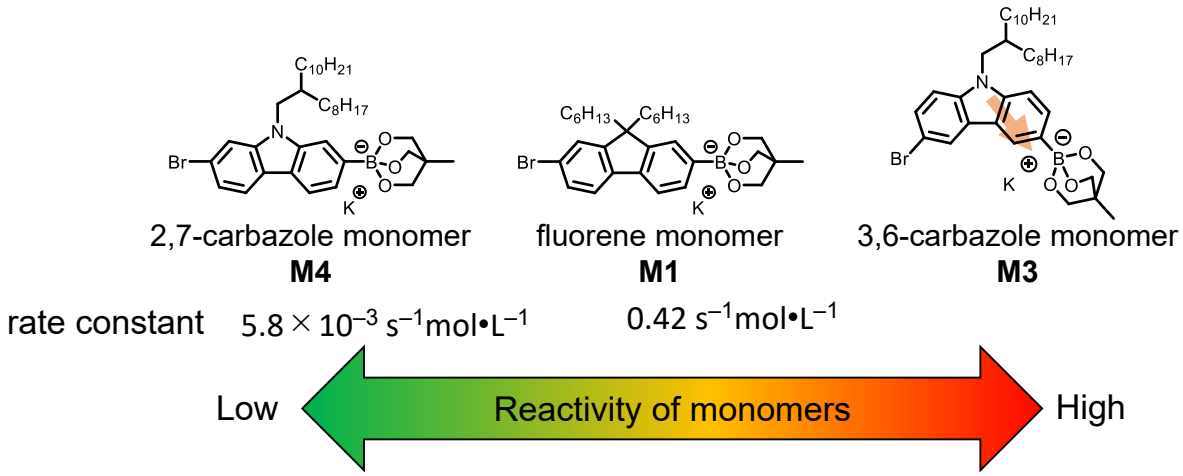

Figure 3-11. Reactivity of triolborate-type fluorene monomer and triolborate-type carbazole monomers.

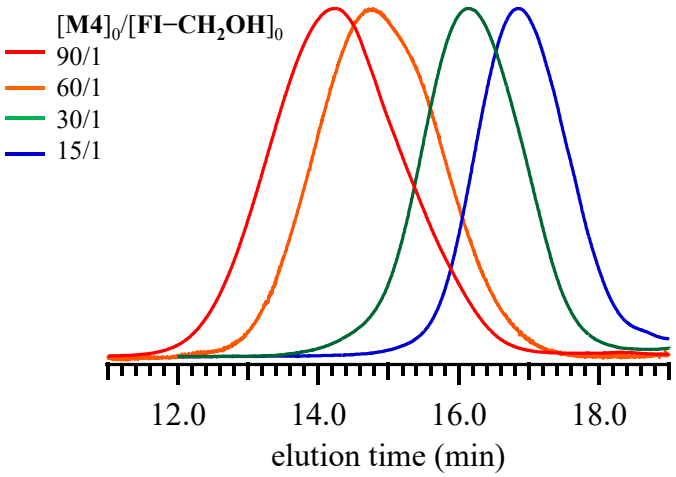

Figure 3-12. SEC traces of **HOCH₂−2,7-PCz** obtained with different [**M4**]₀/[**FI−CH₂OH**]₀ ratios.

3.2.3 Random copolymerization of triolborate salt-type carbazole and fluorene monomers

Recently, π-conjugated copolymers based on carbazole or fluorene groups with varying connectivity, such as at the 2,7- or 3,6-positions, were found to be useful for the extraction of single-walled carbon nanotubes.[31] Therefore, author is interested in testing author SCTP system for the synthesis of poly(2,7-carbazole-*co*-3,6-carbazole) and poly(carbazole-*co*-fluorene)s (Scheme 3-4). First, author examined the random copolymerization of **M3** and **M4** using the initiating system that consisted of **FI−CH$_2$OH**, $Pd_2(dba)_3$•$CHCl_3$, and *t*-Bu_3P, at an [**M3**]/[**M4**]/[**FI−CH$_2$OH**]$_0$/[$Pd_2(dba)_3$•$CHCl_3$]/[*t*-Bu_3P]/[K_3PO_4] ratio of 15/15/1/0.3/2.2/1.5, at 30 °C in a mixture of THF/water (10/1; v/v, [monomers]$_0$ = 10 mmol L^{-1}) (run 13, Table 3-2 run 13). SCTP proceeded to afford 2,7-PCz-*co*-3,6-PCz ($M_{n,SEC}$ = 7800 g mol^{-1}), which exhibited a unimodal SEC elution peak (Figure 3-13). The chemical structure of 2,7-PCz-*co*-3,6-PCz was identified by ^{1}H NMR analysis (Figure 3-14). The major signals were assigned to the polycarbazole backbone (8.6–7.3 ppm: proton A) and 2-octyldodecyl side chain (2.1 ppm: proton B, 4.1 ppm: proton C, 1.8–0.7 ppm: proton D and E). More importantly, a minor signal at 4.7 ppm due to the α-chain end benzyl proton (proton F) was clearly observed, confirming the successful installation of the functional end group. Therefore, the product identified to be the expected copolymer possessed a phenylmethanol residue at the α-chain end (2,7-PCz-*co*-3,6-PCz). The ratio of the 2,7-carbazole unit to the 3,6-carbazole unit in the obtained copolymer was 14:14, which was in good agreement with the monomer feed ratio. The $M_{n,NMR}$ of 2,7-PCz-*co*-3,6-PCz (run 13) was calculated to be 11,500 g mol^{-1} by end-group analysis of the ^{1}H NMR spectrum.

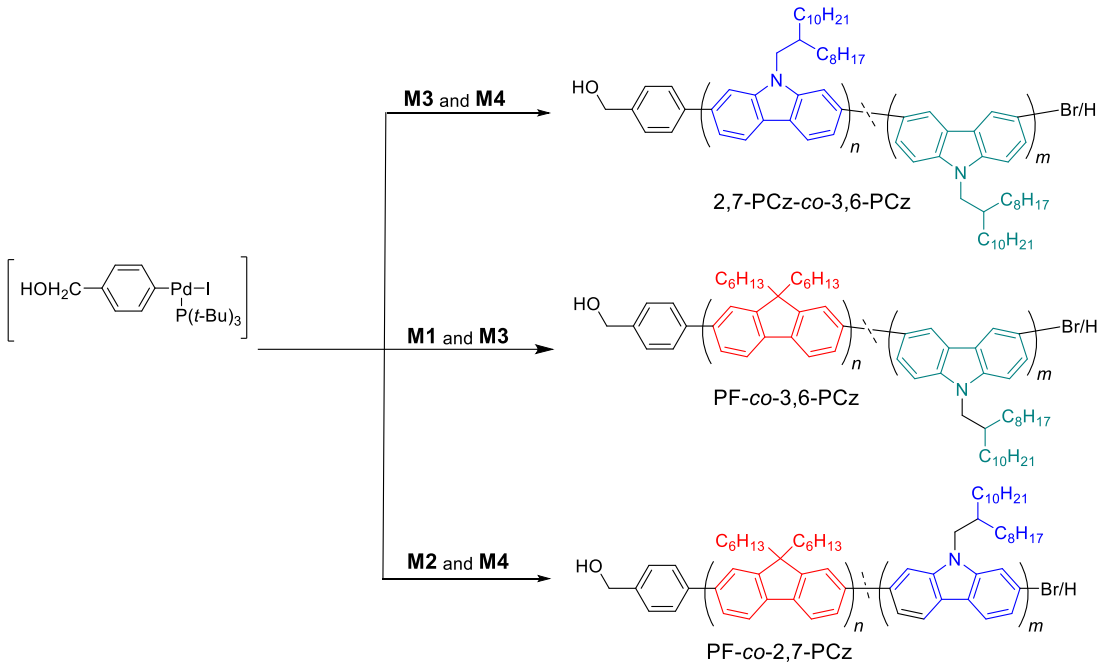

Scheme 3-4. Random copolymerization of **M3**/**M4**, **M1**/**M3**, and **M1**/**M4**

In addition, random copolymerization was carried out for the combination of carbazole and fluorene monomers, i.e., **M1**/**M3** and **M1**/**M4** (Scheme 3-4). Both polymerizations homogeneously proceeded and afforded the corresponding random copolymers, i.e., PF-*co*-3,6-PCz and PF-*co*-2,7-PCz, with $Đ_M$ values of 1.38 and 1.48, respectively. The ^{1}H NMR spectra of the resulted random copolymers showed characteristic signals from both the fluorene and carbazole units (Figure 3-14), which confirmed the successful synthesis of random copolymers.

The thermal and photophysical properties of 3,6-PCz, 2,7-PCz, and fluorene/carbazole copolymers were investigated. 3,6-PCz and 2,7-PCz showed thermal and photophysical properties comparable to the reported data.[13,14] The thermal decomposition temperatures of the random copolymers were comparable to those of the constituent polymers. The UV-Vis and fluorescence spectra of the random copolymers were similar to the superposition of the spectra from the constituent homopolymers (Figures 3-15 and 3-16, Table 3-3).

Table 3-2. Synthesis of PCz and PF-containing random copolymers[a]

run	monomers		random copolymers				yield [d] (%)
	M_A	M_B		$M_{n,SEC}$ [b] (g mol^{-1})	$M_{n,NMR}$ [c] (g mol^{-1})	$Đ_M$ [b]	
13	M3	M4	2,7-PCz-*co*-3,6-PCz	7800	11,500	1.49	72.6
14	M1	M3	PF-*co*-3,6-PCz	9300	12,800	1.38	74.6
15	M1	M4	PF-*co*-2,7-PCz	7800	12,500	1.48	76.1

[a] Polymerization condition: Atmosphere, Ar; solvent, THF/water (v/v) = 10/1; $[M_A+M_B]_0$ = 10 mmol L^{-1}; $[M_A]_0/[M_B]_0/[\text{initiator}]_0/[Pd_2(dba)_3•CHCl_3]/[t\text{-}Bu_3P]/[K_3PO_4]$ = 15/15/1/0.3/2.2/1.5. [b] Determined by SEC using PSt standards. [c] Determined by ^{1}H NMR in $CDCl_3$. [d] Isolated yield.

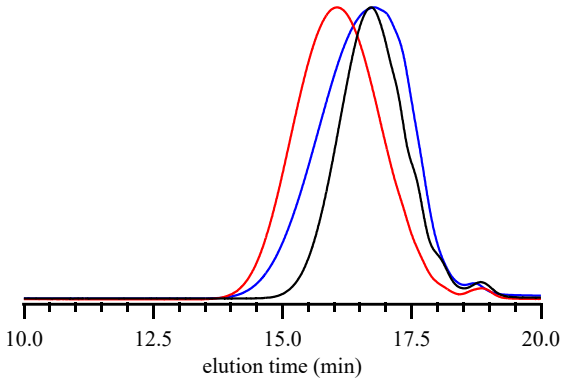

Figure 3-13. SEC traces of 2,7-PCz-*co*-3,6-PCz (black curve), PF-*co*-2,7-PCz (red curve), and PF-*co*-3,6-PCz (blue curve).

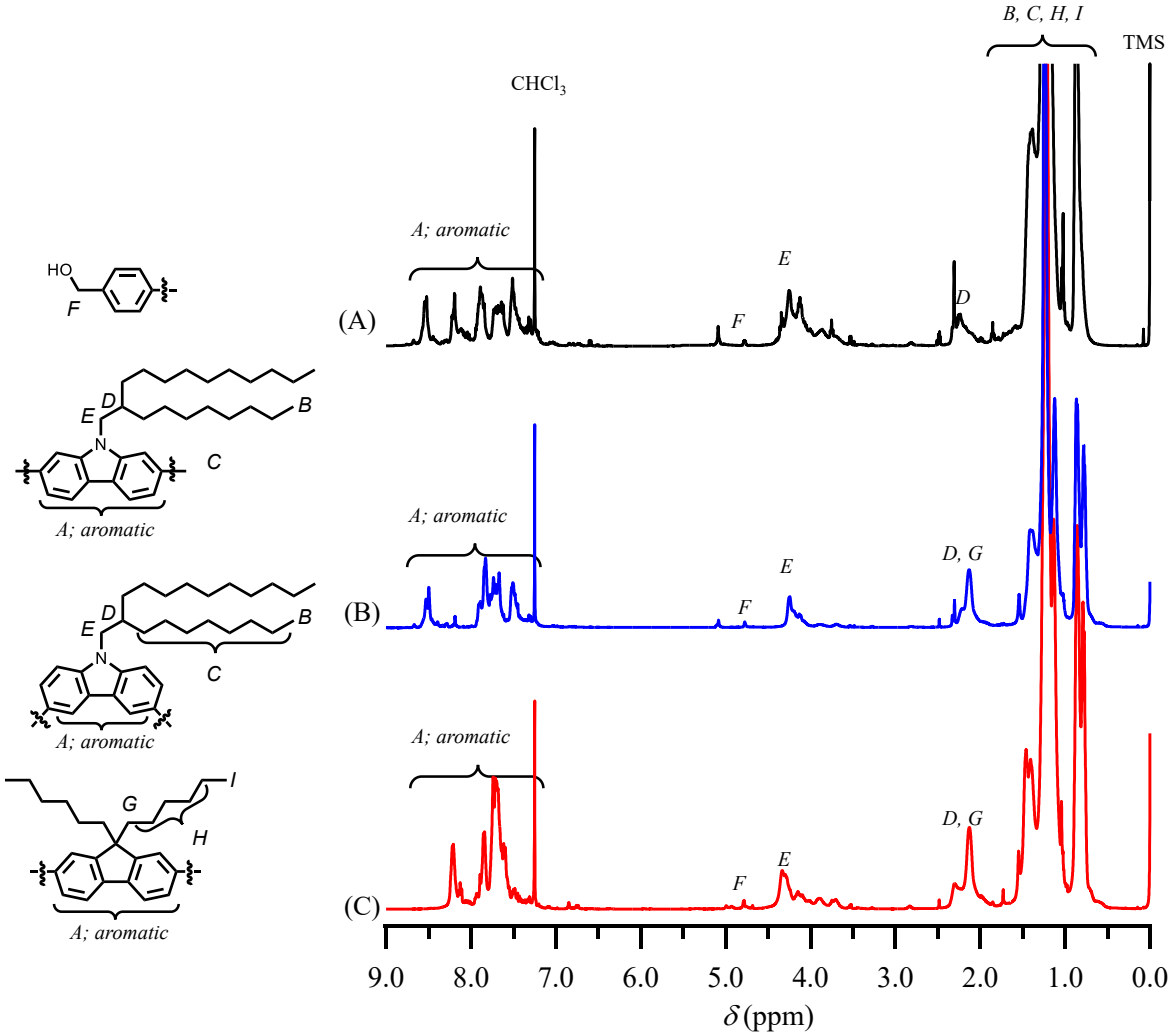

Figure 3-14. ^{1}H NMR spectra of **(**A**)** 2,7-PCz-*co*-3,6-PCz, (B) PF-*co*-3,6-PCz, and (C) PF-*co*-2,7-PCz (400 MHz, $CDCl_3$).

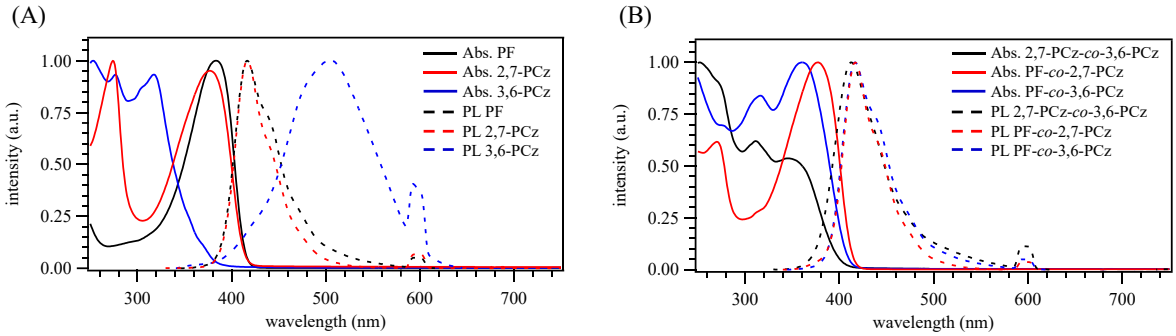

Figure 3-15. Absorption (Abs.) and emission (PL) spectra of (A) homopolymers and (B) random copolymers in $CHCl_3$.

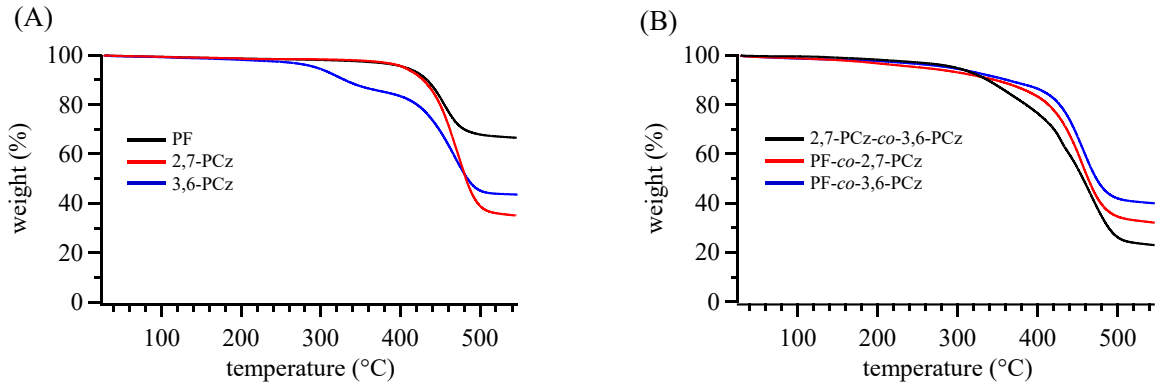

Figure 3-16. TGA results for (A) homopolymers and (B) random copolymers.

Table 3-3. Thermal and photophysical properties of polymers

sample	$T_{d,\ 10\%}$(°C)[a]	solution λ_{max} (nm)[b]	
		ads.	emi.
PF	433	385	417
3,6-PCz-	330	319	509
2,7-PCz-	428	274 (379)	419
2,7-PCz-*co*-3,6-PCz	337	312 (354)	413
PF-*co*-3,6-PCz	362	318 (362)	417
PF-*co*-2,7-PCz	347	272 (378)	419

[a]Determined by TGA measurement. [b]Measurements performed in $CHCl_3$.

3.2.4 Synthesis of 2,7-PCz-containing diblock copolymers using macroinitiators.

Finally, the author employed iodobenzene-terminated macroinitiators for the SCTP of **M4** in order to synthesize 2,7-PCz-containing BCPs (Scheme 3-5). Based on the results in Chapter 2, author reduced the water content as much as possible to prevent the precipitation of the macroinitiator.[23] Author first attempted SCTP with iodobenzene-terminated polystyrene, i.e., PSt−I ($M_{n,NMR}$ = 8300 g mol^{-1}, $Đ_M$ = 1.24), as the macroinitiator under the optimized conditions ([**PSt−I**]$_0$/[**M4**]$_0$ = 1/15; THF/water (v/v) = 5000/1; run 16 in Table 3-4), giving a PSt-*b*-2,7-PCz diblock copolymer. Importantly, the SEC elution peak clearly shifted toward the shorter retention time, which revealed that **M4** polymerization was initiated from PSt−I (Figure 3-17). Moreover, the ^{1}H NMR spectrum of the resulted product exhibited major signals attributable to both the 2,7-PCz and PSt blocks (Figure 3-18), confirming the successful synthesis of PSt-*b*-2,7-PCz. The $M_{n,NMR}$ of the 2,7-PCz block was calculated to be 15,500 g mol^{-1}. In a similar manner, SCTP with the iodobenzene-terminated poly(methyl methacrylate) macroinitiator, i.e., PMMA−I ($M_{n,NMR}$ = 8,900 g mol^{-1}, $Đ_M$ = 1.09), was conducted (run 17 in Table 3-4), which afforded PMMA-*b*-2,7-PCz with a $Đ_M$ of 1.33 (Figures 3-17 and 3-18). These results confirmed the high potential of the present SCTP system for the synthesis of end-functionalized 2,7-PCz and 2,7-PCz-containing BCPs.

Scheme 3-5. Syntheses of PSt-*b*-2,7-PCz and PMMA-*b*-2,7-PCz by SCTP using PSt−I and PMMA−I macroinitiators, respectively

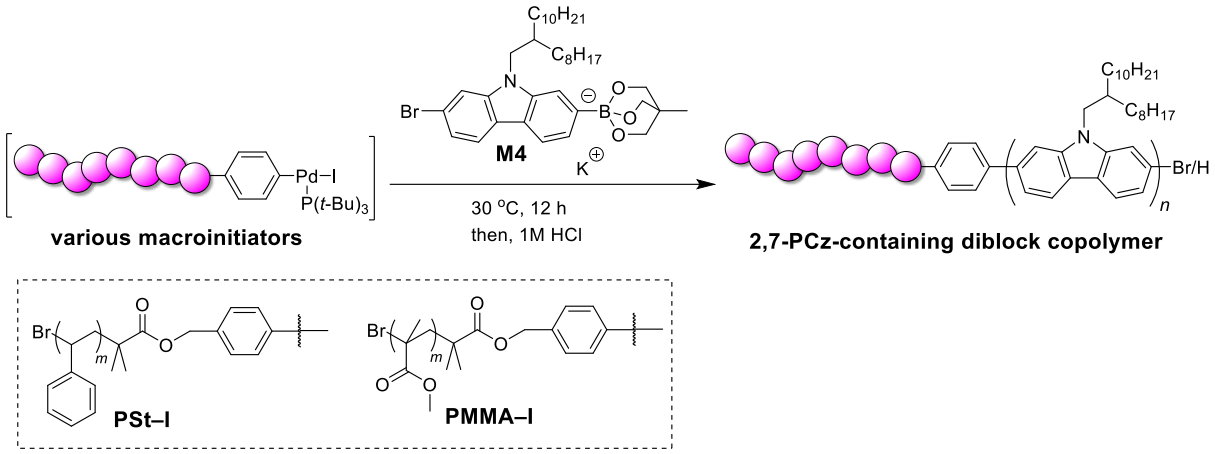

Table 3-4. Polymerization of **M4** using macroinitiators[a]

run	macroinitiator			block copolymer			
		$M_{n,NMR}$[c] (g mol^{-1})	$Đ_M$[b]		$M_{n,NMR}$[c] (g mol^{-1})	$Đ_M$[b]	Yield [d] (%)
16	PSt−I	8300	1.24	PSt-*b*-2,7-PCz	15,500	1.31	78.6
17	PMMA−I	8900	1.09	PMMA-*b*-2,7-PCz	15,700	1.33	73.5

[a] Polymerization condition: atmosphere, Ar; solvent, THF/water (v/v) = 5000/1; [**M4**]$_0$ = 10 mmol L^{-1}; [**M4**]$_0$/[macroinitiator]$_0$/[$Pd_2(dba)_3$•$CHCl_3$]/[*t*-Bu_3P]/[K_3PO_4] = 15/1/1.2/8.8/1.2. [b] Determined by SEC using PSt standards. [c] Determined by ^{1}H NMR in $CDCl_3$. [d]Isolated yield.

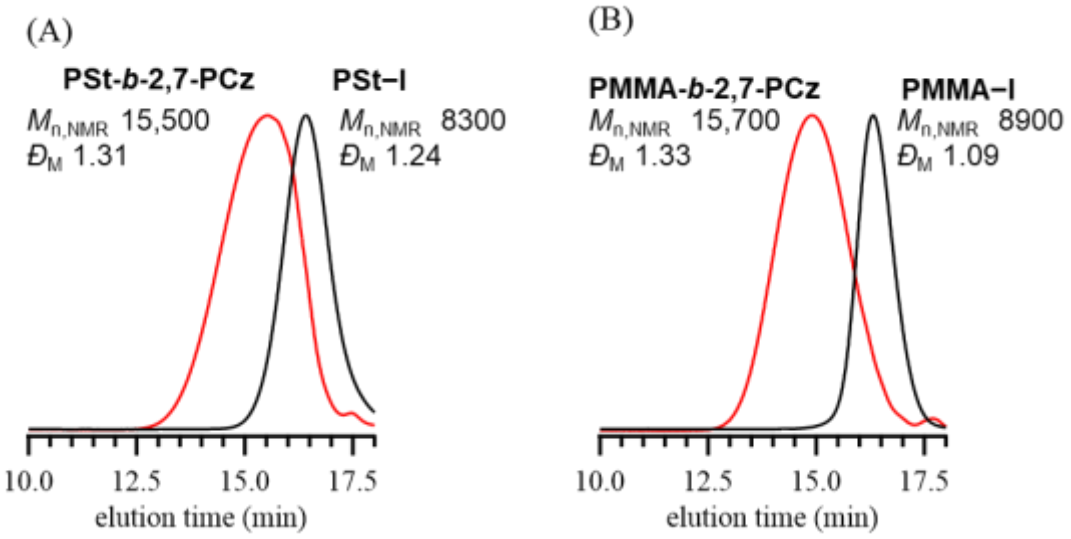

Figure 3-17. SEC traces of (A) PSt-*b*-2,7-PCz and (B) PMMA-*b*-2,7-PCz. The black and red curves represent the macroinitiators and block copolymers, respectively.

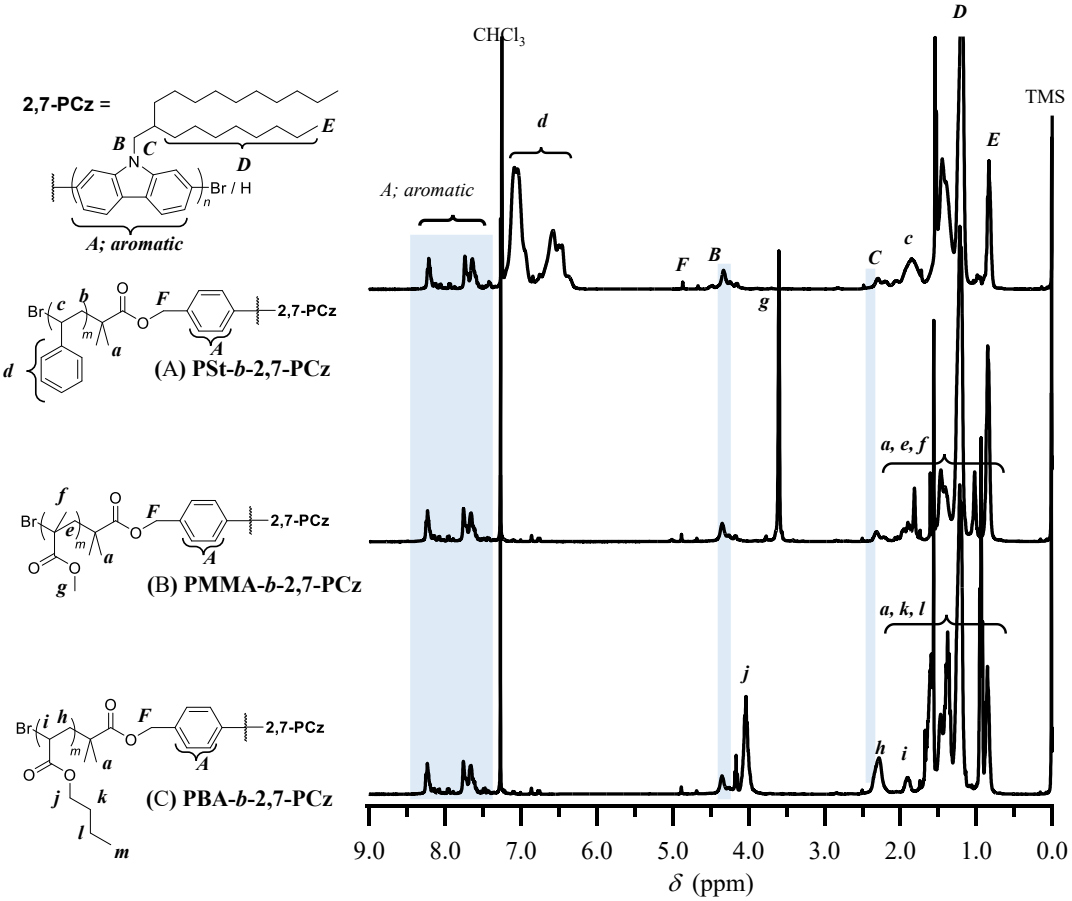

Figure 3-18. ^{1}H NMR spectra of (A) PSt-*b*-2,7-PCz and (B) PMMA-*b*-2,7-PCz (400 MHz, $CDCl_3$).

3.3 Conclusions

In this chapter, the author investigated the SCTP of triolborate salt-type carbazole monomers for the first time. The SCTP of potassium 3-(6-bromo-9-(2-octyldodecyl)-9*H*-carbazole-2-yl)triolborate (**M3**) at low temperatures selectively produced end-functionalized 3,6-PCz, while suppressing the formation of cyclic by-products. The SCTP of potassium 2-(7-bromo-9-(2-octyldodecyl)-9*H*-carbazole-2-yl)triolborate (**M4**) proceeded in a chain-growth mechanism and controlled/living fashion to produce 2,7-PCzs with controlled molecular weights (5080–37,900 g mol^{-1}) and a relatively narrow $Đ_M$ (1.35–1.48). Kinetic and block copolymerization experiments revealed that the SCTP proceeded in chain growth and a controlled/living polymerization manner. Overall, author found that the precise synthesis of 3,6- and 2,7-PCzs can be realized using a triolborate salt-type monomer with higher nucleophilicity than those of conventionally used pinacolboronate-type monomers. In addition, the present SCTP approach enabled the synthesis of random copolymers of *N*-alkyl-3,6- and 2,7-carbazoles, random copolymers of *N*-alkyl-carbazole and 9,9-dialkylfluorene, and 2,7-PCz-containing block copolymers.

3.4 Experimental Section

Materials

2,7-Dibromo-9-(2-octyldecyl)-9*H*-carbazole,[31] 3,6-dibromo-9-(2-octyldecyl)-9*H*-carbazole,[32] iodobenzene-terminated polystyrene (**PSt−I**; $M_{n,NMR}$; 8,300 g mol^{-1}, $Đ_M$; 1.24),[22] 4-iodobenzyl 2-bromo-2-methylpropanoate,[22] potassium 2-(7-bromo-9,9-dihexyl-9*H*-fluorene-2-yl)triolborate,[22] and tris(dibenzylideneacetone)dipalladium(0)-chloroform adduct ($Pd_2(dba)_3$•$CHCl_3$)[33] were prepared according to reported methods.

1,3-Bis(diphenylphosphino)propane (dppp), 2-Dicyclohexylphosphino-2',4',6'-triisopropylbiphenyl (XPhos), 4-iodobenzyl alcohol, methyl methacrylate (MMA), *N*,*N*,*N*',*N*'',*N*''-pentamethyldiethylenetriamine (PMDETA), pinacol, *trans*-2-[3-(4-*tert*-butylphenyl)-2-methyl-2-propylidene]malononitrile, triisopropyl borate, and trimethylolethane were purchased from Tokyo Chemical Industry Co., Ltd. (TCI), and used as received. *n*-Butyllithium (*n*-BuLi; in *n*-hexane as 1.6 mol L^{-1} solution), potassium hydroxide (KOH), and triethylamine (Et_3N) were purchased from Kanto Chemical Co., Inc., and used as received. 2,2'-Bipyridyl, tri(*t*-butyl)phosphine (*t*-Bu_3P), and tripotassium phosphate (K_3PO_4) were purchased from Fujifilm Wako Pure Chemical Co. and used as received. Copper (I) bromide (CuBr) and 2-Dicyclohexylphosphino-2',6'-diisopropoxybiphenyl (RuPhos) were purchased from Sigma-Aldrich Co. and used as received.

Commercially-available dry-THF and dry-toluene (Kanto Chemical Co., Inc., >99.5%, water content, <0.001%) were further purified by an MBRAUN MB SPS Compact solvent purification system equipped with a MB-KOL-C column and a MB-KOL-A column, which were then directly used for the polymerizations.

Instruments

Polymerization was carried out in an MBRAUN stainless steel glovebox equipped with a gas purification system (molecular sieves and a copper catalyst) under a dry argon atmosphere (H_2O, O_2 <0.1 ppm). The moisture and oxygen contents in the glovebox were monitored by an MB-MO-SE 1 moisture sensor and an MB-OX-SE 1 oxygen sensor, respectively.

^{1}H (400 MHz) and ^{13}C NMR (100 MHz) spectra were obtained using a JEOL JNM-ECS400 instrument at 25 °C.

Size exclusion chromatography (SEC) was performed at 40 °C using a Jasco high-performance liquid chromatography system (PU-2080Plus Intelligent HPLC pump, CO-2065Plus Column oven, RI-2031Plus Intelligent RI detector, and Shodex DG-2080-54) equipped with a Shodex KF-G guard column (4.6 mm × 10 mm; particle size, 8 μm) and two Shodex KF-804 columns (linear; particle size, 7 μm; 8.0 mm × 300 mm; exclusion limit, 4 × 10^5) in THF at a flow rate of 1.0 mL min^{-1}. The number-average molecular weight ($M_{n,SEC}$) and dispersity ($Đ_M$) of the polymer were calculated on the basis of a polystyrene calibration.

Matrix-assisted laser desorption ionization time-of-flight mass spectrometry (MALDI-TOF MS) measurement of the polymer was carried out in the reflector mode using an ABSCIEX TOF/TOF/5800 equipped with a 337 nm nitrogen laser (3 ns pulse width). The MALDI-TOF MS samples were prepared by depositing a mixture of the polymer and matrix in THF onto a sample plate. A 1:80 (v/v) ratio of [PCz (1.0 g L^{-1} in THF)]/[*trans*-2-[3-(4-*tert*-butylphenyl)-2-methyl-2-propylidene]malononitrile (10 g L^{-1} in THF)] was used.

Thermogravimetric analysis (TGA) was performed using Hitachi STA200RV under nitrogen atmosphere. All polymer samples were heated up to 550 °C at the heating rate of 10 °C min^{-1}.

Differential scanning calorimetry (DSC) was carried out on a DSC7000X (Hitachi High-Tech Corporation) calibrated with the indium and tin standards. All the polymer samples were heated to 250 °C, cooled to 0 °C, and heated to 300 °C at the heating and cooling rates of 10 °C min^{-1} and 5 °C min^{-1}, respectively.

Absorption spectra were obtained using a JASCO V-670 spectrophotometer. Fluorescence spectra were recorded on a JASCO FP-6500H fluorescence spectrometer at 298 K. The excitation wavelength was 300 nm for all the polymer samples, which were determined by their excitation spectra. The concentration conditions for measuring the absorption and fluorescence spectroscopies in solution were 20 μg mL^{-1} and 2 μg mL^{-1} in $CHCl_3$ for all the polymer samples, respectively.

Synthesis of potassium (bromo-9-(2-octyldecyl)-9*H*-carbazole-2-yl)triolborate

Scheme 3-6. Synthesis of triolborate salt-type carbazole monomers

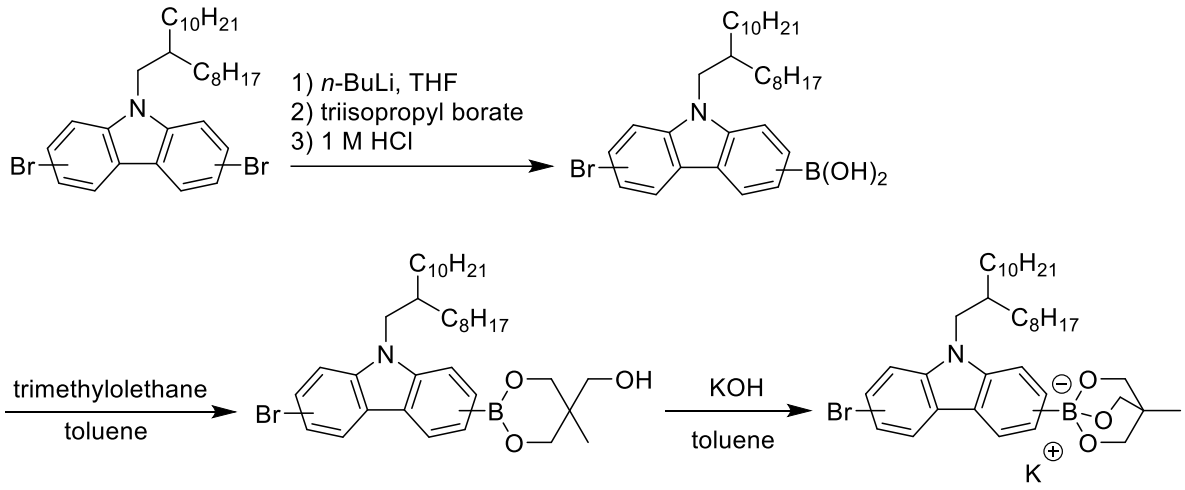

A general protocol is as follows: To a 500 mL three-necked round bottom flask, dibromo-9-alkyl-9*H*-carbazole (2,7-dibromo-9-(2-octyldecyl)-9*H*-carbazole or 3,6-dibromo-9-(2-octyldecyl)-9*H*-carbazole; 7.5 g, 12.4 mmol) was added and dried under vacuum at room temperature for 1.5 h. Dry-THF (100 mL) was introduced to this flask and cooled to −78 °C. *n*-BuLi (8.8 mL, 13.6 mmol, 1.6 mol L^{-1} in *n*-hexane) was injected slowly via a syringe, and the whole mixture was stirred for 3 h under argon atmosphere. Triisopropyl borate (4.3 mL, 18.6 mmol) was then added to this reaction mixture. The mixture was gradually brought back to room temperature and stirred for 12 h under argon atmosphere. The reaction was quenched by the addition of 1 mol L^{-1} HCl (30 mL). The solvent was removed by evaporation, and the residue was dissolved in CH_2Cl_2 and washed with brine. The organic layer was dried over Na_2SO_4 and evaporated completely. The residue was purified by silica gel column chromatography (*n*-hexane/Et_3N = 50/1 (v/v) → *n*-hexane/acetone/Et_3N = 10/3/1 (v/v/v)) to give bromo-9-alkyl-9*H*-carbazole-2-yl boronic acid as a yellow powder.

Bromo-9-alkyl-9*H*-carbazole-2-yl boronic acid (3.5 g, 6.14 mmol) and

trimethylolethane (0.74 g, 6.13 mmol) were suspended in toluene (100 ml). Water was removed by azeotropic distillation for 1 h by a Dean-Stark apparatus. Then, KOH (0.41 g, 7.36 mmol) was added, and the mixture was refluxed for 2 h. The precipitate was collected by filtration, washed with water, and dried under reduced pressure to give potassium bromo-9-alkyl-9*H*-carbazole-2-yl triolborate.

Potassium 2-(7-bromo-9-(2-octyldecyl)-9*H*-carbazole-2-yl)triolborate

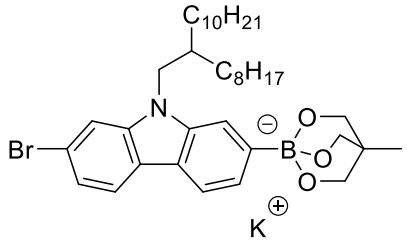

3.89 g, 89.0% yield: Yellow solid

^{1}H NMR (400 MHz, MeOD-d_4): δ (ppm) 8.08 (d, J = 7.8 Hz, 2H, Ar–*H*), 7.88 (s, 1H, Ar–*H*), 7.67 (s, 1H, Ar–*H*), 7.59 (d, J = 7.8 Hz, 1H, Ar–*H*), 7.46 (d, J = 7.3 Hz, 1H, Ar–*H*), 4.86 (s, 6H, −BOC*H*$_2$−), 4.14 (d, 2H, J = 7.3 Hz, −NC*H*$_2$CH−), 2.16 (m, 1H, −NCH$_2$C*H*−), 1.30-1.14 (m, 32H, −CH$_2$(C*H*$_2$)$_7$CH$_3$, −CH$_2$(C*H*$_2$)$_9$CH$_3$), 0.93 (s, 3H, −B(OCH$_2$)$_3$CC*H*$_3$), 0.86 (m, 6H, −(CH$_2$)$_7$C*H*$_3$, −(CH$_2$)$_9$C*H*$_3$).

^{13}C NMR (100 MHz, MeOD-d_4): δ (ppm) 141.1 (Ar), 140.8 (Ar), 130.4 (Ar), 129.9 (Ar), 129.8 (Ar), 124.3 (Ar), 123.7 (Ar), 123.4 (Ar), 119.8 (Ar), 119.6 (Ar), 114.7 (Ar), 114.3 (Ar), 72.7 (−B(O*C*H$_2$)$_3$−), 46.9 (−N*C*H$_2$CH−), 37.3 (−NCH$_2$*C*H−), 36.4 (−B(OCH$_2$)$_3$*C*CH$_3$), 31.8 (−CH$_2$*C*H$_2$(CH$_2$)$_5$CH$_3$, −CH$_2$*C*H$_2$(CH$_2$)$_7$CH$_3$), 29.4 (−CH$_2$CH$_2$(*C*H$_2$)$_4$CH$_2$CH$_3$, −CH$_2$*C*H$_2$(*C*H$_2$)$_6$CH$_2$CH$_3$), 26.2 (−CH$_2$*C*H$_2$(CH$_2$)$_5$CH$_3$, −CH$_2$*C*H$_2$(CH$_2$)$_7$CH$_3$), 22.4 (−(*C*H$_2$)$_6$*C*H$_2$CH$_3$, −(*C*H$_2$)$_8$*C*H$_2$CH$_3$), 16.3 (−B(OCH$_2$)$_3$C*C*H$_3$), 13.2 (−(CH$_2$)$_7$*C*H$_3$,

−$(CH_2)_9CH_3$).

HRMS (ESI): *m*/*z* calcd for $C_{37}H_{56}BO_3NBr^-$: 652.35366; found: 652.35591 $[M–K]^-$

Potassium 3-(6-bromo-9-(2-octyldecyl)-9*H*-carbazole-2-yl)triolborate

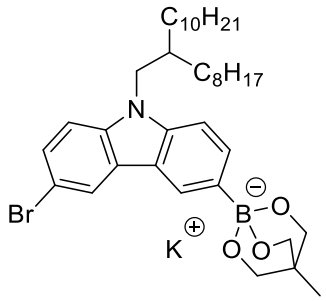

4.18 g, 97.2% yield: Brown solid

^{1}H NMR (400 MHz, DMSO-d_6): δ (ppm) 8.19 (d, J = 1.4 Hz, 1H, Ar–*H*), 8.12 (s, 1H, Ar–*H*), 7.58 (d, J = 8.2 Hz, 1H, Ar–*H*), 7.44-7.38 (m, 2H, Ar–*H*), 7.22 (d, J = 8.2 Hz, 1H, Ar–*H*), 4.14 (d, 2H, J = 7.3 Hz, −NC*H*$_2$CH−), 3.37 (s, 6H, −BOC*H*$_2$−), 2.00 (m, 1H, −NCH$_2$C*H*−), 1.15-1.24 (m, 32H, −CH$_2$(C*H*$_2$)$_7$CH$_3$, −CH$_2$(C*H*$_2$)$_9$CH$_3$), 0.84 (m, 6H, −(CH$_2$)$_7$C*H*$_3$, −(CH$_2$)$_9$C*H*$_3$), 0.59 (s, 3H, −BOCH$_2$CC*H*$_3$).

^{13}C NMR (100 MHz, DMSO-d_6): δ (ppm) 140.7 (Ar), 139.3 (Ar), 132.3 (Ar), 127.0 (Ar), 125.4 (Ar), 124.8 (Ar), 122.5 (Ar), 120.4 (Ar), 111.2, 110.6 (Ar), 107.6 (Ar), 72.7 (−B(O*C*H$_2$)$_3$−), 47.3 (−N*C*H$_2$CH−), 37.4 (−NCH$_2$*C*H−), 35.5 (−B(OCH$_2$)$_3$*C*CH$_3$), 31.5 (−CH$_2$*C*H$_2$(CH$_2$)$_5$CH$_3$, −CH$_2$*C*H$_2$(CH$_2$)$_7$CH$_3$), 29.5 (−CH$_2$CH$_2$(*C*H$_2$)$_4$CH$_2$CH$_3$, −CH$_2$*C*H$_2$(*C*H$_2$)$_6$CH$_2$CH$_3$), 26.3 (−CH$_2$*C*H$_2$(CH$_2$)$_5$CH$_3$, −CH$_2$*C*H$_2$(CH$_2$)$_7$CH$_3$), 22.7 (−(*C*H$_2$)$_6$*C*H$_2$CH$_3$, −(*C*H$_2$)$_8$*C*H$_2$CH$_3$), 17.0 (−B(OCH$_2$)$_3$C*C*H$_3$), 14.5 (−(CH$_2$)$_7$*C*H$_3$, −(CH$_2$)$_9$*C*H$_3$).

HRMS (ESI): *m*/*z* calcd for $C_{37}H_{56}BO_3NBr^-$: 652.35366; found: 652.35580 $[M–K]^-$

Synthesis of bromo-9-(2-octyldecyl)-9*H*-carbazole-2-yl 4,4,5,5-tetramethyl-1,2,3dioxaborolane

Scheme 3-7. Synthesis of pinacol boronate monomers

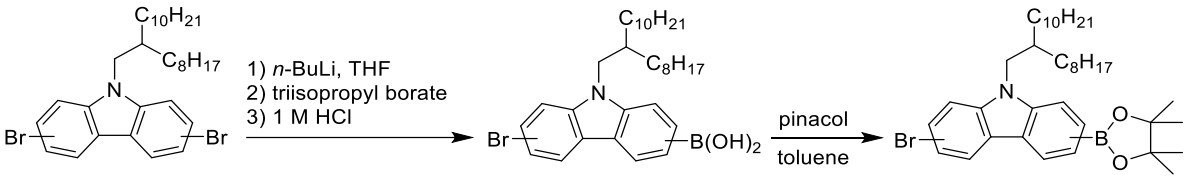

A general protocol is as follows: To a 500 mL three-necked round bottom flask, dibromo-9-alkyl-9*H*-carbazole (2,7-dibromo-9-(2-octyldecyl)-9*H*-carbazole or 3,6-dibromo-9-(2-octyldecyl)-9*H*-carbazole; 7.5 g, 12.4 mmol) was added and dried under vacuum at room temperature for 1.5 h. Dry-THF (100 mL) was introduced to this flask and cooled to −78 °C. *n*-BuLi (8.8 mL, 13.6 mmol, 1.6 mol L^{-1} in *n*-hexane) was injected slowly via a syringe, and the whole mixture was stirred for 3 h under argon atmosphere. Triisopropyl borate (4.3 mL, 18.6 mmol) was then added to this reaction mixture. The mixture was gradually brought back to room temperature and stirred for 12 h under argon atmosphere. The reaction was quenched by the addition of 1 mol L^{-1} HCl (30 mL). The solvent was removed by evaporation, and the residue was dissolved in CH_2Cl_2 and washed with brine. The organic layer was dried over Na_2SO_4 and evaporated completely.

To 500 mL flask containing toluene (280 mL), the obtained residue and pinacol (1.5 g, 13.0 mmol) were added and refluxed for 12 h. The solvent was removed by evaporation, and the residue was dissolved in diethylether. After wash with brine, the organic layer was dried over Na_2SO_4, and concentrated. The residue was purified by silica gel column chromatography (*n*-hexane/acetone/Et_3N = 94/4/2 (v/v/v)) to give bromo-9-alkyl-9*H*-carbazole-2-yl 4,4,5,5-

tetramethyl-1,2,3dioxaborolane.

2-(7-Bromo-9-(2-octyldecyl)-9*H*-carbazole-2-yl)4,4,5,5-tetramethyl-1,2,3dioxaborolane

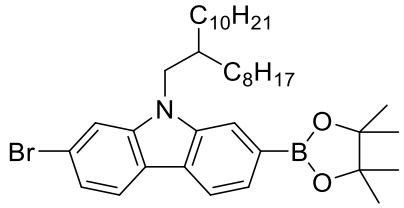

4.20 g, 56.8% yield: Yellow liquid

^{1}H NMR (400 MHz, $CDCl_3$): δ (ppm) 8.06 (d, J = 7.8 Hz, 2H, Ar–*H*), 7.87 (s, 1H, Ar–*H*), 7.69 (s, 1H, Ar–*H*), 7.56 (d, J = 7.8 Hz, 1H, Ar–*H*), 7.47 (d, J = 7.3 Hz, 1H, Ar–*H*), 4.14 (dd, 2H, J = 7.3, 2.3 Hz, −NCH_2CH−), 2.16 (m, 1H, −NCH$_2$C*H*−), 1.19–1.40 (m, 44H, −CH(CH_2)$_7$CH$_3$, −CH(CH_2)$_9$CH$_3$, −BOC(CH_3)$_2$−), 0.85–0.89 (m, 6H, −(CH$_2$)$_7$CH_3, −(CH$_2$)$_9$CH_3).

^{13}C NMR (100 MHz, $CDCl_3$): δ (ppm) 141.1 (Ar), 140.8 (Ar), 130.4 (Ar), 129.9 (Ar), 129.8 (Ar), 124.3 (Ar), 123.7 (Ar), 123.4 (Ar), 119.8 (Ar), 119.6 (Ar), 114.7 (Ar), 114.3 (Ar), 73.7 (−BO*C*(CH$_3$)$_2$−), 46.9 (−N*C*H$_2$CH−), 37.9 (−NCH$_2$*C*H−), 31.9 (−*C*H$_2$(CH$_2$)$_6$CH$_3$, −*C*H$_2$(CH$_2$)$_8$CH$_3$), 29.7 (−CH$_2$CH$_2$(*C*H$_2$)$_4$ CH$_2$CH$_3$, −CH$_2$*C*H$_2$(*C*H$_2$)$_6$CH$_2$CH$_3$), 26.6 (−CH$_2$*C*H$_2$(CH$_2$)$_5$CH$_3$, −CH$_2$*C*H$_2$(CH$_2$)$_7$CH$_3$), 25.0 (−BOC(*C*H$_3$)$_2$−), 22.7 (−(*C*H$_2$)$_6$*C*H$_2$CH$_3$, −(*C*H$_2$)$_8$*C*H$_2$CH$_3$), 14.2 (−(CH$_2$)$_7$*C*H$_3$, −(CH$_2$)$_9$*C*H$_3$.

HRMS (ESI): *m*/*z* calcd for $C_{38}H_{59}BO_2NBrNa^+$: 674.37144; found: 674.37190 $[M+Na]^+$

3-(6-Bromo-9-(2-octyldecyl)-9*H*-carbazole-2-yl)4,4,5,5-tetramethyl-1,2,3dioxaborolane

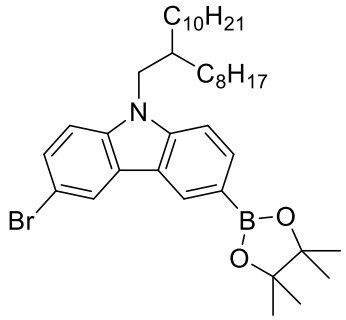

3.70 g, 46.8% yield: Yellow liquid

^{1}H NMR (400 MHz, $CDCl_3$): δ (ppm) 8.54 (s, 1H, Ar–*H*), 8.23 (d, *J* = 1.8 Hz, 1H, Ar–*H*), 7.91 (dd, *J* = 8.2, 0.9 Hz, 1H, Ar–*H*), 7.52-7.50 (m, 1H, Ar–*H*), 7.35 (d, *J* = 8.2 Hz, 1H, Ar–*H*), 7.25-7.22 (m, 1H, Ar–*H*), 4.12 (dd, 2H, *J* = 7.3, 2.3 Hz, −NC*H*$_2$CH−), 2.06 (m, 1H, −NCH$_2$C*H*−), 1.19–1.40 (m, 44H, −CH(C*H*$_2$)$_7$CH$_3$, −CH(C*H*$_2$)$_9$CH$_3$, −BOC(C*H*$_3$)$_2$−), 0.85–0.89 (m, 6H, −(CH$_2$)$_7$C*H*$_3$, −(CH$_2$)$_9$C*H*$_3$).

^{13}C NMR (100 MHz, $CDCl_3$): δ (ppm) 143.3 (Ar), 139.7 (Ar), 132.7 (Ar), 128.3 (Ar), 128.0 (Ar), 124.9 (Ar), 123.3 (Ar), 121.6 (Ar), 120.6 (Ar), 112.1 (Ar), 110.5 (Ar), 108.7 (Ar), 83.7 (−BO*C*(CH$_3$)$_2$−), 47.9 (−N*C*H$_2$CH−), 37.9 (−NCH$_2$*C*H−), 31.9 (−*C*H$_2$(CH$_2$)$_6$CH$_3$, −*C*H$_2$(CH$_2$)$_8$CH$_3$), 29.7 (−CH$_2$CH$_2$(*C*H$_2$)$_4$ CH$_2$CH$_3$, −CH$_2$*C*H$_2$(*C*H$_2$)$_6$CH$_2$CH$_3$), 26.6 (−CH$_2$*C*H$_2$(CH$_2$)$_5$CH$_3$, −CH$_2$*C*H$_2$(CH$_2$)$_7$CH$_3$), 25.0 (−BOC(*C*H$_3$)$_2$−), 22.7 (−(*C*H$_2$)$_6$*C*H$_2$CH$_3$, −(*C*H$_2$)$_8$*C*H$_2$CH$_3$), 14.2 (−(CH$_2$)$_7$*C*H$_3$, −(CH$_2$)$_9$*C*H$_3$.

HRMS (ESI): *m*/*z* calcd for $C_{38}H_{59}BO_2NBrNa^+$: 674.37144; found: 674.37240 [M+Na]$^+$

Synthesis of iodobenzene-terminated polymethyl methacrylate

Scheme 3-8. Synthesis of iodobenzene-terminated poly(methyl methacrylate)

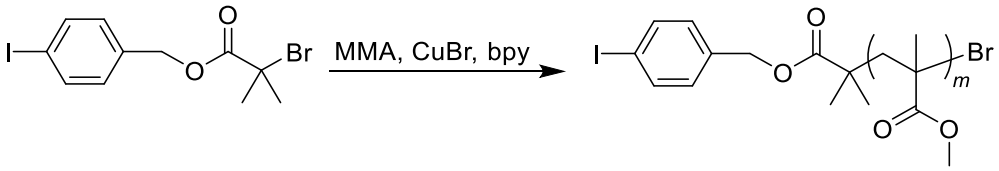

CuBr (15.0 mg, 105 μmol, 1.0 eq.) was evacuated for 30 min in a Schlenk flask and backfilled with argon. Methyl methacrylate monomer was passed through a basic Al_2O_3 column in order to remove the inhibitor. A mixture of methyl methacrylate monomer (1.05 g, 10.5 mmol, 100 eq.), 2,2'-bipyridyl (bpy; 16.3 mg, 105 μmol, 1.0 eq.), and 4-iodobenzyl 2-bromo-2-methylpropanoate (39.9 mg, 105 μmol, 1.0 eq.) were subjected to three freeze-pump-thaw cycles. Next, the liquid mixture was transferred to the Schlenk flask containing CuBr for the polymerization. The polymerization was performed in a preheated oil bath at 90 °C, and the monomer conversion was monitored by ^{1}H NMR at different polymerization time interval. The polymerization was terminated by bubbling air into the solution. The crude product was passed through a neutral Al_2O_3 column and eluted with THF to remove the catalyst. The mixture was purified by reprecipitation using THF as a good solvent and cold MeOH as a poor solvent to give iodobenzene-terminated polymethyl methacrylate (**PMMA−I**; 349 mg, 17.2% yield) as a white powder.

$M_{n,SEC}$ = 8000 g mol^{-1} (THF); $M_{n,NMR}$ = 8900 g mol^{-1} ($CDCl_3$), $Đ_M$ = 1.09.

^{1}H NMR ($CDCl_3$, 400 MHz): δ (ppm) 7.71-7.10 (m, Ar–*H*), 6.49-6.39 (m, Ar–*H*), 5.01 (s, –C*H*$_2$O–), 3.60 (s, O–C*H*$_3$), 2.07-1.81 (m, –C*H*$_2$–), 1.44-0.83 (m, –C(=O)C(C*H*$_3$)$_2$–, –C*H*$_3$).

Polymerization of potassium 3-(6-bromo-9-(2-octyldecyl)-9*H*-carbazole-2-yl)triolborate

Scheme 3-9. Polymerization of triolborate salt-type 3,6-carbazole monomer

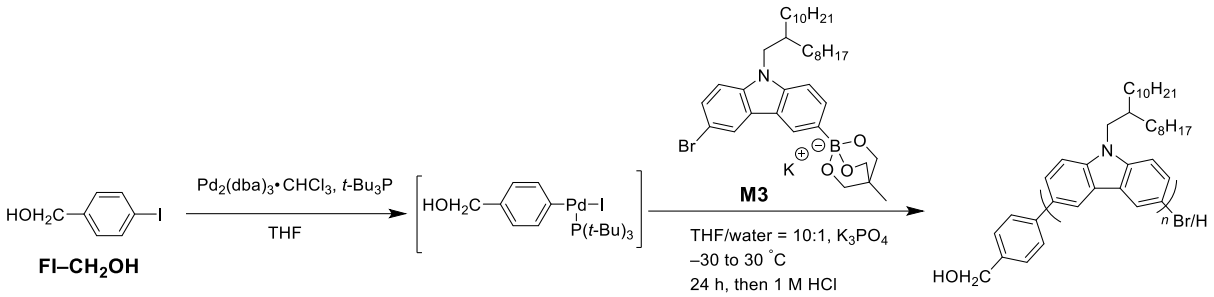

In the glovebox, 4-iodobenzyl alcohol (**FI−CH$_2$OH**; 30 μL, 1.4 μmol, as 0.050 mol L^{-1} stock solution in THF), $Pd_2(dba)_3$•$CHCl_3$ (0.40 mg, 0.43 μmol), and *t*-Bu_3P (6.0 μL, 3.2 μmol, as 0.5 mol L^{-1} stock solution in THF) were placed in a vial and dissolved in THF (200 μL), after stirring for 1 h at room temperature. The vial containing the stock solution of the Pd-initiator was sealed and taken out from the glovebox. In a 30 mL recovery flask, a mixture of THF (3.9 mL), deionized water (388 μL), potassium 3-(6-bromo-9-(2-octyldecyl)-9*H*-carbazole-2-yl)triolborate (**M3**; 30 mg, 0.043 mmol), and K_3PO_4 (0.46 mg, 2.2 μmol) were deoxygenated by argon bubbling at least for 1 h. The stock solution of the Pd-initiator was quickly added to the mixture under an argon atmosphere, and the entire mixture was vigorously stirred for 24 h at −10 °C. To the reaction mixture, 1 mol L^{-1} HCl (5 mL) was added to terminate the polymerization. The solvent was removed by evaporation, and the residue was dissolved in CH_2Cl_2 and washed with brine. The organic layer was dried over Na_2SO_4 and concentrated. The mixture was filtered, and the filtrate was evaporated under reduced pressure. The resulting solution was concentrated and precipitated using THF as a good solvent and cold poor solvent (MeOH/acetone = 2/1 (v/v)) to give **HOCH$_2$−3,6-PCz**. The polymerization results are listed in Table 3-1.

11.6 mg, 60.1% yield: Yellow solid.

$M_{n,SEC}$ = 6300 g mol^{-1} (THF); $M_{n,NMR}$ = 6700 g mol^{-1} ($CDCl_3$), $Đ_M$ = 1.19.

$T_{d,\ 10\%}$ = 330 °C, Abs. (λ_{max}) = 319 nm ($CHCl_3$); Emi. (λ_{max}) = 509 nm ($CHCl_3$).

^{1}H NMR (400 MHz, $CDCl_3$): δ (ppm) 8.62–8.23 (m, Ar–*H*), 7.93–7.77 (m, Ar–*H*), 7.54–7.36 (m, Ar–*H*), 4.75 (s, –C*H*$_2$O–), 4.14 (s, −NC*H*$_2$CH−), 2.33–1.97 (m, −NCH$_2$C*H*−), 1.49–1.06 (br, −CH$_2$(C*H*$_2$)$_7$CH$_3$, −CH$_2$(C*H*$_2$)$_9$CH$_3$), 0.91–0.76 (m, −(CH$_2$)$_7$C*H*$_3$, −(CH$_2$)$_9$C*H*$_3$).

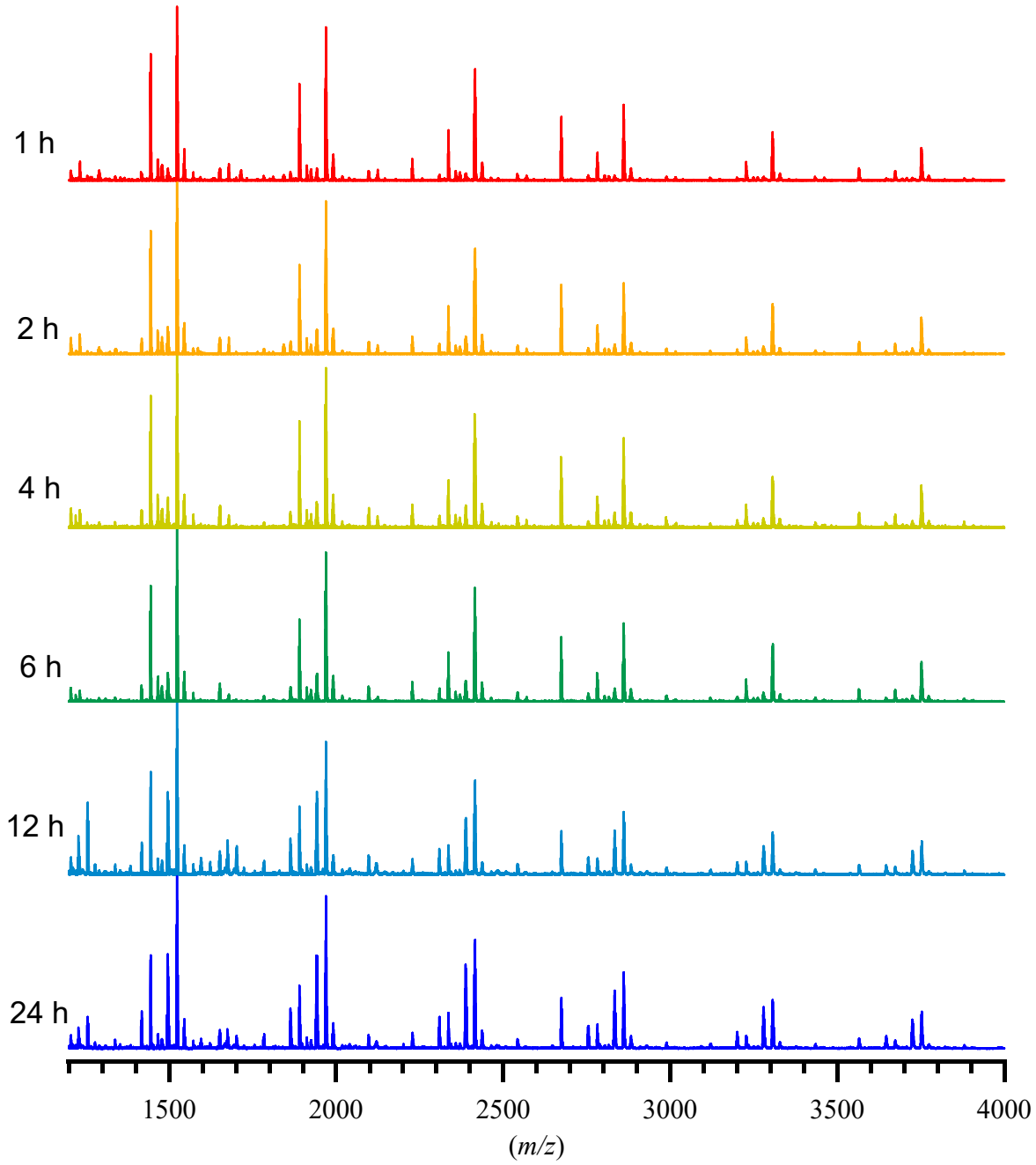

Figure 3-19. Expanded MALDI-TOF mass spectra ranging from 1200 to 4000 Da of 3,6-PCz.

Polymerization of potassium 2-(7-bromo-9-(2-octyldecyl)-9*H*-carbazole-2-yl)triolborate

Scheme 3-10. Polymerization of triolborate salt-type 2,7-carbazole monomer

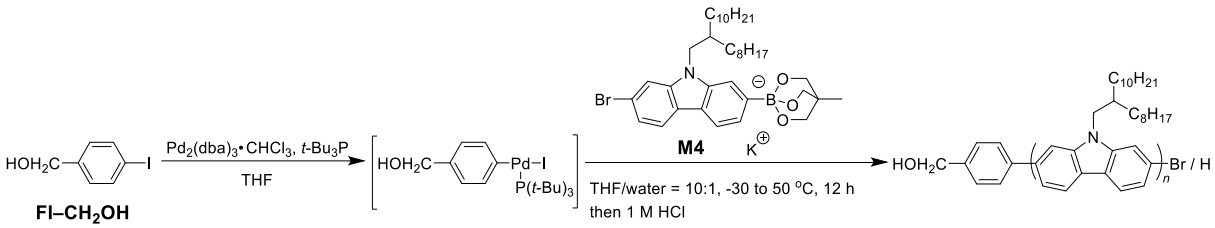

In the glovebox, 4-iodobenzyl alcohol (**FI−CH₂OH**; 30 μL, 1.4 μmol, as 0.050 mol L^{-1} stock solution in THF), $Pd_2(dba)_3$•$CHCl_3$ (0.40 mg, 0.43 μmol), and *t*-Bu_3P (6.0 μL, 3.2 μmol, as 0.5 mol L^{-1} stock solution in THF) were placed in a vial and dissolved in THF (200 μL), after stirring for 1 h at room temperature. The vial containing the stock solution of the Pd-initiator was sealed and taken out from the glovebox. In a 30 mL recovery flask, a mixture of THF (3.9 mL), deionized water (388 μL), potassium 2-(7-bromo-9-(2-octyldecyl)-9*H*-carbazole-2-yl)triolborate (**M4**; 30 mg, 0.043 mmol), and K_3PO_4 (0.46 mg, 2.2 μmol) were deoxygenated by argon bubbling at least for 1 h. The stock solution of the Pd-initiator was quickly added to the mixture under an argon atmosphere, and the entire mixture was vigorously stirred for 12 h at −10 °C. To the reaction mixture, 1 mol L^{-1} HCl (5 mL) was added to terminate the polymerization. The solvent was removed by evaporation, and the residue was dissolved in CH_2Cl_2 and washed with brine. The organic layer was dried over Na_2SO_4 and concentrated. The mixture was filtered, and the filtrate was evaporated under reduced pressure. The resulting solution was concentrated and precipitated using THF as a good solvent and cold poor solvent (MeOH/acetone = 2/1 (v/v)) to give **HOCH₂−2,7-PCz**. The polymerization results are listed in Table 3-1.

14.4 mg, 74.8% yield: Yellow solid.

$M_{n,SEC}$ = 3700 g mol^{-1} (THF); $M_{n,NMR}$ = 5080 g mol^{-1} ($CDCl_3$), $Đ_M$ = 1.23.

$T_{d,\,10\%}$ = 428 °C; T_g = 122 °C, Abs. (λ_{max}) = 379, 274 nm ($CHCl_3$); Emi. (λ_{max}) = 419 nm ($CHCl_3$).

^{1}H NMR (400 MHz, $CDCl_3$): δ (ppm) 8.16–7.84 (m, Ar–*H*), 7.77–7.50 (m, Ar–*H*), 4.75 (s, –C*H*$_2$O–), 4.14 (s, −NC*H*$_2$CH−), 2.33–1.97 (m, −NCH$_2$C*H*−), 1.49–1.06 (br, −CH$_2$(C*H*$_2$)$_7$CH$_3$, −CH$_2$(C*H*$_2$)$_9$CH$_3$), 0.91–0.76 (m, −(CH$_2$)$_7$C*H*$_3$, −(CH$_2$)$_9$C*H*$_3$).

Evaluation of the living nature of the SCTP of triolborate salt-type monomer

Scheme 3-11. Kinetic study for SCTP of M4

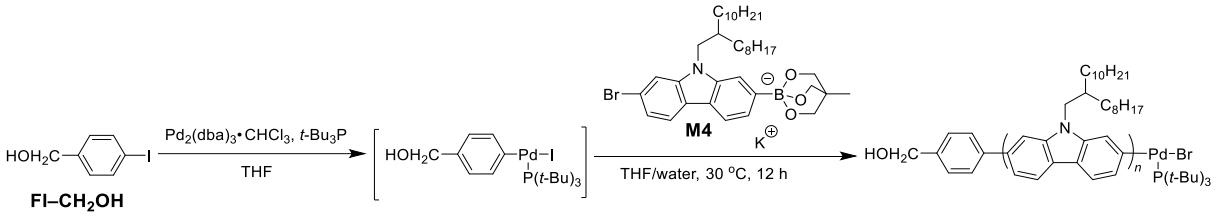

In the glovebox, **FI−CH$_2$OH** (192 μL, 9.62 μmol, as 0.5 mol L^{-1} stock solution in THF), $Pd_2(dba)_3$•$CHCl_3$ (3.0 mg, 2.87 μmol), and *t*-Bu_3P (42.3 μL, 21.1 μmol, as 0.5 mol L^{-1} stock solution in THF) were placed in a vial and dissolved in THF (3 mL), then stirring for 1 h at room temperature. The vial containing the stock solution of the Pd-initiator was sealed and taken out from the glovebox. In a 100 mL recovery flask, a mixture of THF (23 mL), deionized water (2.6 mL), **M4** (200 mg, 0.289 mmol), and K_3PO_4 (3.06 mg, 14.4 μmol) were deoxygenated by argon bubbling at least for 1 h. The stock solution of the Pd-initiator was quickly added to the mixture under an argon atmosphere, and the entire mixture was vigorously stirred for 12 h at 30 °C. A small aliquot (2 mL) of the reaction mixture was collected at 1.0, 3.0, 6.0, and 12 h. Each aliquot was quenched with 1 mol L^{-1} HCl solution and extracted with CH_2Cl_2. The separated organic layer was evaporated under reduced pressure to get a residue. Half of the residue was dissolved in $CDCl_3$ to determine the conversion of monomer by ^{1}H NMR (conversions of 42.3%, 63.3%, 85.6%, and 98.5% were observed for 1.0, 3.0, 6.0, and 12 h, respectively). The other half of the residue was dissolved in THF, and the solution was filtered. The filtrate was analyzed by SEC to determine the Mn and $Đ_M$ values of the polymers. The $M_{n,SEC}$ ($Đ_M$) values of each polymer initiated by $Pd_2(dba)_3$•$CHCl_3$/*t*-Bu_3P/**FI−CH$_2$OH**/K_3PO_4 for 1.0, 3.0, 6.0, and 12 h were 3100 (1.20), 5300 (1.23), 7500 (1.30), and 9200 g mol^{-1} (1.31) respectively. The polymerization results are listed in Table 3-5.

Table 3-5. Monomer conversion, molecular weight, and dispersity at each reaction time[a]

reaction time (h)	conversion (%)	$M_{n,SEC}$[b] (g mol^{-1})	$Đ_M$[b]	$M_{n,NMR}$[c] (g mol^{-1})
1.0	42.3	3100	1.20	4300
3.0	63.3	5300	1.23	7300
6.0	85.6	7500	1.30	10,000
12	98.5	9200	1.31	11,500

[a]Polymerization conditions: Ar atmosphere; solvent, THF/water (v/v) = 10/1; [**M4**]$_0$ = 10 mmol L^{-1}; [**M4**]$_0$/[**FI−CH$_2$OH**]$_0$/[$Pd_2(dba)_3$•$CHCl_3$]/[*t*-Bu_3P]/[K_3PO_4] = 30/1/0.3/2.2/1.5. [b]Determined by SEC (PSt standards, THF, 40 °C). [c]Determined by ^{1}H NMR spectrum in $CDCl_3$.

Post-polymerization experiment for the SCTP of triolborate

Scheme 3-12. Block copolymerization experiment to confirm living nature of SCTP of M4

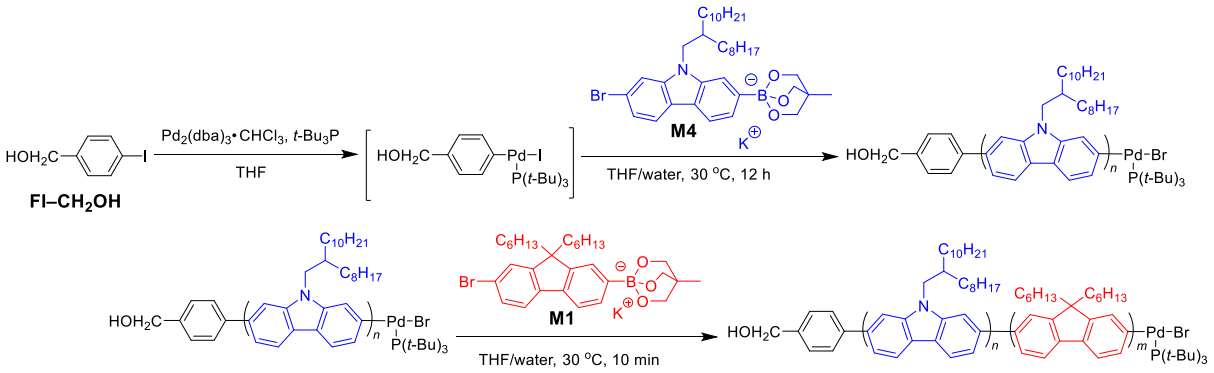

In the glovebox, **FI−CH$_2$OH** (1.15 mL, 0.58 mmol, as 0.5 mol L^{-1} stock solution in THF), $Pd_2(dba)_3$•$CHCl_3$ (178.6 mg, 0.173mmol), and *t*-Bu_3P (2.53 mL, 1.27 mmol, as 0.5 mol L^{-1} stock solution in THF) were placed in a vial and dissolved in THF (15 mL), then stirring for 1 h at room temperature. The vial containing the stock solution of the Pd-initiator was sealed and taken out from the glovebox. In a 100 mL recovery flask, a mixture of THF (3.9 mL), deionized water (388 μL), **M4** (30 mg, 0.043 mmol), and K_3PO_4 (0.46 mg, 2.2 μmol) were deoxygenated by argon bubbling at least for 1 h. The stock solution of the Pd-initiator was quickly added to the mixture under an argon atmosphere, and the entire mixture was vigorously stirred for 12 h at 30 °C. After withdrawing a small aliquot of the mixture, **M1** (25 mg, 0.043 mmol) was then added, and the whole mixture was stirred for 10 min at 30 °C. The final products were obtained as a yellow solid.

2,7-PCz-*b*-PF

30 mg, 88.6% yield: Yellow solid.

$M_{n,SEC}$ = 7800 g mol^{-1} (THF); $M_{n,NMR}$ = 9400 g mol^{-1} ($CDCl_3$), $Đ_M$ = 1.38.

^{1}H NMR (400 MHz, $CDCl_3$): δ (ppm) 8.16–7.50 (m, Ar–*H*), 4.75 (s, –C*H*$_2$O–), 4.14 (s, −NC*H*$_2$CH−), 2.33–1.97 (m, −NCH$_2$C*H*−, Ar–(C*H*$_2$(CH$_2$)$_4$CH$_3$)$_2$), 1.49–1.06 (br, −C*H*$_2$−), 0.91–0.66 (m, −C*H*$_3$).

Molecular weight control

Scheme 3-13. Molecular weight control of 2,7-PCz

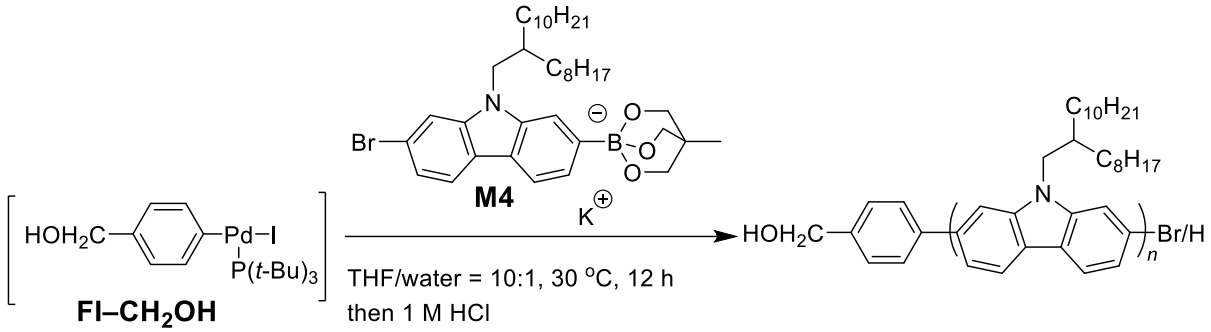

The SCTP of **M4** was conducted with the optimized condition while varying the $[\mathbf{M4}]_0/[\mathbf{FI{-}CH_2OH}]_0$ ratio (30/1, 60/1, and 90/1) for aiming at synthesizing the higher molecular weight PFs. The final product of **HOCH₂−PF** was obtained as a yellow solid. The polymerization results are listed in Table 3-1.

Polymerization of bromo-9-(2-octyldecyl)-9*H*-carbazole-2-yl 4,4,5,5-tetramethyl-1,2,3dioxaborolane

Scheme 3-14. Polymerization of pinacolboronate-type carbazole monomers

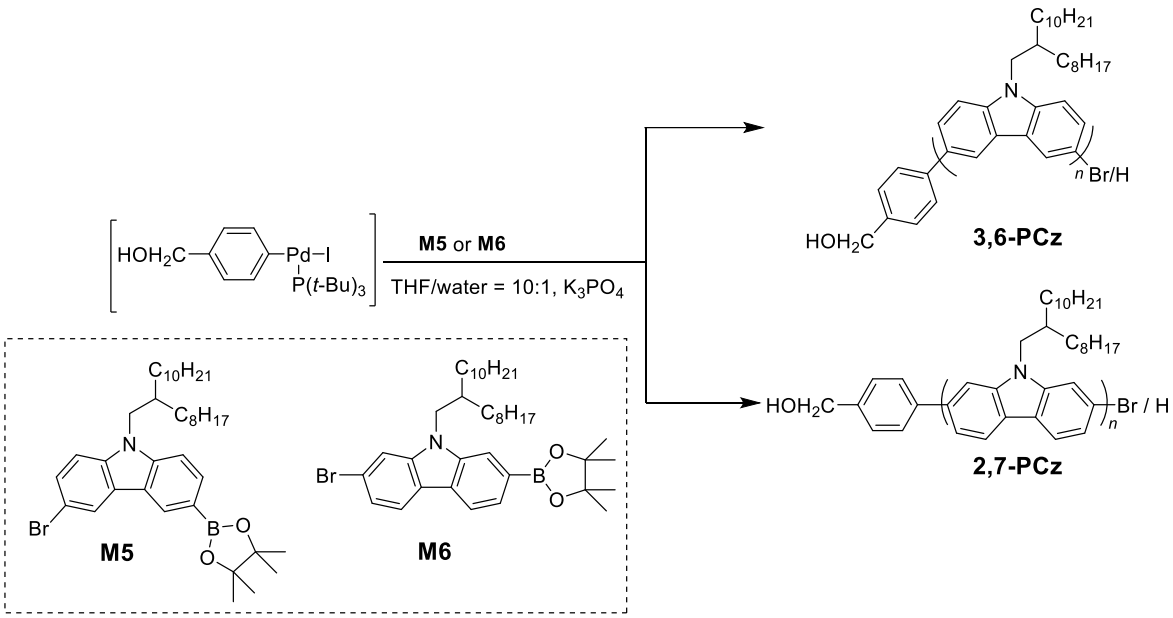

The PCzs were synthesized by the SCTP of pinacolboronate-type carbazole monomer (**M5** or **M6**; 3.45 mL, 0.86 mmol) with **HOCH$_2$−PF** (115 μL, 57.5 μmol, as 0.50 mol L^{-1} stock solution in THF), $Pd_2(dba)_3$•$CHCl_3$ (17.9 mg, 17.2 μmol), *t*-Bu_3P (253 μL, 127 μmol, as 0.5 mol L^{-1} stock solution in THF) in a mixture of THF (86 mL), K_3PO_4 (18.3 mg, 86.3 μmol), and deionized water (8.6 mL).

Synthesis of PCz or PF containing random copolymers

Scheme 3-15. Random copolymerization of M3/M4, M1/M3, and M2/M4

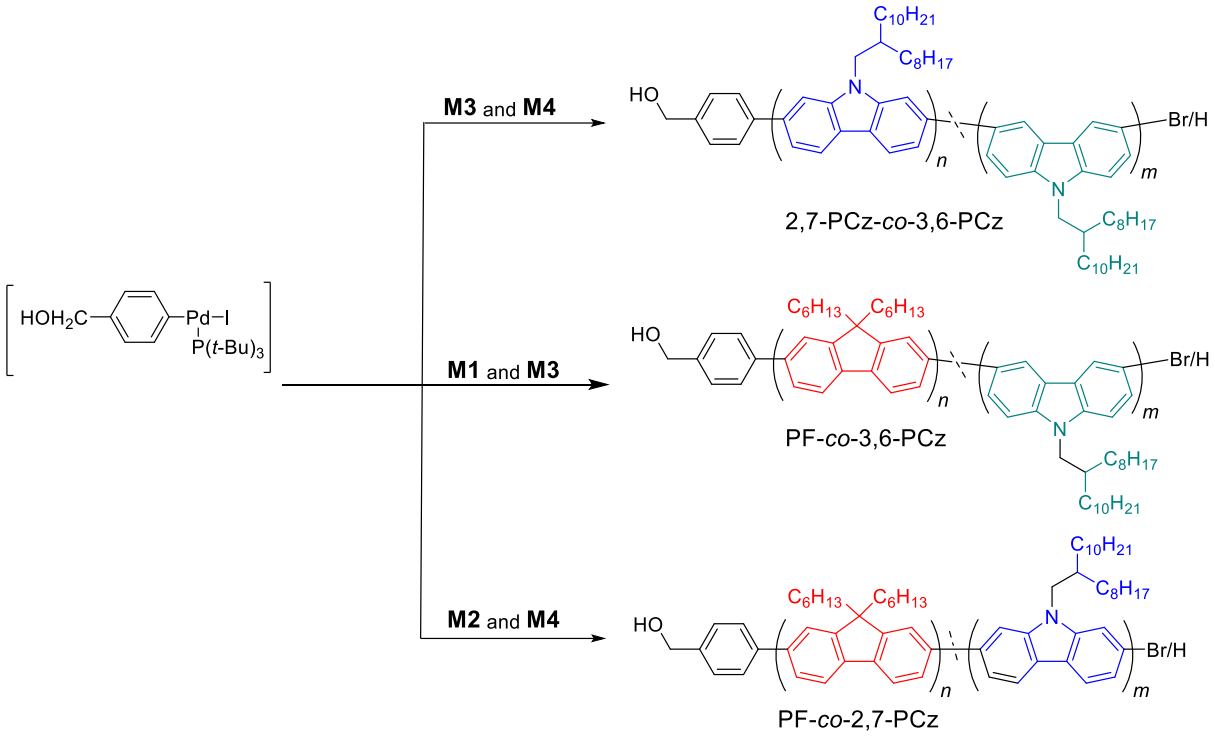

The PCz- or PF-containing random copolymers were synthesized by the SCTP of triolborate salt-type monomer (21.7 μmol) and the other monomer (21.7 μmol) with **FI−CH$_2$OH** (58 μL, 28.9 μmol, as 0.50 mol L^{-1} stock solution in THF), $Pd_2(dba)_3$•$CHCl_3$ (0.90 mg, 8.7 μmol), *t*-Bu_3P (127 μL, 63.5 μmol, as 0.50 mol L^{-1} stock solution in THF) in a mixture of THF (3.88 mL), K_3PO_4 (0.92 mg, 4.3 μmol), and deionized water (388 μL). The final products were obtained as a yellow solid. The polymerization results are listed in Table 3-2.

2,7-PCz-*co*-3,6-PCz

28 mg, 72.6% yield: Yellow solid.

$M_{n,SEC}$ = 7800 g mol^{-1} (THF); $M_{n,NMR}$ = 11,500 g mol^{-1} ($CDCl_3$), $Đ_M$ = 1.49.

$T_{d,\ 10\%}$ = 337 °C, Abs. (λ_{max}) = 354, 312 nm ($CHCl_3$); Emi. (λ_{max}) = 413 nm ($CHCl_3$).

^{1}H NMR (400 MHz, $CDCl_3$): δ (ppm) 8.62–8.23 (m, Ar–*H*), 8.16–7.84 (m, Ar–*H*), 7.77–7.36 (m, Ar–*H*), 4.75 (s, –C*H*$_2$O–), 4.14 (s, −NC*H*$_2$CH−), 2.33–1.97 (m, −NCH$_2$C*H*−), 1.49–1.06 (br, −CH$_2$(C*H*$_2$)$_7$CH$_3$, −CH$_2$(C*H*$_2$)$_9$CH$_3$), 0.91–0.76 (m, −(CH$_2$)$_7$C*H*$_3$, −(CH$_2$)$_9$C*H*$_3$).

PF-*co*-3,6-PCz

25 mg, 74.6% yield: Yellow solid.

$M_{n,SEC}$ = 9300 g mol^{-1} (THF); $M_{n,NMR}$ = 12,300 g mol^{-1} ($CDCl_3$), $Đ_M$ = 1.38.

$T_{d,\ 10\%}$ = 362 °C, Abs. (λ_{max}) = 362, 318 nm ($CHCl_3$); Emi. (λ_{max}) = 417 nm ($CHCl_3$).

^{1}H NMR (400 MHz, $CDCl_3$): δ (ppm) 8.62–8.23 (m, Ar–*H*), 8.16–7.84 (m, Ar–*H*), 7.77–7.36 (m, Ar–*H*), 4.75 (s, –C*H*$_2$O–), 4.14 (s, −NC*H*$_2$CH−), 2.33–1.97 (m, −NCH$_2$C*H*−, Ar–(C*H*$_2$(CH$_2$)$_4$CH$_3$)$_2$), 1.49–1.06 (br, −C*H*$_2$−), 0.91–0.66 (m, −C*H*$_3$).

PF-*co*-2,7-PCz

26 mg, 76.1% yield: Yellow solid.

$M_{n,SEC}$ = 7800 g mol^{-1} (THF); $M_{n,NMR}$ = 12,500 g mol^{-1} ($CDCl_3$), $Đ_M$ = 1.48.

$T_{d,\ 10\%}$ = 347 °C, T_g = 167 °C, Abs. (λ_{max}) = 378, 272 nm ($CHCl_3$); Emi. (λ_{max}) = 419 nm ($CHCl_3$).

^{1}H NMR (400 MHz, $CDCl_3$): δ (ppm) 8.16–7.50 (m, Ar–*H*), 4.75 (s, –C*H*$_2$O–), 4.14 (s, −NC*H*$_2$CH−), 2.33–1.97 (m, −NCH$_2$C*H*−, Ar–(C*H*$_2$(CH$_2$)$_4$CH$_3$)$_2$), 1.49–1.06 (br, −C*H*$_2$−), 0.91–0.66 (m, −C*H*$_3$).

Synthesis of 2,7-PCz-containing diblock copolymers using macroinitiators

Scheme 3-16. Synthesis of PSt-*b*-2,7-PCz and PMMA-*b*-2,7-PCz by SCTP using macroinitiators

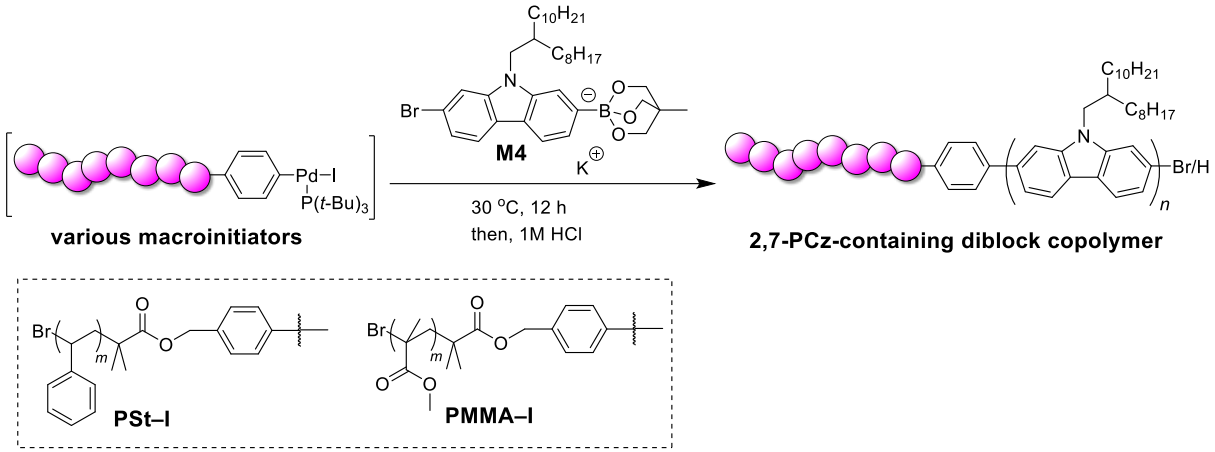

The 2,7-PCz-containing diblock copolymers were synthesized by the SCTP of **M4** (30 mg, 43.3 μmol) with the macroinitiators (2.89 μmol, 1.0 eq.; **PSt−I**; $M_{n,NMR}$; 8300 g mol^{-1}, $Đ_M$; 1.24 and **PMMA−I**, $M_{n,\,NMR}$ = 8900, $Đ_M$ = 1.09), $Pd_2(dba)_3$•$CHCl_3$ (3.6 mg, 3.47 μmol, 1.2 eq.), and *t*-Bu_3P (51 μL, 25.4 μmol, as 0.5 mol L^{-1} stock solution in THF, 8.8 eq.) in a mixture of THF (3.84 mL), K_3PO_4 (0.74 mg, 3.4 μmol, 1.2 eq.), and deionized water (0.80 μL). The resulting solution was concentrated and precipitated using THF as a good solvent and cold mixed solvent of MeOH/acetone (= 1/1 (v/v)) as a poor solvent to give the 2,7-PCz-containing diblock copolymers. The final products were obtained as a yellow solid.

PSt-*b*-2,7-PCz

30 mg, 78.6% yield: Yellow solid.

$M_{n,SEC}$ = 13,600 g mol^{-1} (THF); $M_{n,NMR}$ = 15,500 g mol^{-1} ($CDCl_3$), $Đ_M$ = 1.31.

^{1}H NMR (400 MHz, $CDCl_3$): δ (ppm) 8.16–7.84 (m, Ar–*H*), 7.77–7.50 (m, Ar–*H*), 6.49–6.39 (m, Ar–*H*), 5.01 (s, –C*H*$_2$O–), 4.14 (s, −NC*H*$_2$CH−), 2.33–1.97 (m, −NCH$_2$C*H*−, Ar−C*H*$_2$−), 1.92 (s, –C*H*$_3$), 1.49–1.06 (br, −CH$_2$(C*H*$_2$)$_7$CH$_3$, −CH$_2$(C*H*$_2$)$_9$CH$_3$), 0.91–0.76 (m, −(CH$_2$)$_7$C*H*$_3$, −(CH$_2$)$_9$C*H*$_3$).

PMMA-2,7-PCz

33 mg, 73.5% yield: Yellow solid.

$M_{n,SEC}$ = 12,900 g mol^{-1} (THF); $M_{n,NMR}$ = 15,700 g mol^{-1} ($CDCl_3$), $Đ_M$ = 1.33.

^{1}H NMR (400 MHz, $CDCl_3$): δ (ppm) 8.16–7.84 (m, Ar–*H*), 7.77–7.10 (m, Ar–*H*), 6.49-6.39 (m, Ar–*H*), 5.01 (s, –C*H*$_2$O–), 3.60 (s, O–C*H*$_3$), 4.14 (s, −NC*H*$_2$CH−), 2.33–1.97 (m, −NCH$_2$C*H*−, –C*H*$_2$–), 1.49–1.06 (br, −CH$_2$(C*H*$_2$)$_7$CH$_3$, −CH$_2$(C*H*$_2$)$_9$CH$_3$, –C(=O)C(C*H*$_3$)$_2$–), 0.91–0.76 (m, −C*H*$_3$).

3.5 References

1. F. Xu, J.-H. Kim, H. U. Kim, J.-H. Jang, K. S. Yook, J. Y. Lee, and D.-H. Hwang, *Macromolecules* **2014**, *47*, 7397–7406.
2. J. Huang, Y. H. Niu, W. Yang, Y. Q. Mo, M. Yuan, and Y. Cao, *Macromolecules* **2002**, *35*, 6080–6082.
3. Z. A. Li, Y. Liu, G. Yu, Y. Wen, Y. Guo, L. Ji, J. Qin, Z. Li, *Adv. Funct. Mater.* **2009**, *19*, 2677–2683.
4. S.-J. Liu, W.-P. Lin, M.-D. Yi, W.-J. Xu, C. Tang, Q. Zhao, S.-H. Ye, X.-M. Liu, W. Huang, *J. Mater. Chem.* **2012**, *22*, 22964–22970.
5. J. Luo, G. Xie, S. Gong, T. Chen, C. Yang, *Chem. Commun.* **2016**, *52*, 2292–2295.
6. T. Michinobu, H. Kumazawa, E. Otsuki, H. Usui, and K. Shigehara, *J. Polym. Sci. A Polym. Chem.* **2009**, *47*, 3880–3891.
7. L. Yi and X. Wang, *Comp. Theor. Chem.* **2011**, *969*, 71–75.
8. F. Peng, X. Wang, T. Guo, J. Xiong, L. Ying, Y. Cao, *Organic* **2019**, *67*, 34–42.
9. J. Li, F. Dierschke, J. Wu, A. C. Grimsdale, and K. Müllen, *J. Mater. Chem.* **2006**, *16*, 96–100.
10. N. Blouin and M. Leclerc, *Acc. Chem. Res.* **2008**, *41*, 1110–1119.
11. S. Wakim, S. Beaupré, N. Blouin, B.-R, Aich, S. Rodman, R. Gaudiana, Y. Tao, and M. Leclerc, *J. Mater. Chem.* **2009**, *19*, 5351–5358.
12. J. -F. Morin and M. Leclerc, *Macromolecules* **2001**, *34*, 4680–4682.
13. Z.-B. Zhang, M. Fujiki, H.-Z. Tang, M. Motonaga, and K. Torimitsu, *Macromolecules* **2002**, *35*, 1988–1990.
14. R. Schroot, U. S. Schubert, and M. Jager, *Macromolecules* **2016**, *49*, 8801–8811.
15. H. Wen, Z. Ge, Y. Liu, T. Yokozawa, L. Lu, X. Ouyang, and Z. Tan, *Eur. Polym. J.* **2013**, *49*, 3740–3743.
16. R. Schroot, U. S. Schubert, and M. Jager, *Macromolecules* **2017**, *50*, 1319–1330.
17. (a) *Organic Synthesis via Boranes*, *Vol*. 2 (Eds.: H. C. Brown and M. Zaidlewicz), Aldrich, Milwaukee. 2001; (b) *Science of Synthesis, Houben-Weyl Methods of Molecular Transformations*, *Vol*. 6 (Eds.: D. E. Kaufmann and D. S. Matteson), Thieme, Stuttgart. 2005; (c) *Boronic Acids* (Ed.: D. G. Hall), Wiley-VCH, Weinheim. 2005.
18. (a) N. Miyaura, A. Suzuki, *Chem*. *Rev*., 1995, **95**, 2457−2483; (b) N. Miyaura, Organoboron Compounds. *Top*. *Curr*. *Chem*., 2002. **219**, 11−59; c) *Organic Synthesis via Boranes*, *Vol*. 3 (Eds.: A. Suzuki and H. C. Brown), Aldrich, Milwaukee. 2003; (d) *Metal-Catalyzed Cross-Coupling Reactions*, 2nd ed. (Eds.: A. Meijere and F. Diederich), Wiley-VCH, Weinheim. 2004, 41−123.
19. Y. Yamamoto, M. Takizawa, X.-Q. Yu, and N. Miyaura, *Angew. Chem. Int. Ed.* **2008**, *47*, 928–931.
20. G.-Q. Li, Y. Yamamoto, and N. Miyaura, *Tetrahedron* **2011**, *67*, 6804–6811.
21. S. Sakashita, M. Takizawa, J. Sugai, H. Ito, and Y. Yamamoto, *Org. Lett.* **2013**, *15*, 4308–4311.
22. S. Kobayashi, K. Fujiwara, T. Yamamoto, K. Tajima, Y. Yamamoto, T. Isono, T. Satoh, *Polym. Chem.*

2020, *11*, 6832–6839.

23. H.-H. Zhang, C.-H. Xing, Q.-S. Hu, and K. Hong, *Macromolecules* **2015**, *48*, 967–978.
24. J. Lee, H. Park, S.-H. Hwang, I.-H. Lee, and T.-L. Choi, *Macromolecules* **2020**, *53*, 3306–3314.
25. T. Beryozkina, V. Senkovskyy, E. Kaul, and A. Kiriy, *Macromolecules* **2008**, *41*, 7817–7823.
26. N. Doubina, A. Ho, A. K.-Y. Jen, and C. K. Luscombe, *Macromolecules* **2009**, *42*, 7670–7677.
27. N. Marshall, S. K. Sontag, and J. Locklin, *Macromolecules* **2010**, *43*, 2137–2144.
28. C. Adamo, C. Amatore, I. Ciofini, A. Jutand and H. Lakmini, *J. Am. Chem. Soc.* **2006**, *128*, 6829–6836.
29. M. Butters, J. N. Harvey, J. Jover, A. J. J. Lennox, G. C. L.-Jones, and P. M. Murray, *Angew. Chem.* **2010**, *122*, 5282–5286.
30. F. Lemasson, N. Berton, J. Tittmann, F. Hennrich, M. M. Kappes, and M. Mayor, *Macromolecules* **2012**, *45*, 713–722.
31. A. Y. Fedorov, A. A. Shchepalov, A. V. Bol´shakov, A. S. Shavyrin, Y. A. Kurskii, J. P. Finet, and S. V. Zelentsov, *Russian chemical bulletin* **2004**, *53*, 370−375.
32. X. Zhu, S. R. Bheemireddy, S. V. Sambasivarao, P. W. Rose. R. T. Guzman. A. G. Waltner, K. H. DuBay, and K. N. Plunkett, *Macromolecules* **2016**, *49*, 127−133.
33. S. Zalesskiy and V. P. Ananikov, *Organometallics* **2012**, **31**, 2302−2309.

Chapter 4

Conclusions

The Suzuki–Miyaura catalyst-transfer polycondensation (SCTP) using triolborate salt-type fluorene and carbazole monomers was performed, which are more nucleophilic than boronic acid derivatives. This is a novel synthesis approach for well-defined π-conjugated polymers and their block copolymers (BCPs). These new monomers were highly effective for precisely synthesizing high-molecular-weight end-functionalized polyfluorenes (PFs) and polycarbazoles (PCzs) with narrow dispersity. Furthermore, PF/PCz-containing BCPs were directly obtained by conducting SCTP using a variety of macroinitiators. The key to this approach was to use a solvent with reduced water content to suppress macroinitiator aggregation. The significant achievements and findings of this study are summarized as follows.

Chapter 2 "Suzuki–Miyaura Catalyst-Transfer Polycondensation of Triolborate Salt-Type Fluorene Monomer"

PFs and PF-containing block and graft copolymers were successfully synthesized by SCTP using a triolborate salt-type fluorene monomer, viz. potassium 2-(7-bromo-9,9-dihexyl-9*H*-fluorene-2-yl)triolborate. Kinetic and post-polymerization experiments revealed that SCTP proceeded via chain growth and controlled/living polymerization. This is the first report of successful chain-growth polycondensation using a triolborate salt-type monomer and demonstrates the suitability of this monomer for the synthesis of π-conjugated polymers for the first time. PF-containing block and graft copolymers were successfully synthesized by starting with various macroinitiators. This was complicated to achieve by the conventional SCTP of pinacolboronate-type fluorene monomers. The strategy proposed in this chapter is based on the coil-first/graft-from approach, which is an easy and convenient method to synthesize PF-containing BCPs.

Chapter 3 "Suzuki–Miyaura Catalyst-Transfer Polycondensation of Triolborate Salt-Type Carbazole"

Given the promising results demonstrated in Chapter 2, the suitability of triolborate salt-type monomer for polymerization was investigated, not only for fluorene but also for carbazoles (3,6- and 2,7-carbazole) as a representative example of a heteroaromatic monomer. At low temperatures, the SCTP of potassium 3-(6-bromo-9-(2-octyldecyl)-9H-carbazole-2-yl)triolborate selectively produced end-functionalized 3,6-PCz while suppressing the formation of cyclic byproducts. The existing SCTP could not achieve this. It was made possible for the first time by using a triolborate salt-type monomer with high nucleophilicity. The SCTP of potassium 2-(7-bromo-9-(2-octyldecyl)-9*H*-carbazole-2-yl)triolborate proceeded in a chain-growth, and controlled/living manner produces 2,7-PCzs with controlled molecular weights and narrow dispersity. This is the first example of synthesizing 2,7-PCz by SCTP using a triolborate-salt-type monomer. The current SCTP approach enables the synthesis of random copolymers of *N*-alkyl-3,6- and 2,7-carbazoles, random copolymers of *N*-alkyl-carbazole, and 9,9-dialkylfluorene, and 2,7-PCz-containing block copolymers.

In conclusion, the author successfully established precise synthesis strategies for narrowly dispersed, end-functionalized PF, PCz, and PF/PCz-containing BCPs by the SCTP of triolborate salt-type fluorene and carbazole monomers. One of the essential findings of the present study is that triolborate salt-type monomers can be polymerized even at low temperatures, thus suppressing side reactions such as protodeboronation and chain transfer reactions. Furthermore, while the pinacolborate-type monomers used in conventional SCTP require large amounts of base and water, SCTP using triolborate salt-type monomers can significantly reduce the amount of base and water. Moreover, the ability to carry out SCTP with much less water and the base has led to the developing of a new method to produce conjugated BCPs based on the coil-type macroinitiator method (Figure 4). Therefore, we believe that the

newly established SCTP system using triolborate salt-type monomers can lead to significant progress in fabricating high-quality π-conjugated polymers with unique structures and functions. This will eventually contribute to developing organic light-emitting diodes, organic field-effect transistors, organic photovoltaics, and organic memory devices.

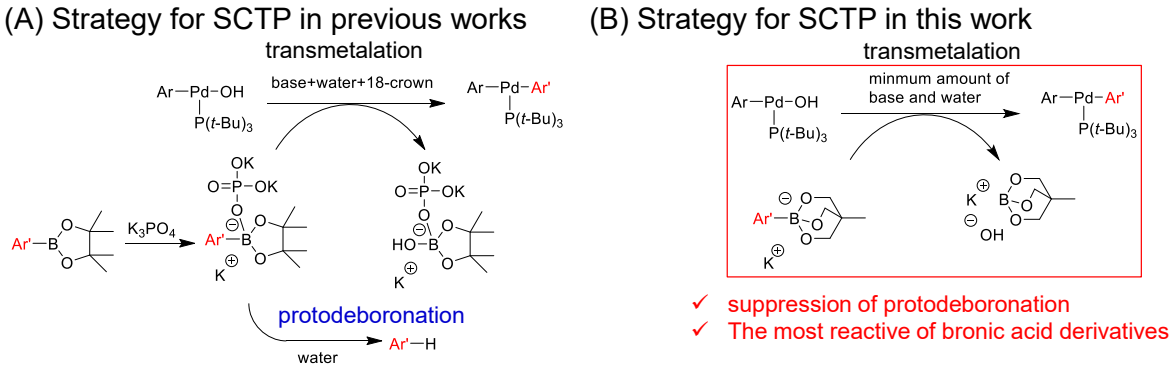

Figure 4. Suzuki–Miyaura coupling reaction for the precise synthesis of a π-conjugated polymer. (A) Conventional synthesis of the π-conjugated polymer by SCTP of pinacolborate-type monomer. (B) The strategy for the precise synthesis of the π-conjugated polymer through SCTP of triolborate salt-type monomer.